POLITECNICO DI MILANO

Facoltà di Ingegneria Industriale

Corso di Laurea in Ingegneria Energetica

Dipartimento di Energia

Preliminary Design of Different Fully Renewable Stand Alone for Residential Buildings in a Greek Island

Supervisor: Prof. Marco Astolfi
Co-Supervisor: Kostas Braimakis

Candidate

Giacomo Manzoni
Matr. 853130

AA 2017-2018

Acknowledgements

Index

List of figures

List of tables

Notes

Sommario

L'energia ha giocato nella storia dell'umanità un ruolo centrale, e questo risulta ancora più vero al giorno d'oggi. La sfida del cambiamento climatico coinvolge l'essere umano a livello globale: per questo motivo, soluzioni innovative e sostenibili sono al centro di numerose ricerche. La tesi si propone di analizzare differenti sistemi di trigenerazione (CCHP, Combined Cooling Heating and Power) in un contesto rurale, un'isola greca, off-grid e completamente rinnovabili. I sistemi analizzati includono differenti integrazioni dei componenti, i quali comprendono un micro ORC (Organic Rankine Cycle), una caldaia a biomassa, uno storage termico (TES, Thermal Energy Storage), collettori solari a tubi evacuati (ETC, Evacuated Tube Collector), batterie agli ioni di Litio (BESS, Battery Energy Storage System) e pannelli fotovoltaici (PV). Viene proposta anche una comparazione con un sistema esclusivamente fotovoltaico integrato con batterie, stand-alone. Le performance dei sistemi sono state valutate tramite una simulazione off-design mediante due distinti codici Matlab® sviluppati dall'autore. I risultati vengono comparati in termini economici attraverso l'annuity dell'impianto. Il layout che risulta più economico e compatto, e che garantisce una continua produzione di energia, è un micro ORC con storage termico, storage elettrico, caldaia a biomassa e collettori solari, integrato con pannelli fotovoltaici. La annuity del sistema risulta 5499 € annui, con un'affidabilità del 100%. A parità di annuity, l'impianto fotovoltaico accoppiato con batterie mostra un'affidabilità minore (90-95%), e delle dimensioni superiori. Si conclude che in un contesto rurale come un'isola greca, nonostante l'alto costo dell'elettricità generata da motori diesel, i sistemi stand-alone completamente rinnovabili non risultano competitivi senza un sistema di incentivazione.

Parole Chiave: ORC, CCHP, stand-alone, off-design, Grecia

Abstract

Energy has played in mankind's history a central role, and this is even more evident nowadays. The climate change challenge involves the entire world: for this reason, many innovative and sustainable solutions are under research to stop it. The thesis analyses different trigeneration systems (CCHP, Combined Heat Cooling and Power) in a rural context, a Greek Island, off-grid and fully renewable. The systems investigated include different degrees of integration of RES (Renewable Energy Sources), in particular: a micro ORC (Organic Rankine Cycle), a biomass boiler, a thermal storage (TES, Thermal Energy Storage), ETCs (Evacuated Tube Collectors), BESS (Battery Energy Storage System), and PVs (Photovoltaic Panels). It is proposed a benchmark with a photovoltaic field coupled with batteries, without a back-up generator. Performances of the systems have been evaluated with the aid of a Matlab® codes developed by the author. The results are economically benchmarked according to the annuity of the plants. The cheapest and most reliable system is a micro ORC, which includes TES, BESS, ETCs, PVs and the biomass boiler. The annuity given is 5499€ per year, with a reliability of 100%. With the same annuity, the PV-BESS plant shows a lower reliability (90-95%), and larger dimensions. Thus, although the high cost of electricity provided by diesel generator in a Greek island, fully renewable stand-alone systems are not competitive without a subsidisation system.

Key Words: ORC, CCHP, stand-alone, off-design, Greece

1 Introduction

1.1 Introduction

Energy has played a central role in the development of our society, and nowadays we depend on it even more. The challenge of the mankind in this century is to find feasible and sustainable alternatives to fossil fuel to shift the energy production towards more environmental-friendly solutions.

The IEA 2017 Energy Outlook shows the world energy consumption and its future trends. In the document, it is forecasted a 28% growth in the global energy demand: in 2015 world energy consumption increases from 575 quadrillion BTU ($1.68 * 10^8\ TWh/year$) to 663 quadrillion BTU ($1.94 * 10^8\ TWh/year$) by 2030 and then to 736 quadrillion BTU ($1.94 * 10^8\ TWh/year$) by 2040. [1]

The increase of the global energy demand will have an impact on environment: the over exploitation of the natural resources, the pollution of the air and oceans, the massive greenhouse gases (GHG) production, will lead finally to climate change. The concern about it started in 1992 thanks to the Bruntland Report, and it has reached the world population's attention, that claims for better policies and a change of paradigm. [2] The most important international treaty that have tried to provide nations a guideline to reduce the GHG emissions is the Kyoto Protocol, signed by 180 countries in 1997 and effective since 2005. Currently, 192 countries signed it. Those countries "in order to promote sustainable development shall implement and/or further elaborate policies and measures in accordance with its national circumstances, such as research on, promotion, development and increased use of new and renewable forms of energy". [3] In 2010, the European Commission proposed Europe 2020 strategy, an inclusive, sustainable and smart strategy of growth, which includes even more ambitious targets in terms of energy, the so-called three 20 targets:

1. To reduce greenhouse gas emissions by at least 20% compared to 1990 levels
2. Increase the share of renewable energy in final energy consumption to 20%
3. achieve a 20% increase in energy efficiency

In 2014, European members agreed that research is an investment in our future and started the Horizon 2020 Framework Programme. Horizon 2020 is the biggest EU Research and Innovation programme ever with nearly €80 billion of funding available over 7 years. [4] Among all the objectives of the Programme, there is a section, "Secure, Clean and Efficient Energy", devoted to support the transition to a reliable, sustainable

and competitive energy system. 5391 million have been allocated to this section. On the Work Program 2016-2017 about the energy sector, more ambitious milestones to be reached by 2030 are listed:

- Diversify energy sources – so Europe can quickly switch to other supply channels if the financial or political cost of importing from the East becomes too high.

- Help EU countries become less dependent on energy imports.

- at least 27% for the share of renewable energy consumed within the EU

- at least 27% improvement of energy efficiency

- Reduce Europe's energy use by 27% or greater by 2030

- Build on the EU's target of emitting at least 40% less greenhouse gases by 2030

- Make the EU the world number one in renewable energy and lead the fight against global warming

[5]

Despite all the policies and programs developed, the shift to cleaner energy is a long and challenging path, but Europe has highlighted the most important aspects: diversification, improvement of renewable, reduction of the emissions and enhancement of efficiency.

One of the most relevant sector in terms of GHG emissions is the building sector: global building-related CO_2 emissions have continued to rise by nearly 1% per year since 2010, and it represents the 6% of the total share, as in Figure 1. [6]
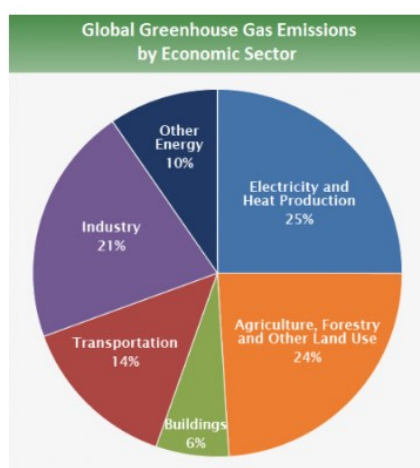
Figure 1 – Global GHG Emissions by Economic Sector [6]

Moreover, the untapped efficiency potential of the building sector claim to be up to 80%, meaning that large improvement in this sector should be undertaken. [7]

Furthermore, as previously said, the global energy demand is growing: this growth in the residential sector is linked with a larger demand in terms of electricity and air conditioning. This increase in terms of energy consumption could be a problem for those off-grid rural areas, that requires targeted solutions. [8]

In fact, the building sector includes both urban and rural areas and different solutions should be considered according to the utility following the guidelines of the EU: diversificating, promoting renewables and reducing the emissions. Based on these premises, renewable combined generation, such as cogeneration (CHP e combined heating and power) or trigeneration (CCHP e combined cooling, heating and power), has become an even more attractive energy alternative, particularly on a medium- and small-scale basis (below 1 MW) also thanks to its higher efficiency with respect to the traditional separated generation. The application of these technologies in decentralized, off-grid areas can additionally contribute to the improvement of the socioeconomic environment, providing fuel independence and decreased energy costs. [9]

The aim of this thesis is to provide a sustainable solution for such complex rural scenario, comparing different CCHP schemes, completely driven by renewable, in a off-grid context: a Greek Island.

1.2   Greece in a glance

Figure 2 – Aegean Sea and Greek Islands [10]

Greece is a member of the European Union since 1981, with approximately 11 million of inhabitants and a GDPpc of 17,890 US$. It is a very peculiar country thanks to its morphology, in fact, Greece has approximately 2000 of islands, with a population of over 1.3 million of people. [11] The Total Primary Energy Supply (TPES) of the country is 22.9 Mtoe (-24% since 2006), the TPES pc is 2.1 toe (IEA average: 4.4 toe), while the Total Final Consumption (TFC) reached is peak in 2007 (21.8 Mtoe), then decreased by 30% in 2015 (15.4 Mtoe); but the last year (2016) shows an encouraging positive trend (16.8 Mtoe). The decrease of this values can be attributed to the financial crisis of 2009, which is still burdening the economy of the country, that has started to recover only this year with a +0.3% of GDP.

Greece has a large amount of coal production that covers the domestic demand for coal, which is used mainly in the power sector. Coal is still the dominant fuel in electricity generation, accounting for almost a third of the total generation, but its use is decreasing. Regarding the renewables, they have doubled the share of TPES from 5.9% to 12.5% in the period 2006-2016. Oil is the most-significant fuel (50% of TPES, 54% of TFC), and the country is almost entirely dependent on oil imports. The transport sector, which is the

largest energy-consuming sector due to shipping, is dominated by oil products, and large shares of fuel oil are being used in the residential sector.
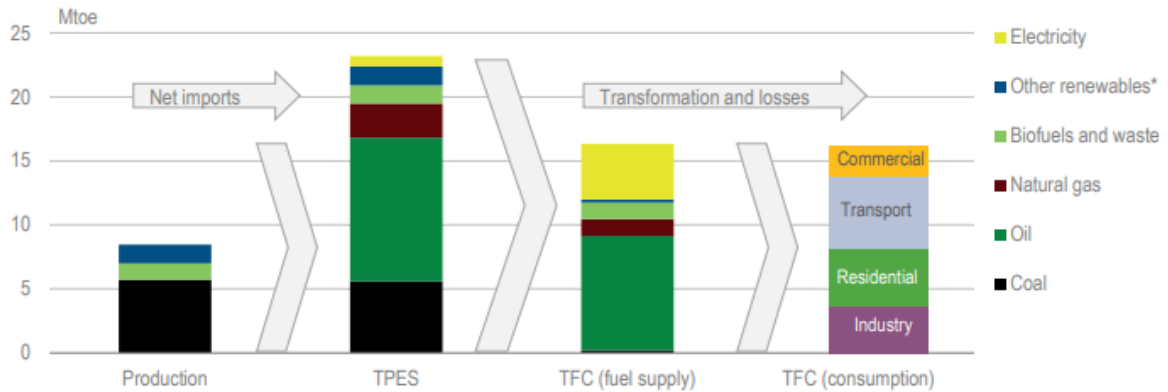
Figure 3 – Energy Transformation in Greece: from Production to Consumption [12]

Furthermore, Greece has a large share of oil consumed in power generation. Oil power plants generated 11% of the total electricity production in 2015, which was the highest among all IEA member countries. This is because many of Greece's islands, namely Non-Interconnected Islands (NII), are not yet connected to the mainland electricity grid, as in Figure 4, but are supplied by isolated systems that rely on diesel generation (90.2% of the consumption). [12]

Figure 4 - Greek National Grid [12]

The relatively small grid of the islands are not interconnected each other, nor they are able to deal with high-fluctuating technologies such as renewable ones (wind or PV), nor with high seasonality of peak power consumption. Hence, despite the high potential in terms of sun (up to 1800 kWh/m2, assuming optimal tilt angle, south oriented [13]) and wind energy (8-11 m/s at hub height [14]), they can stand a maximum penetration of renewables of 25-30% in terms of share. [10] Moreover, islands are strongly affected by seasonality and tourism: the yearly rate of increase in demand of electricity has grown more in the islands with respect to the grid connected network; the load factor is lower than that of the continent; many problems related to seasonal peak power production arise. This results in a higher electricity cost of generation in the NIIs. [15]

The average cost of production of these plants in August 2017 reached 336,96 €/MWh, according to the Hellenic Electricity Distribution Network Operator, which is over seven times the price in the main grid (50 €/MWh). [16] The extra-cost of generation is not charged on the customers of the islands because the Greek regulatory system provides for a public service obligation (PSO) to supply power to consumers on NIIs at the same electricity prices of the mainland. Island suppliers are compensated for the difference between their (high) cost of generation and the system marginal price on the mainland through a fund that is financed by a fee charged to all electricity consumers. The total cost for this PSO is in the range 500 M€ to 700 M€ per year.

At the same time, it's not only a mere issue of higher prices for the consumers, but also in terms of emissions. As previously mentioned, Greece maintains a high reliance on coal and diesel in electricity generation, which results in a high carbon intensity of the country. In 2015, Greece emitted 582 gCO2/kWh, while IEA member countries emitted on average 390 gCO2/kWh. As we can see, the high reliance on diesel generator in the NIIs affects the whole country, in terms of higher prices, higher emissions, and lower generation efficiency. [12] So, appropriate energy planning and development in the non-connected islands could lower energy prices across the country, and at the same time, ensuring the economic survival and well being of Aegean island communities. The need to untap the high renewable energy potential of the Aegean islands has led to the ambitious project of connecting most Aegean islands to the mainland grid. [10]
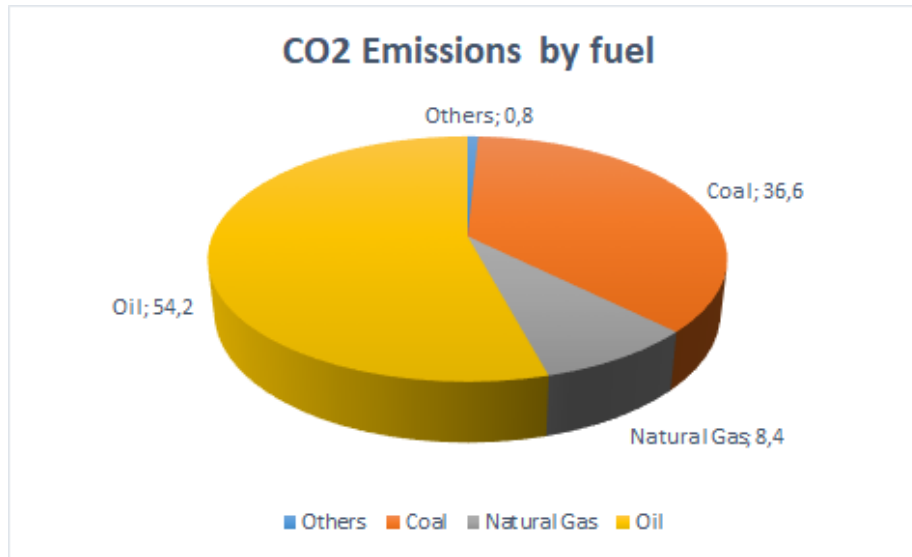
Figure 5 – CO2 Emissions by Fuel in Greece

The project of interconnecting the Greek Islands with the mainland started in 2010, and it contemplates four phase nowadays; actually is at the end of the first phase.

- The first phase will connect the port of Lavrio, in the south of Attica region, with Syros, Paros, Mykonos and Tinos, and it will be completed at the end of 2018.
- The second phase will provide the connection Paros-Naxos, Naxos-Mykonos and un upgrade in south Euvoia. The completion is expected for the end of 2019.
- The third phase is ratified yet, and it will provide an undersea cable between Lavrio and Syros. Also, a "small" (2 x 140 MW) connection between Chrete and Peloponnese within 2020, and a "big" one (2 x 500 MW) within 2022.
- The fourth phase, which has not been ratified and it is still matter of study includes several projects in order to connect further islands. [16]

Still, this ambitious program can not connect the over 2000 islands in the short period, because many of them will be left isolated anyway, also just because of their geographical position. Hence, hybrid and renewable solutions should be taken into account in order to deal with this complex scenario, suggesting as viable in a short term perspective, decentralized electric production and off-grid stand-alone plants. [12] The aim is not only to decrease the generation of costly diesel plants in the islands, but also to reduce the dependence on foreign fossil fuels in the entire country while, at the same time, moving towards national and E.U. clean energy goals lowering the emissions.

The aim of this thesis will be to find the most sustainable and economically feasible micro-scale off-grid solution: only fully renewable driven plants will be insvestigated.

1.3 The Shift of the Paradigm: from Centralized Power Generation to Decentralized Systems

1.3.1 The Challenges of Decentralization

At the end of the first era of electrification the power generation was centralized with huge thermal power plants, and large transmission and distribution grids had been built, meant for many consumers and cost-effective thanks to the size effect. Technological advances in decentralized power generation however, have made these technologies more competitive and continue to shift the calculus towards increased deployment. The spectrum of centralization to decentralization can be distinguished in three levels:

- Centralized power generation, with a reticulated electrical network serving a (usually heavily populated) geographic area.
- Mini or micro grid: a grid serving the needs of a community or defined loads.
- Decentralized power generation: an individual unit covering the need of one household or load.

The two last levels may involve the use of local storage capacity (batteries). Typical systems include Solar Home Systems with PV, diesel generators, or biomass gasification. The main criterion governing the choice of a decentralized solution is the relative cost of the technology compared to a centralized technology. This cost is a function of the geographic scenario (the cost function of extension is proportional to distance and increases with geographic obstacles) and the consumption density. [17]

Moreover, there is a social aspect related to the concern of the inhabitants as well as the increase of the public willingness for "green technologies". Hence, it is an opportunity to reduce the environmental impact employing hybrid solution embracing renewable energy sources. Renewable technologies can help the rural population to lower their dependence on fossil fuel, which implies lower imports at national level, resulting in an improvement in terms of energy diversification for the country.

On the other hand, many problems arise when a stand-alone plant has to be sized. The former is the energy source choice (hydro, sun, wind, biomass) and its availability in the selected location. Secondly, the degree of hybridization: from a conventional diesel generator, to a hybrid (for instance a genset-wind-pv plant), until a fully renewable plant. Thirdly, the economical feasibility of such plants must not be taken for granted: indeed, many studies highlights how heavy is the impact of the site location (and hence the renewable energy source availability), the required reliability of the system and the load factor on the LCOE. [18] Moreover, one of the major obstacles to the deployment of

decentralized renewables is the high initial cost. Finally, maintenance is a crucial issue for decentralized power systems: local technicians must be able to fix or replace the components. The lack of proper maintenance, local manufacturers, trained technicians, is one of the major causes of system failure, along with a misuse of the device. [17]

1.3.2   Photovoltaic systems

The typical solution for stand-alone application are the photovoltaic panels (PV), thanks to their market that, after an initial economic push with Feed-in-Tariffs and incentives, is still able to increase year by year (+50% in the last year: for the first time the solar PV additions are larger than any other fuel in terms of installed GW [19]). This results in a standardization of the product that leads to a decrease of its specific cost of installation. Nowadays, the specific cost per installed, which slightly changes according to the country and if the system is grid-connected or not, is, for residential on-grid, 3€/W [20]; for rural off-grid it is 11€/W [21]. Moreover, the standardization process covers a wide range of rated power output (30-300 W), allowing simple customized solutions for the customers.

The typical layouts of pure PV plant and hybrid PV plant are presented in figure 9.
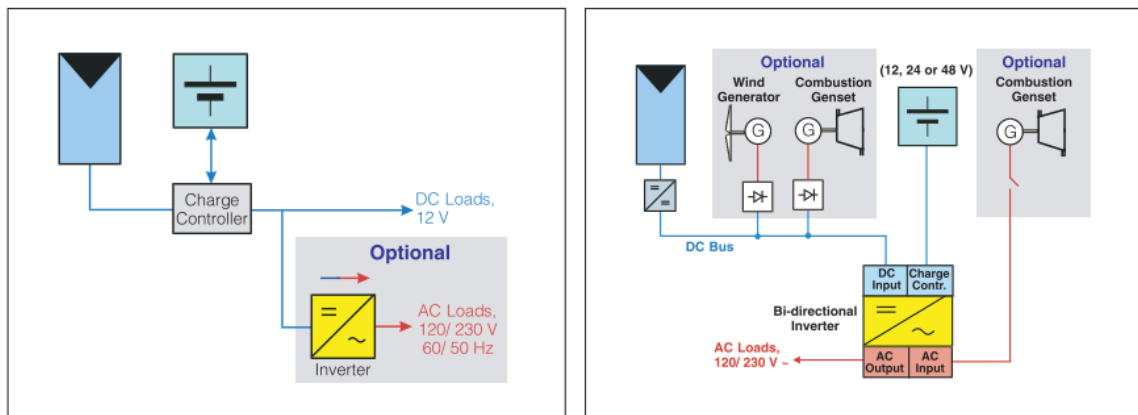
Figure 6 - Typical Layouts: on the left, the pure PV coupled with BESS (Battery Energy Storage System); on the right, a hybrid configuration that considers also an optional small wind turbine and an optional back-up diesel generator. [22]

Many investigations have been carried out to estimate the effectiveness of these systems, considering different electric load requirements according to different utilities. For instance, a 6 kW - 80 batteries (6V, 225Ah) plant for a small hospital with a total load capacity of 31 kWh in Iraq has been simulated with the aid of HOMER software. Beside the massive greenhouse gases emissions' reduction (-14.9 ton/year of CO2), the COE (Cost of Electricity) of the PV is 0.238 US$/kWh while the diesel generator one is 1.332

US$/kWh. This is due to the poor efficiency of the diesel generator at small loading, to its short lifetime, and to high price of gasoline. [23]

In Kynthos island, in Greece, a pure PV system has been projected in order to cover the needs of a farm: it has a nominal power of 2.1 kW, coupled with lead-acid batteries, with a capacity of 50 kWh. The study aims to compare its investment cost with the cost of utility grid extension and connection to the main one, and the outcomes is that the PV array is cost effective if the grid access is further than 1 km. [21]

A hybrid solution wind-PV-BESS, with a nominal capacity of 3 kW, 2.5 kW, and 41,852 kWh respectively, has been investigated in Samothrace Island, Greece. The COE of the system is 0.302 €/kWh, while a LPG generator-wind-BESS has a COE of 0.484 €/kWh. The yearly electric energy requirement is 13,082 kWh. [24] But, as previously said, hybrid stand-alone systems are very sensitive to the load requested and its seasonality, to the location, and finally to the desidered reliability of the grid. In fact, another case-study involving three different cities Cape Corse, Ajaccio, Calvì of Corse island, France, shows a COE of 0.882 €/kWh, 1.383 €/kWh and 1.373€/kWh respectively. The installed capacity is 800 W of PV and 800 W of Wind for Cape Corse, 1200 W of PV and 400W of wind for Ajaccio, and 850 W of PV and 1000W for Calvì, for a total annual electric load of 1,095 kWh. As we can see, a lower electric requirement, a lower installed capacity and a different geographical location with different weather conditions heavily affect the cost of electricity produced and the economical feasibility of such plant. [25]

1.3.3 Micro-ORCs

Nowadays, photovoltaic and its hybridization are not the only solutions available. In fact, many researches are focused on converting the solar power other ways, exploiting the solar thermal energy, instead of the photovoltaic effect, which directly converts the sun power into electric energy. Solar thermal driven plants use sunlight as a heat source to supply power for thermodynamic system: Organic Rankine Cycle (ORC) and, to a lesser extent, Stirling-engine systems are proven technologies with low-medium temperature concentrating solar-thermal collectors. Moreover, ORC systems show strong potential for use in small-scale systems (<10 kWe) with lower temperature, with both non- and low-concentrating collectors. Although water is the most commonly used working fluid in a Rankine cycle, organic fluids are more suitable in low grade heat applications because of their interesting thermo-physical properties at low temperature. [26] The main advanteges of employing an organic compound instead of water are several:

- Less heat is needed during the evaporation process.
- The evaporation process takes place at lower pressure and temperature.

- The expansion process ends in the vapor region and hence the superheating is not required and the risk of blades erosion is avoided.
- The smaller temperature difference between evaporation and condensation also means that the pressure drop ratio will be much smaller and thus simple single stage turbines can be used, reducing the dimensions of the engine.
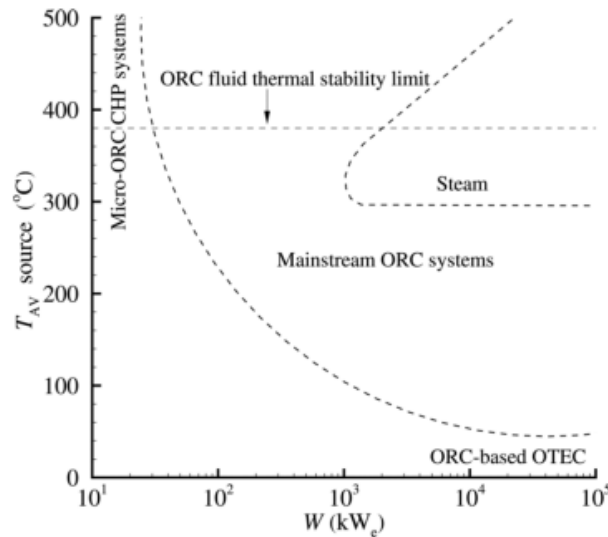
Figure 7 – Fields of application of ORC versus steam power systems in terms of average temperature and power capacity. [27]

Hence, ORCs are the most suitable candidate to exploit low grade heat source, with a reasonable efficiency and compactness. The fields of application of such thermodynamic system are many, thanks to its intrinsic capability of covering a large field of low-to-medium rated power output. [27]

Geothermal power plant: Geothermal fluid properties are extremely site dependent and these sources are characterized by a wide range of temperatures, from about 80 ºC to 300 ºC, and available thermal power. ORC power plants are usually adopted for the conversion of liquid-dominated geothermal reservoirs, with temperatures around 120-150 ºC. The most common layout is the pure binary cycle where the geothermal fluid is pumped to the surface, cooled down releasing heat to the working fluid and, eventually, reinjected into the reservoir to avoid or limit its depletion. The cumulative capacity installed is 10 GW worldwide.

WHR (Waste Heat Recovery): Many fields of application are under investigation nowadays, in fact, ORC potential is particularly strong in all those sectors where it is possible to recover waste heat and the use of a steam cycle is not feasible for technoeconomical reasons. Research and Development are now investigating the opportunity of recovering thermal power from waste heat of fuel cells, but also coupling an ORC with on-road diesel engine of trucks, or commercial ships. Nevertheless, the industrial sector, that release to the ambient a huge amount of waste heat during the manufacturing process has started to increase its interest towards ORCs. The most involved industries are those that release to the ambient huge amount of thermal power expecially the petrochemical sector, the glass sector, the ceramic sector and the cement industry, which was the first one installing a bottoming ORC.

OTEC (Ocean Thermal Energy Conversion): no commercial applications are available on the market, but ORCs can theoretically exploit the temperature difference between surface and deep water. OTEC engines have a critical efficiency, usually in the range of 3-5%, due to the low thermal gradient and, in order to be effective, the minimum temperature difference between the ocean surface layer and deep water should be around 20 °C. This fact limits this kind of application to tropical and equatorial areas where the difference in temperature between the surface and the water 800–1000 m deep is in the range of 20–25 °C.

Biomass conversion: Biomass is the name given to any organic matter which can be both vegetable and animal material such as wood from forests, crops, seaweed, material left over from agricultural and forestry processes, and organic industrial wastes. Biomass is one of the earliest sources of energy, especially in rural areas where it is often the only accessible and affordable source of energy. Compared to other renewable technologies such as solar or wind, biomass has few problems with energy storage; in a sense, biomass is stored energy.
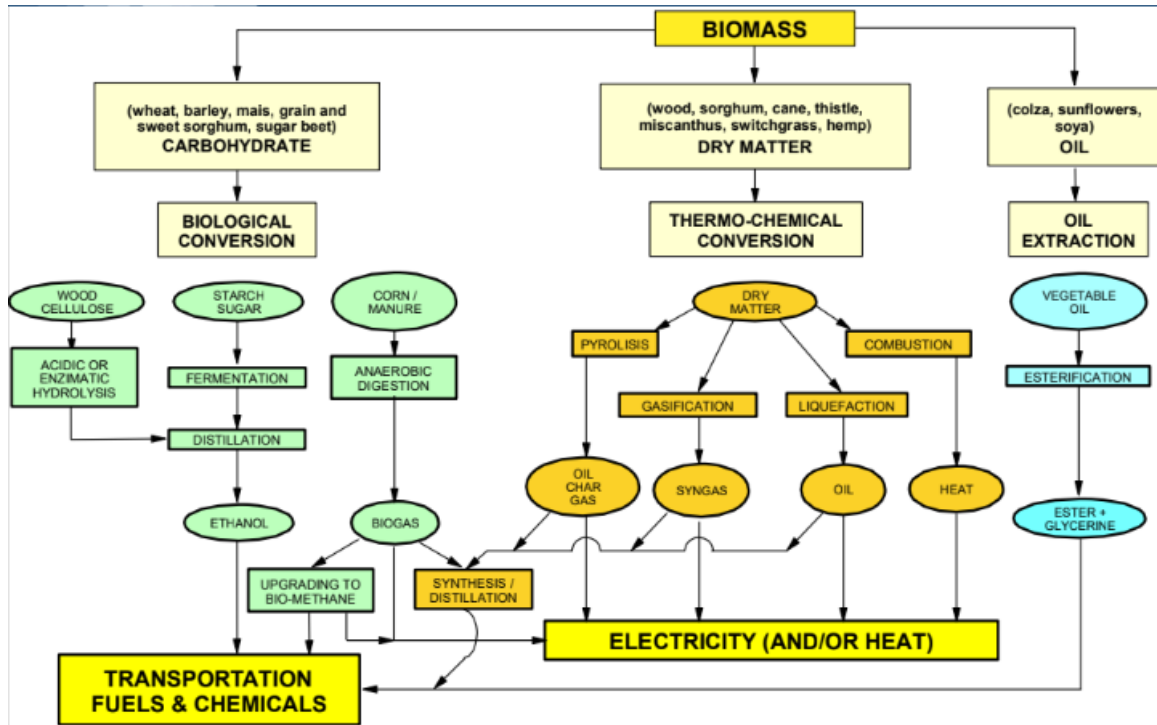
Figure 8 – The different processes to convert Biomass into energy

In Europe, starting from early 2000's more than 200 power plants fuelled with various type of biomass have been installed, making this application one of the fields of major success for ORCs, partly thanks to the favorable legislation. These plants are in the MW_{el} range. But also, the use of biomass is usually coupled with cogenerative ORC plants in CHP units: Biomass ORC CHP plants at medium scale (100–1500 kW) have been successfully demonstrated and are now commercially available. The medium-scale biomass-fired ORC-based CHP plants have already been successfully demonstrated in Admont (400 kWe) and Lienz (1000 kWe), which use silicon oil as working medium and thermo-oil as heating medium, achieving 18% electrical efficiency and 80% overall CHP efficiency. [28] Small scale systems of few kW are still under development.

At the University of Notthingam, a prototype of a micro-scale ORC CHP has been tested with modest results. The system consists on a 50 kW_{th} biomass boiler that provide the thermal input for the ORC which produces 860.7 W, with an efficiency of conversion of 1.41%. Those results are far from the thermodynamic model, which forecasted 7-8% of net electric efficiency, and an expander efficiency of 85%, while the tests shows an expander efficiency of 52.4%. The CHP efficiency is 78.9%.
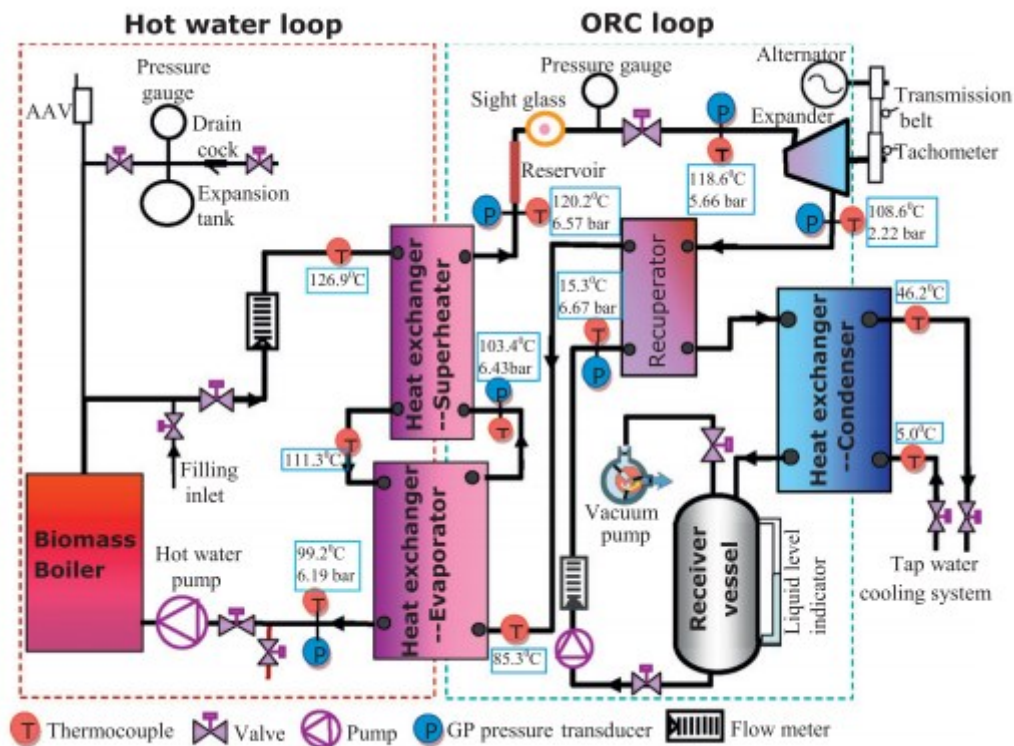
Figure 9 – Plant layout, on the left-hand side the hot water loop for the cogenerative purpose, on the right-hand side the ORC loop for power production. The cycle is a superheated regenerative. [28]

The main reasons that the author found out to justify the poor efficiency of the cycle and the large gap between the model and the test rig were attributed to the expander efficiency assumed versus the tested one (85% vs 52.3%) and to the alternator efficiency assumed versus the tested one (90% vs 50.9%). [28]

Solar thermal power systems: different plant layouts have been investigated, according to the solar thermal collectors employed: CSP (Concentrated Solar Power), PT (Parabolic Trough) or Linear Fresnel; or ETC (Evacuated Tube Collectors)

Concentranted Solar Power systems work with the principle of concentrating solar power on a tube bundle in which the heat transfer fluid flows, thanks to mirrors that are put in place in different arrays. The shape of the mirrors can be 2-D extruded, and in such case the tracking system is one-axis tracking, or, a 3-D extruded with a two-axis tracking system.
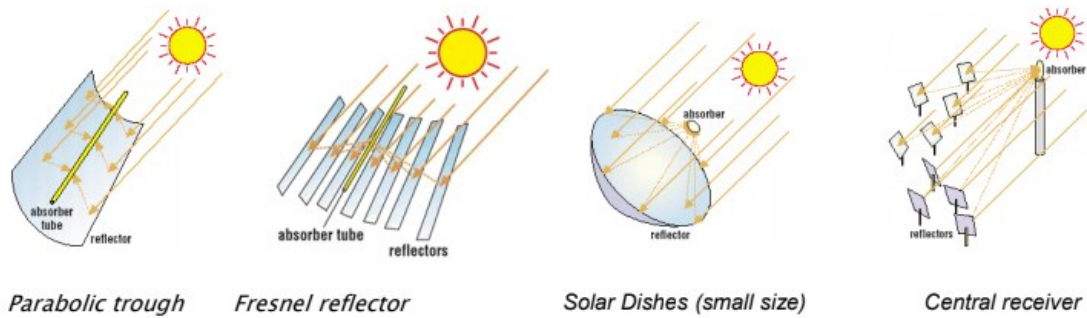
Figure 10 – Linear, 2-D: Parabolic Trough and Fresnel Reflector, one degree of freedom of tracking. 3-D: Parabolic dish, usually with a PV or a Stirling engine, and Tower receiver, two degrees of freedom of tracking of the mirrors.

Researchers at MIT and University of Liège have collaborated with the Non-governmental organization STG International to delevope and implement a small scale concentrated solar thermal technology utilizing medium temperature collectors and an ORC in a remote region of Lesotho.
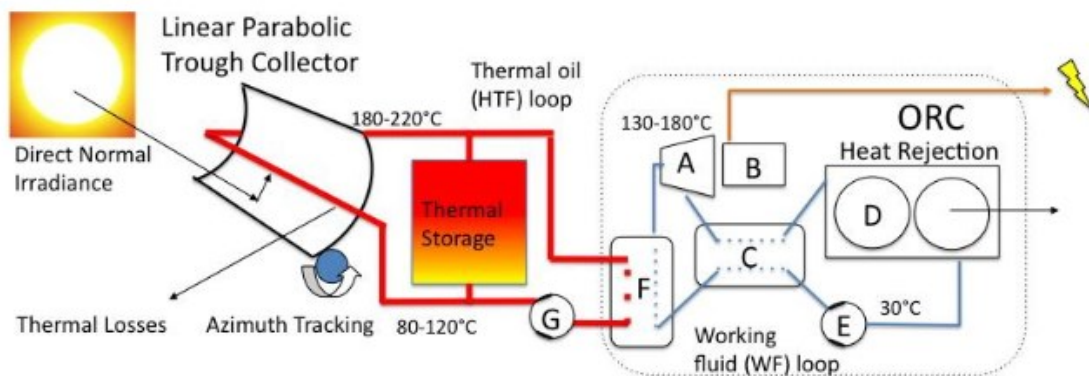
Figure 11 - Conceptual scheme of the solar ORC with components listed as follows A:expander, B: generator, C: recuperator, D: air condenser, E: working fluid pump, F: evaporator, G: HTF pump. [17]

Because no thermal power blocks are currently manufactured in the kilowatt range a small-scale ORC has to be designed for this application. The design is based on modified commercially available components e.g. Heating Ventilation and Air Conditioning (HVAC) scroll compressors (for the expander), and industrial pumps and heat exchangers. At present, no volumetric expander is available on the market. In order to reduce the cost of a practicable system, the expander is obtained by adapting an off-the-shelf hermetic scroll compressor to run in reverse, which has been successfully tested. The proposed technology thus presents the advantage of utilizing off-the-shelf components that are available locally through, e.g. global industrial component supply

chains. This constitutes an important difference with the PV systems where the major part of the components must be imported.

The main characteristics of the plant are:

- 3kWe of net power output
- 75 m^2 of Concentrating Parabolic Trough (PTC) field, single axis tracking
- $\eta_{\text{solar-to-electric}} = 8\%$
- LCOE=0.25$/kWh, which compares favourably with PV (0.3$/kWh).

The study shows a lower conversion efficiency solar-to-electric with respect to photovoltaic panels, but with a lower LCOE and moreover, with also a heating effect that the typical PV systems are not able to cover. [17]

Another option to collect the solar power is using non-concentrated devices such as Flat Tube Collectors (FTC), but they are not meant to produce electricity because of their very low temperature level heat production (<100°C): their usual application is DHW (Domestic Hot Water) production. Hence, the only viable solution to gather solar power and convert it inot electric energy with non-concentrated systems is to use Evacuated Tube Collectors (ETC). They are able to produce heat at a low-medium temperature level, up to 230°C, which is more suitable for power production applications.
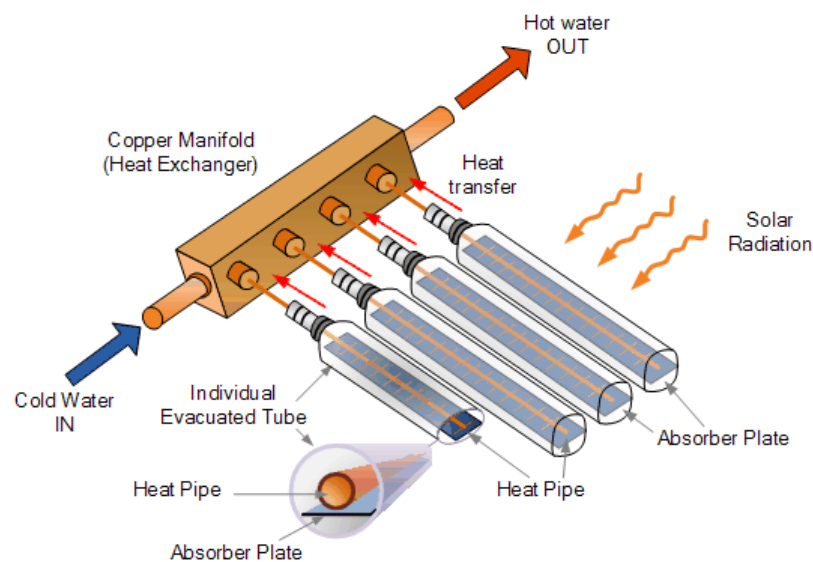
Figure 12 – Evacuated Tube Collector layout [29]

It is interesting also to investigate on the opportunity of employing ETC (Evacuated Tube Collectors) instead of concentrating the radiation, because the market for commercial and residential ETC is more developed and can lead to significative cost reduction of the plant. Moreover, ETC have a simpler installation procedure, since no tracking system is

required, and they can exploit not only the direct beam radiation, but also the diffuse one. It has been demonstrated, that a small-scale ORC of 1 kW reaches 4.4-6.4 % of solar-to-thermal efficiency in the UK climate zone, and a 6.3-7.7% in the Cyprus climate zone. The solar array was assumed to be 15 m^2, a typical size that can be easily integrated on a residential dwelling.
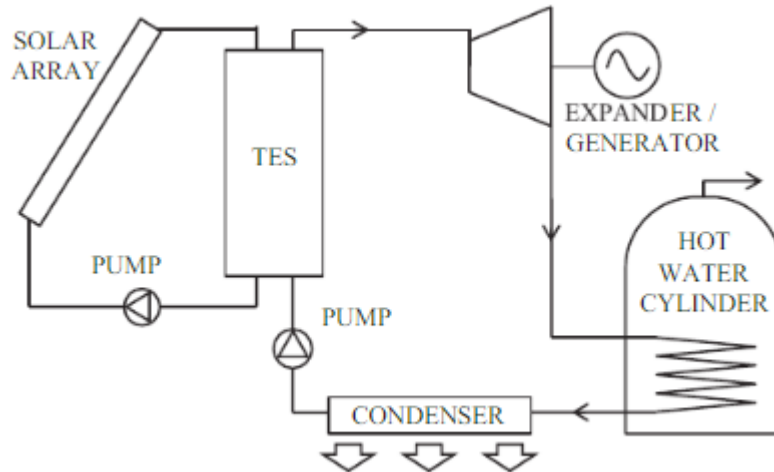
Figure 13 – A pure Solar ORC plant scheme, including a Thermal Energy Storage (TES) [26]

The solar array was able to provide 4 hours of continuos operation at 1 kW of power output in the summer season, 3 hours in the mid season and 0.75 hour in winter time in the UK region, providing 25-30% of the electricity consumption of a residential utility. In Cyprus, the hours were 7, 6 and 3 respectively. Furthermore, a peculiar care is suggested when selecting the evacuated tube collector, because their performance is extremely variable according to several factors, including:

- The average temperature of the fluid inside the collector.
- The application they are going to drive, i.e. power generation, domestic hot water, space heating.
- The inlet temperature of the fluid in the collector

In particular, both the climatic region shows a peak of the efficiency of the solar collectors as a function of the inlet temperature in the 95-135 °C range. [26] Finally, in order to perform a realistic simulation throughout the whole year it is crucial to have an accurate dataset of ambient temperature and radiation, because using average daily data can lead to an error on the energy output of the collector up to 26%. The best practice would be to have data with a time interval of 15 mins, but the error using hourly data is negligible and impressively lower than that using daily averages [30]

As we have seen, many research with very different results have been carried out to investigate the potential of micro CHP ORCs, that show promising performances, although they are extremely site-dependent and affected by the selected technology and its integration with renewables.

The solutions investigated and benchmarked by this thesis include power production, air-conditioning and space-heating, namely CCHP (Combined Cooling Heat and Power) systems. The first system investigated is a micro CCHP ORC (Organic Rankine Cycle) driven by a Biomass Boiler and integrated with TES (Thermal Energy Storage). Then, the benefit introduced by Evacuated Tube Collectors (ETC) and BESS (Battery Energy Storage System) is investigated, and finally, the addition of PV (Photovoltaic) panels is explored. As term of comparison, a simple PV field coupled with BESS for a single house utility will be used, thus leading to a benchmark between fully renewable plants. The utility is assumed remote from the program of interconnection of NIIs on a long-term perspective and hence, the two systems are considered stand-alone. The two plants are completely driven by renewables and the aim is to preliminarly design them thanks to an annual off-design simulation of 8760 hours. Electric energy is provided by the micro ORC and the PV panels respectively. Air conditioning is provided by a Vapour Compression Cycle (VCC), while both cases of space heating provided by radiators panel and Heat Pump (HP) are considered.

2 Introduction to the Test Case

The utility considered for the case study of this thesis, it is a residential dwelling for a single family of 100 m^2, located on an island close to Athens, in the Attica region of Greece. Before discussing the system proposed, it is crucial to forecast the demand in terms of energy, and to collect the weather data, in order to understand the potential of the location in terms of radiation.

2.1   Electric Load Demand Forecast

The electric load has been implemented and modelled thanks to LoadProGen, a useful Matlab tool provided by Politecnico di Milano. [31] The software generates load curves starting from the nominal power of the appliances. Moreover, the software allows to introduce two different degrees of uncertainty on the load curve: the first one is related to the total functioning time of the appliance, the second one is related to the functioning window of the appliance. In fact, many appliances are switched on and off along the day, others follow cyclical operations, (i.e. the fridge) and it is very important to randomize the functioning cycles of them to obtain more realistic curves. According to this randomization, three different load curves for each season are obtained as output: then, these three different scenarios are randomly mixed along the season.

Four different macro scenarios, one per each season have been modelled, to take into account the different utilization of the appliances, which slightly changes season by season. The main differences are related to the utilization of lights, that slightly decrease during summer and mid-seasons with respect to winter thanks to the larger duration of the days. At the same time, the functioning window of the outdoor lights is increased a bit, because of the larger exploitation of the outdoor space during warm season and a small decrease in the functioning hours of the electic stoves is assumed. A constant load of 75 W is also assumed as base-load, hence a zero-load scenario would never happen during the year.

The nominal power of the appliances considered are listed in Table 1.

Table 1 - List of the typical appliances considered and their nominal power to forecast the load curve.

Appliances	Nominal Power [W]
Lights, Living Room	100
Lights, Bedroom	60
Lights, Bath	20
Outdoor Lights	40
Fridge	140
PC/Phone Charger	100
Stereo/TV	150
Electric Stove	1000
Electronics	75
Washing Machine	1000

The load curves generated according to the nominal power of the appliances in Table 1 are summarized by the Figure 14.
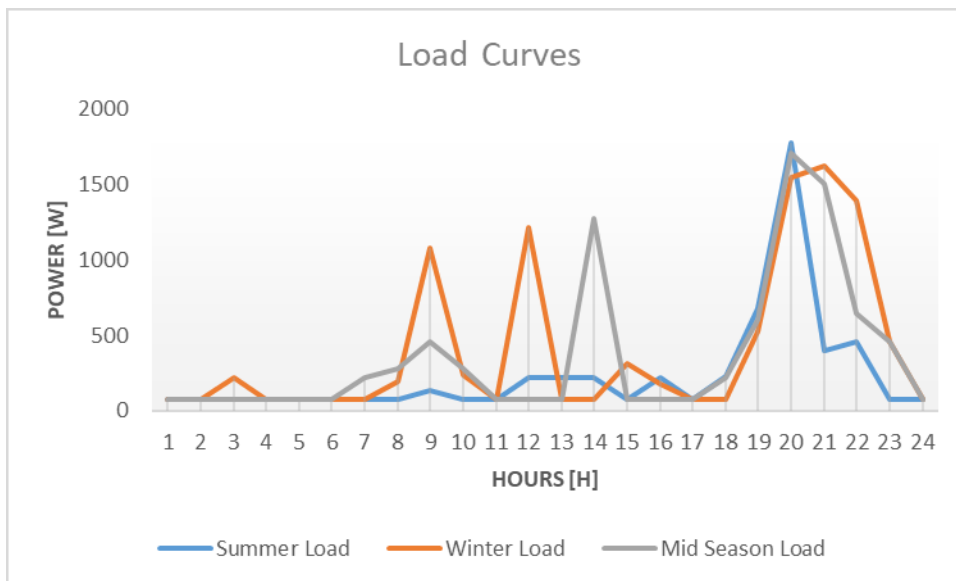
Figure 14 – The different shapes of Load Curves, according to the differences that occur seasonally

Then, to better understand the distribution of the load demand throughout the whole year, and appreciate the differences of energy requirement, a visualization on a heat map is provided.
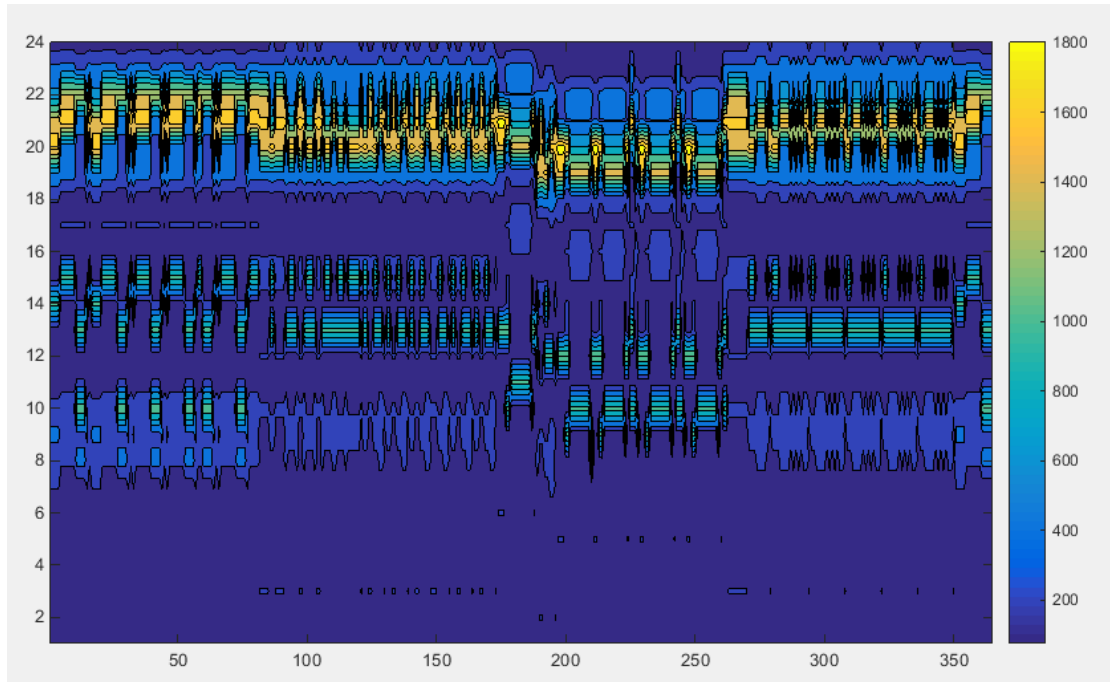
Figure 15 – On the y-axis are the hours of the day, on the x-axis are the days of the year. On the right-hand side there is the legend: blue for low load demand, yellow represents the high ones.

As it is possible to notice, dinner time is the peak period of the day because of the utilization of the electric stove and other appliances. During lunch time, the largest consumption is given, depending on the randomization process, by the washing machine or the electric stove. The brighter blue stripes during night time are the phone charger that are randomly activated. Finally, we can state that more than half of the hours (54.43%) of the year the electric load is just given by the base load, expecially during night time, which is not a very favourable condition for designing the equipment of a stand-alone application. The yearly amount of electric energy required is 2,784 kWh, which is aligned with typical values of residential utility. [25] The highest peak of electric load estimated is 1885 W.

2.2   Cooling and Heating Load

Since the aim of the case study is to perform a simulation of a trigeneration system, it is crucial not only to forecast the electric load, but also the loads in terms of space heating and air conditioning. Indeed, the sizing of the component is based on those input expecially because it is an off-grid application, and peaks must be carefully considered. The cooling and heating load have been estimated with the MIT Advisor Tool [http://designadvisor.mit.edu/design/], which is an online tool that allow to estimate them for a utility, starting from the weather data. Some assumptions have been made about the residential building considered and used as input parameter for the simulation of the software:

- Area: 10 m x 10, m 100 m^2
- Building: Residential
- 4 Facades exposed to the outdoor ambient
- Wall Surface: 85 %
- Window Surface: 15%
- Occupancy: 1/25 person/m^2
- Lighting: 1 W/m^2
- Wall Thermal Resistance: 2 m^2 °C/W
- Glass type: single glazed
- Orientation: N/S E/W
- Roof: Bitumen Roof, Thermal Resistence 2 m^2 °C/W
- Indoor Air Temperature: MAX=22°C, min=18°C
- Max Relative Humidity=:60%
- Ventilation Rate: 5.5 l/s/person [32]

The output of the software is both a chart and a table that collect the heating and cooling load in terms of $\frac{W}{m^2}$ for a typical day of each month of the year. Hence, it has been used the typical day repeated along the entire duration of the month to perform an 8760 hours simulation. The peak values for the heating and cooling load are, respectively, 3.680 kW$_{th}$ and 4.830 kW$_{th}$, while the total amount of energy required is 4,207.8 kWh$_{th}$ and 2,917.3 kWh$_{th}$ respectively. Typical values for a mild climate span in a range of 4-25 kWh$_{th}$ for heating, according to the different country: national average estimated in Greece is 8,000 kWh$_{th}$ of heating per year, resulting in the same order of magnitude. The space heating can be provided both by radiators and a heat pump. In the first case, the heating load is modelled as a heat requirement exchanged in a heat exchanger, while in the second case it is calculated starting from the COP of the heat pump. The air-conditioning will be

provided by a Vapour Compression Cycle, driven by the micro ORC or the PV field and the peak of Cooling load estimated is 4,830. W_{th}. Alternatively, the air-conditioning is provided by the heat pump.

DHW, Domestic Hot Water, is not considered in the case study.
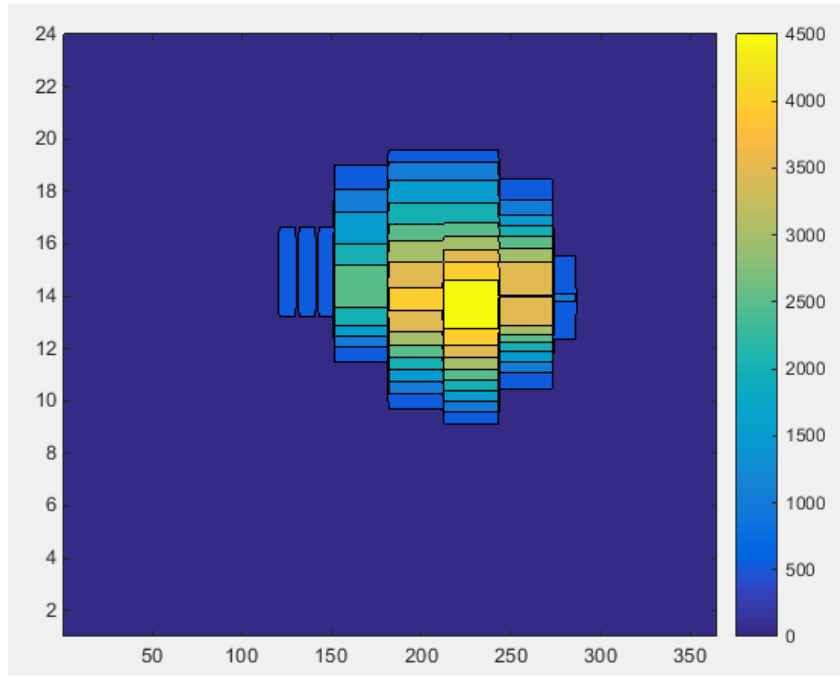
Figure 16 - Cooling load, repeated over the 8760 hours of the year. It is possible to notice the specular behaviour with respect to the Heating Load
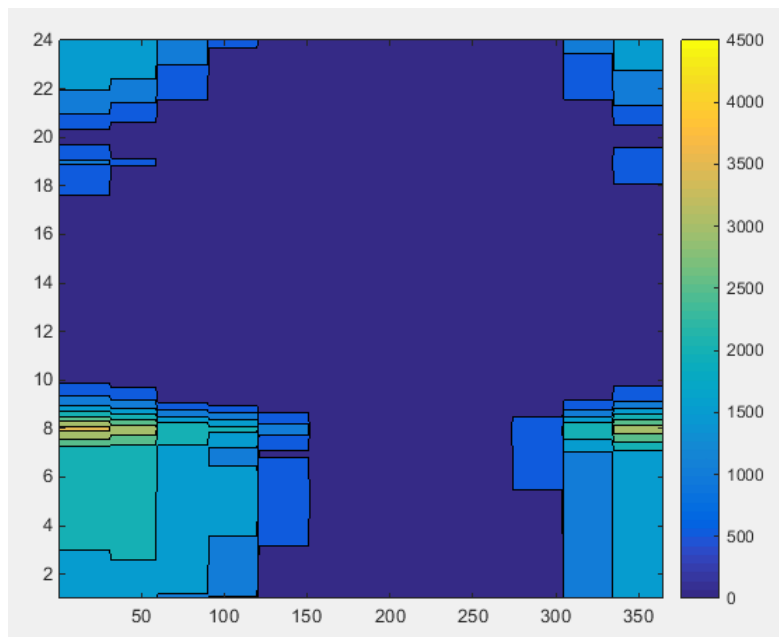
Figure 17 - Heating load, repeated over the 8760 hours of the year.

2.3   Weather Data

The weather data of Athens are considered for the case study, assuming a similar temperature/radiation behaviour in the close islands of the Attica. The weather data required to perform the simulation are the ambient temperature and the radiation data. The ambient temperature affects the efficiencies of many components of the plant, as well as the radiation is important to estimate the radiation potential of the region.

Ambient temperature and radiation data have been taken from Energy+® database. [33]

2.3.1   Ambient Temperature

The weather of Athens is typically very hot and dry, in fact Athens is together with Madrid one of the driest cities of Europe. The average temperature on a year basis is 18°C, as in
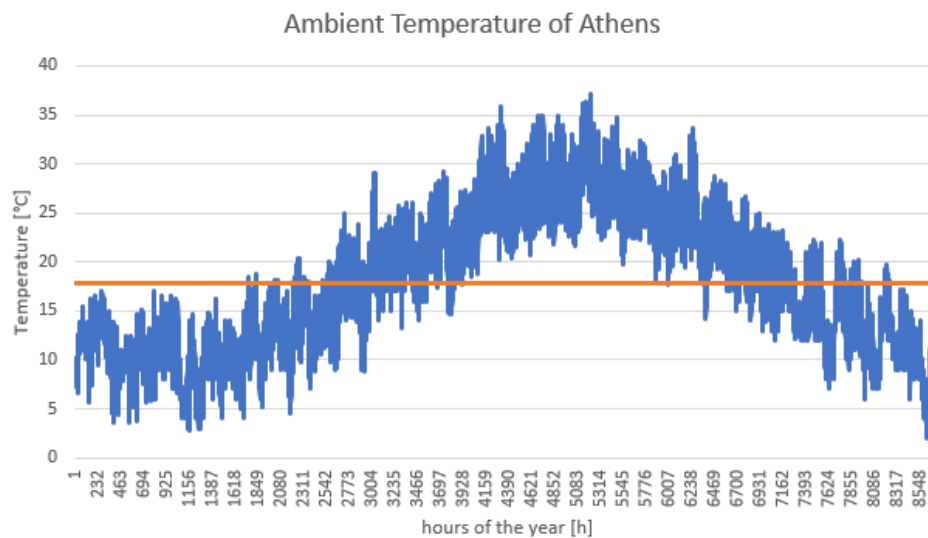
Figure 18 - Ambient Temperature of Athens along the year. The straight line represents the average over the year.

.

Ambient temperature is a crucial parameter because it affects several operating conditions:

- The evacuated tube collector efficiency and its thermal losses towards ambient.
- The condensing temperature of the ORC, and thus the thermodynamic efficiency of the cycle.
- The condensing temperature of the VCC
- The condensing and evaporating temperature of the Heat Pump, and thus its COP.
- The rated power output of the PV panel.

The dataset of temperatures have been taken from Energy+ database. [33]
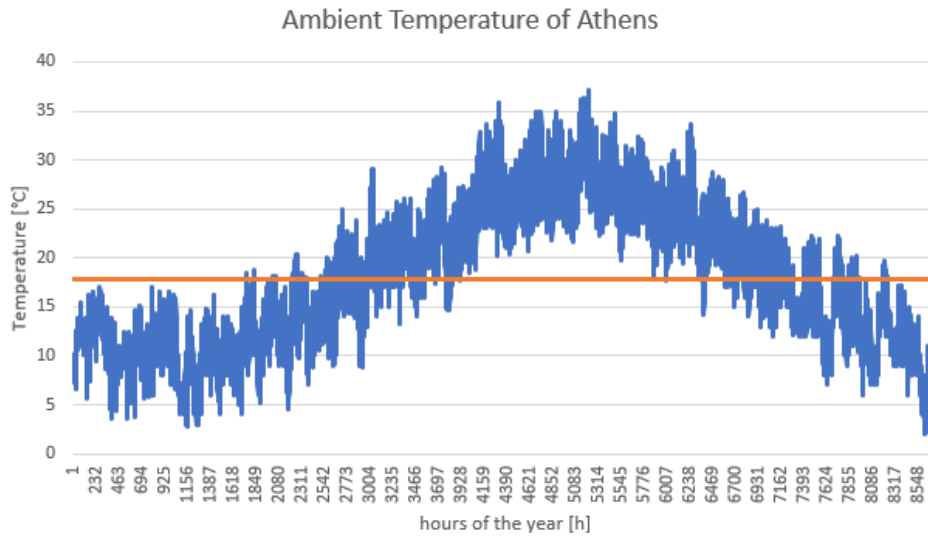
Figure 18 - Ambient Temperature of Athens along the year. The straight line represents the average over the year.

As we can see in Figure 18, the temperatures in this geographical region can reach very high peaks, and strengthen the need for air-conditioning in the building. Furthermore, the PV panels with these high temperatures see a heavy reduction in terms of power produced, while, on the other hand, the efficiency of the ETC would raise because the thermal losses towards the ambient will be reduced. At the same time both the thermodynamic power cycle of the ORC and the cooling cycle of the VCC would be penalized in terms of efficiency by these high values of ambient temperature. In general, in power and reverse thermodynamic cycles the ambient temperature is linked with the condensing temperature (If air-condensed) that, if it raises up, lead to a lower theoretical power production of the turbine and a higher work of the compressor, lowering the efficiency. Hence, a good dataset of ambient temperature is fundamental to include these effects and to develop a more realistic model.

2.3.2   Radiation
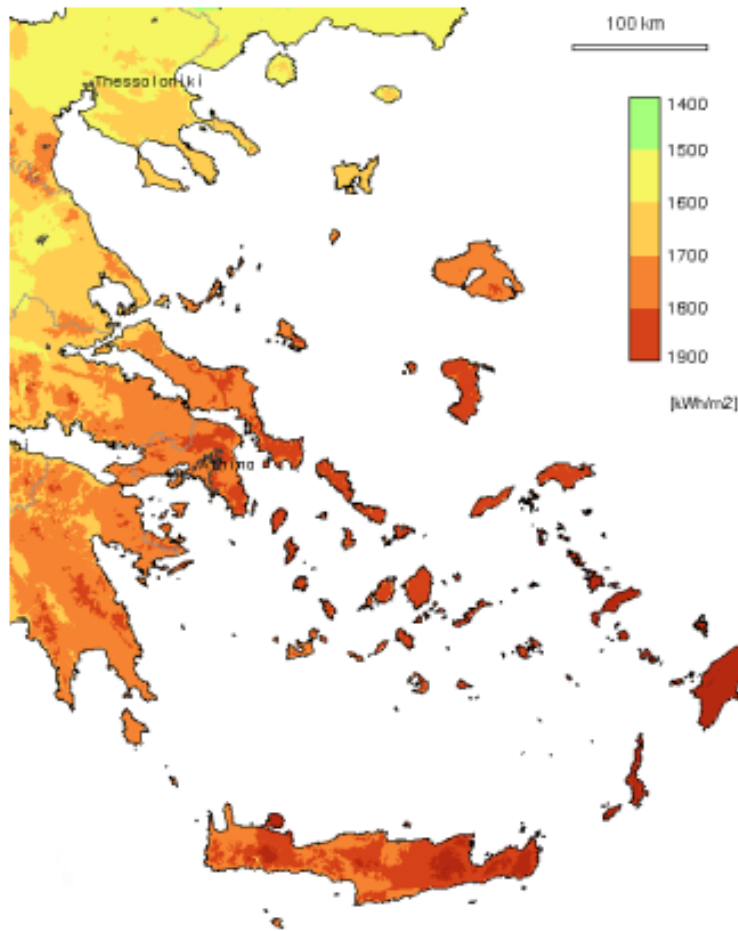
Figure 19 – Solar Potential in the Greek Islands [13]

As it is possible to notice in Figure 19, there is a very high potential in terms of solar power in Greece, which theoretically justifies the integration of solar technologies, both thermal and photovoltaic, in the plant scheme. As previously mentioned, an hourly dataset of radiation can lead to small errors in terms of evaluation of the solar potential of the location. Moreover, the selected data include cloudy days, or days in which sun does not shine at all, improving the veridicity of the simulation.

The radiation is used as input parameter to determine both the electric power production of the PV panels and the thermal power production of the ETC. Both the technologies are able to exploit the Direct Normal Radiation (DNI) and the Diffuse Radiation (DR).

As well as temperature data, radiation's data have been taken from Energy+. [33]

3 Mathematical Modeling and List of the Components.

The aim of this chapter is to introduce the system proposed, from a mathemathical point of view, providing the set of equations and the assumptions done in the simulation phase. Firstly, it will be presented the load modelling: how it will be provided heating, cooling and electricity to the dwelling, then, it will be presented how this energy demand will be covered by the CCHP system. The analysis will be carried out component by component. Equations refers to steady-state conditions, due to the off-design nature of the simulation, hence, dynamics has not been investigated. Figure 20 shows the different combinations investigated in this thesis.
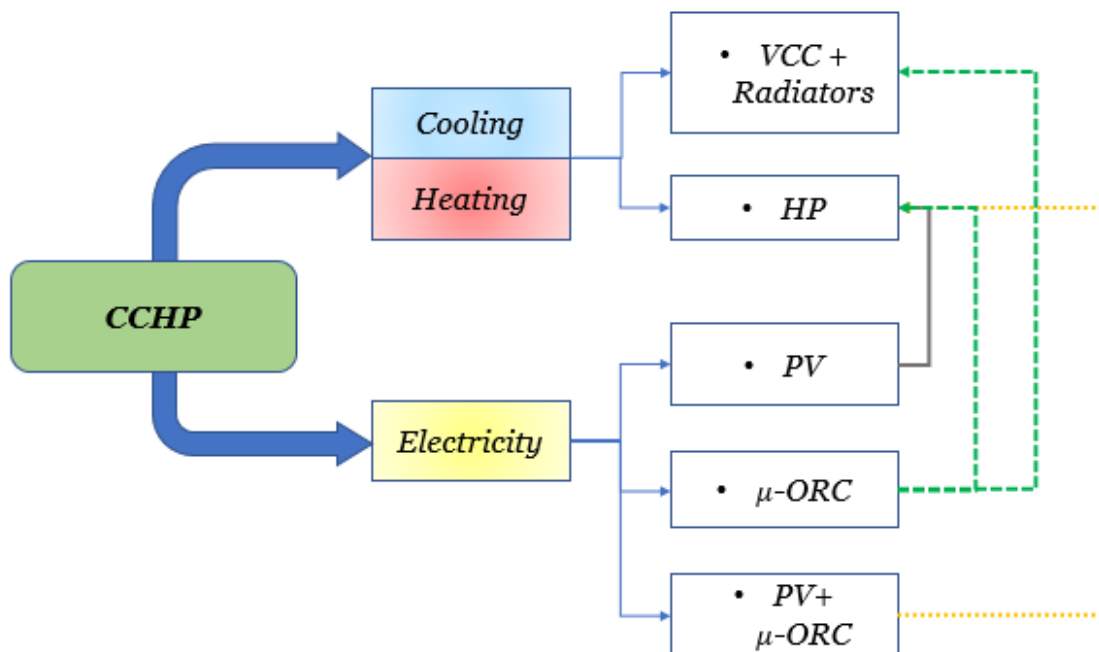
Figure 20 – Different combinations of solutions proposed in the case study.

3.1 Electricity, Space Heating and Air Conditioning

The aim of this section is to deepen the modelling of the loads: in particular, the way in which they are met. After the assessment of the amount of electricity and thermal power required to forecast the demand, it is crucial to analyse which device suite with such loads, to obtain the input to simulate the yearly simulation.

3.1.1 Electric Load

The Electric load is provided by two different engines, the first one considered is a micro ORC, which is a thermodynamic engine, suitable for small applications. The power generated at the shaft of the micro turbine is converted into AC electric power thanks to a generator with a fixed and constant efficiency, $\eta_{generator} = 0.95$. Alternatively, if PV panels have been integrated, electricity will be provided also by them. The second one considered, is a photovoltaic panels' field, that directly converts the radiation incident on the panel into DC electric power, which is subsequently converted into AC power with an inverter with a variable efficiency, function of the part load conditions, and sent to the house.

The generic equation for the hourly electric power that the two different engines should produce are, respectively:

$$Load = \frac{\sum_{i=1}^{n} appliances, i}{\eta_{generator}}$$

$$Load = \frac{\sum_{i=1}^{n} appliances, i}{\eta_{inverter}}$$

3.1.2 Space Heating

The thermal power required for space heating has been assessed in the previous chapter: now, it is crucial to focus how it will be provided. In this thesis, two solutions are proposed and investigated: radiators, and a heat pump. Radiators are a viable solution only when micro ORC is present, since the PV field is not able to produce thermal power, but only electricity. Hence, the micro ORC is studied both with radiators and heat pump, while the PV field is analysed only with the heat pump. Moreover, since HP is electrically driven, the addition of PV panels to the micro ORC have been investigated only in that scenario.

Radiators

Once it is forecasted the thermal power required in terms of W$_{th}$, the space heating model with radiators consists simply in a heat exchanger in which a mass flow rate whithdrawn from the hot storage transfers the thermal power required, then it reaches the cold storage. The mass flow rate required at the heat exchanger, namely $\dot{m}_{heating}$, is estimated with:

$$\dot{Q}_{heating} = \dot{m}_{heating} \cdot c_p \cdot \Delta T_{heating}$$

The $\Delta T_{heating}$ is considered constant, and it is the temperature difference that the heat transfer fluid experiences at the heat exchanger devoted to space heating: it is equal to the temperature difference between the hot and the cold storage. $\Delta T_{heating} = 25°C$.

Moreover, it has been considered the electric consumption to move such mass flow rate devoted to space heating. The work of the pump has been computed with:

$$\dot{W}_{aux,heating} = \dot{m}_{heating} \cdot \frac{\Delta P_{heating}}{\eta_{pump} \cdot \rho \cdot \eta_{gen}}$$

$\Delta P_{heating} = 0.5 \; bar$ and $\eta_{pump} = 0.7$ have been assumed.

Another option could have been to use the waste heat from the condenser of the ORC, but this choice would lead to a higher condensing temperature of the ORC to produce heat at an acceptable grade of temperature (radiator panels require a temperature of 60°C, floor heating 40°C, meaning that the condensing temperature should be 80-60°C), penalising the efficiency of the thermodynamic cycle, which is already penalised because of its size. In such way, the mass flow rate for space heating is produced by a combination of ETCs and biomass boiler.

Thermal losses along the pipeline are neglected.

Heat Pump – Heating Mode

The other solution proposed and analysed in this thesis is an air-air heat pump, because the availability of water was not proved for the selected location. A heat pump is a device that produces both space heating and air-conditioning, and here it is modelled its behaviour in space heating mode. The HP cycle have been modelled as a black-box: the thermodynamic cycle has not been investigated.

Since it is known a priori the heating requirement of the utility, it is possible to estimate the size of this component. Thus, the size of the heat pump is assumed to be 5kW, which is a commercial size that can cover the heating peak load estimated of 3.680 kW$_{th}$ and also the cooling peak load of 4,830 kW$_{th}$. The nominal COP for heating mode is 4.11. [34]

The COP of a heat pump is typically more dependent on ambient temperature, which affect the evaporating temperature of the cycle, with respect to part load conditions because typically the heat pumps are on-off mode. Hence, it is crucial to set up equations able to include the effects of variations of ambient temperature on the performances of the heat pump. After a literature review, a curve has been interpolated which describes the behaviour of the heat pump in heating mode as a function of ambient temperature. [35]

The equation describing the COP, heating mode, is:

$$COP_{heating} = COP_{heating,nom} \cdot (a \cdot T_{amb}^2 + b \cdot T_{amb} + c)$$

where:

- $a = 8.403 * 10^{-5} \, °C^{-2}$
- $b = 0.0391 \, °C^{-1}$
- $c = 2.108$

Then, it is computed the electric power required to operate the heat pump, thanks to the definition of the COP, considering the efficiency of the generator:

$$Pel_{HP} = \frac{Heating_{load}}{COP_{heating} \cdot \eta_{gen}}$$

Auxiliaries are included in the efficiency definition.

3.1.3 Air Conditioning

Air conditioning is a primary need for the utility considered because of the high temperature reached in the warm season. Once the cooling load in terms of thermal power have been estimated, it is crucial to compute the electric power required by the compressor, that will be considered an electric load too. The air conditioning is provided by a Vapour Compression Cycle, if space heating is provided by radiators, while it is provided by a heat pump in reverse mode, if the heat pump is considered. The air-conditioning is electrically powered by the micro ORC or by PV panels.

Heat Pump – Cooling Mode

As previously said, the hat pump is able to operate reversely and provide also air conditioning. The modelling process is the same of heating mode: the cooling COP is a function of the ambient temperature. [35]

$$COP_{cooling} = COP_{cooling,nom} \cdot (d \cdot T_{amb}^3 + e \cdot T_{amb}^2 + f \cdot T_{amb} + g)$$

where:

- $d = -4.444 * 10^{-5} \, °C^{-3}$
- $e = 0.001219 \, °C^{-2}$
- $f = 0.0131 \, °C^{-1}$
- $g = 0.8305$

$$Pel_{HP} = \frac{Cooling_{Load}}{COP_{cooling} \cdot \eta_{gen}}$$

VCC, Vapour Compression Cycle

The Vapour Compression cycle have been modelled as a black-box as well, because it is known a priori the cooling requirement of the utility, and hence it is possible to estimate the size of this component. Thus, the size of the VCC is assumed to be 5kW, which is a commercial size that can cover the peak load estimated of 4,830 W. The modelling of the VCC cycle is the same of the HP reverse way, the same COP coorelation is used to obtain the power consumption of the compressor. This decision is justified by the necessity of providing a fair comparison between the two systems. To calculate the power of the compressor, the definition has been used:

$$COP_{cooling} = \frac{Cooling_{load}}{Pel_{VCC}}$$

The nominal COP assumed is $COP_{cooling,nom} = 3.6$, the same of the heat pump.

Finally, to estimate the power requirement of the VCC, the electric power is divided by the efficiency of the generator:

$$Pel_{VCC} = \frac{Cooling_{load}}{COP_{cooling} \cdot \eta_{gen}}$$

Auxiliaries of the VCC are included in the efficiency.

From now on, Pel_{VCC} represents both the power of the VCC of air-conditioning and the power of the Heat Pump, Pel_{HP}.

3.2   Micro ORC

Here is presented an introduction to the components and the mathematical set of equations for each component that will be considered in the plant layout showed in Figure 21. In the figure, all the possible combinations are present in terms of intergration of renewables, except for the simple PV-BESS, that will be discussed in its own section.
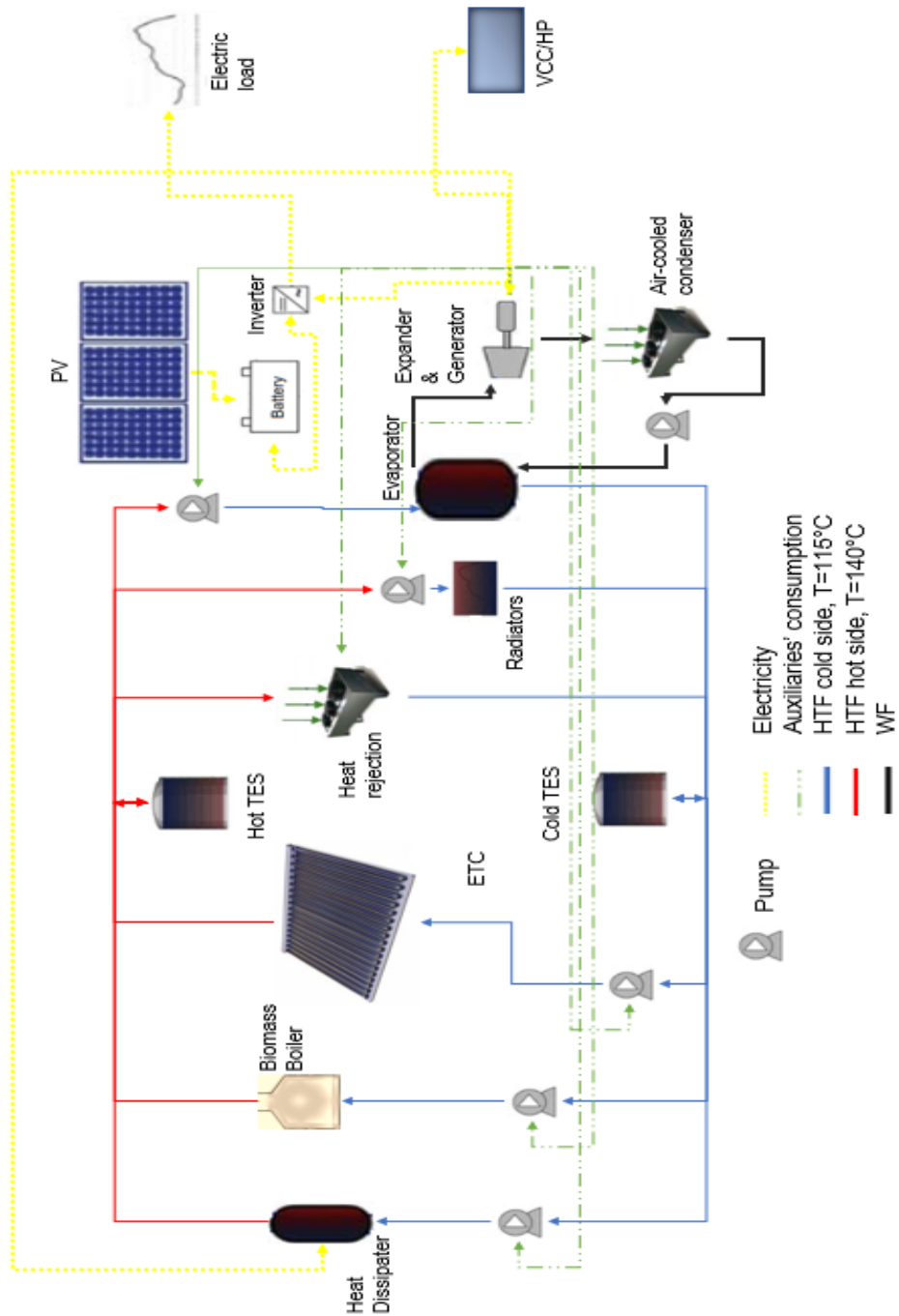
Figure 21 – Micro ORC Plant Layout

3.2.1   Micro-ORC

The micro Organic Rankine Cycle will provide the electric power required by the appliances of the house and the power for the compressor of the VCC (or HP). The micro ORC is considered as a black-box and the thermodynamic cycle has not been computed nor optimized. Neither the working fluid of the ORC has been considered.

The aim is to find an optimal size in terms of kW, because the nominal power output of the cycle is a free parameter of the case study, and it can be designed according to the integration with the other components. The operating condition of the cycle have been assumed in the range of [20-110] % of the nominal power, meaning that the ORC can not produce less than the lower bound and more than the upper one. In the first case, ORC operating at minimum load, namely $ORCmin$, the surplus of electric power must be stored or rejected: it can be stored in the BESS, or, alternatively, if not considered, a mass flow rate from the cold tank is withdrawn, heated up with an electric dissipator, and sent to the hot tank. In the second case, ORC operating at maximum load, namely $ORCmax$, if the engine is not able to produce the electric power required, hence, the BESS tries to cover the unmet load, if there is not enough charge, or they aren't present, an unmet load occurs.

$$ORC_{min} = 20\% \; ORC_{nom}$$

$$ORC_{max} = 110\% \; ORC_{nom}$$

The production requires a heat input which is provided by a combination of the biomass boiler, the solar field and the thermal storage, according to the degree of integration and the control strategy, that will be further explained in the description of each component. The heat production requires auxiliaries which are powered by the ORC too.

The scheme of the control strategy is presented in Figure 22.
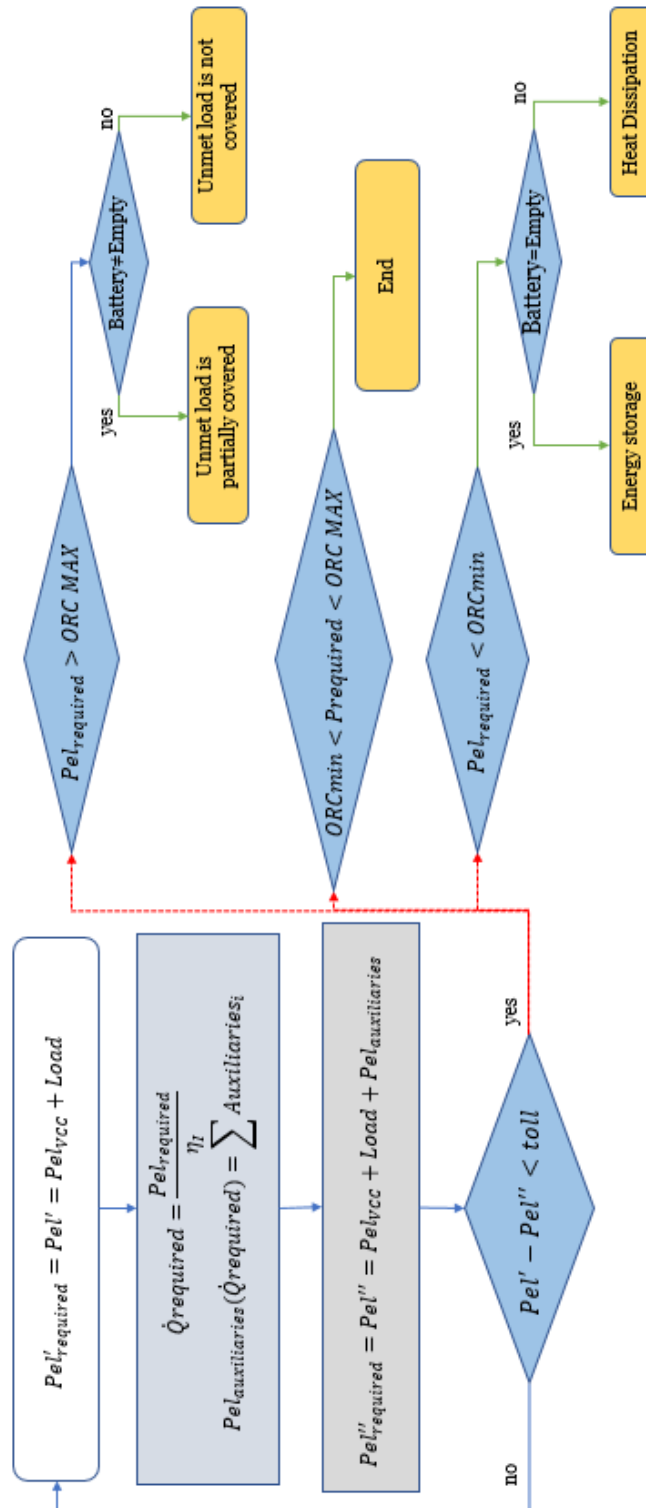
Figure 22 – The flow chart represents the control strategy of the micro ORC and the macro-scenarios occurring according to its functioning.

Assumptions

- $\eta_{generator} = 0.95$, constant [37]

- $\eta_{pump} = 0.7$, constant

- $\eta_{II,nominal} = 0.5$ [37]

- Air-condensed with ambient air, $\Delta T_{pinch} = 15°C, \Delta T_{air} = 5°C$, constant

- $Teva_{in} = 140\,°C, Teva_{out} = 115\,°C \rightarrow \Delta T_{eva} = 25\,°C$, constant

- $\Delta P_{eva} = 0.5$ bar, constant [37]

- Second law efficiency includes auxiliaries of the Organic Rankine Cycle

Efficiency

The power required by the utility is given by:

$$Pel_{required} = \frac{Load + Pel_{VCC} + Pel_{auxiliaries}}{\eta_{gen}}$$

or Pel_{HP} instead of Pel_{VCC} if the heating and cooling is provided by the heat pump. *Load* is the electric load of the house, Pel_{VCC} is the power required by the VCC compressor, and $Pel_{auxiliaries}$ is the electric work required to operate the thermal production loop. The term $Pel_{auxiliaries}$ will be further discussed in every section dedicated to the components of the plant.

The first principle efficiency is evaluated with the production between the second law efficiency and the Lorentz efficiency. The second law efficiency is a function of the load of the Organic Rankine Cycle, while the Lorentz efficiency is a function of the ambient temperature. In such way, it is possible to have an accurate estimation of the first principle efficiency, which involves the different operating conditions that the cycle have to deal with.

The condensing temperature at each condition is required to compute the Lorentz's efficiency:

$$Tcond_{air} = T_{amb} + \Delta T_{air} + \Delta T_{pinch}$$

$$\eta_{Lorentz} = 1 - \frac{Tcond_{air}}{\Delta TML_{eva}}$$

The second law efficiency have been interpolated from a publication of Turboden®, a Mitsubishi® company, which is one of the world leader's of designing, manufacturing and maintaining Organic Rankine Cycles. [38] In the publication, a curve of second law

efficiency-nominal efficiency ratio as a function of the percentage of load is provided, and the interpolation is computed with the aid of Matlab®:

$$\frac{\eta_{II}}{\eta_{IInom}} = \frac{a \cdot P + b}{P^2 + c \cdot P + d}$$

where:

- $a = 15.41$
- $b = -0.2654$
- $c = 12.64$
- $d = 1.566$
- $P = \frac{Power\ output}{ORCnom}$

An efficiency map has been drawn to better comprehend the trend of the efficiency as a function of ambient temperature and percentage of load, available in Figure 23. It is possible to visualize the influence of the ambient temperature, which, as previously mentioned, affects negatively the performance of the cycle increasing the condensing temperature, resulting in a lower power at the shaft of the micro turbine.
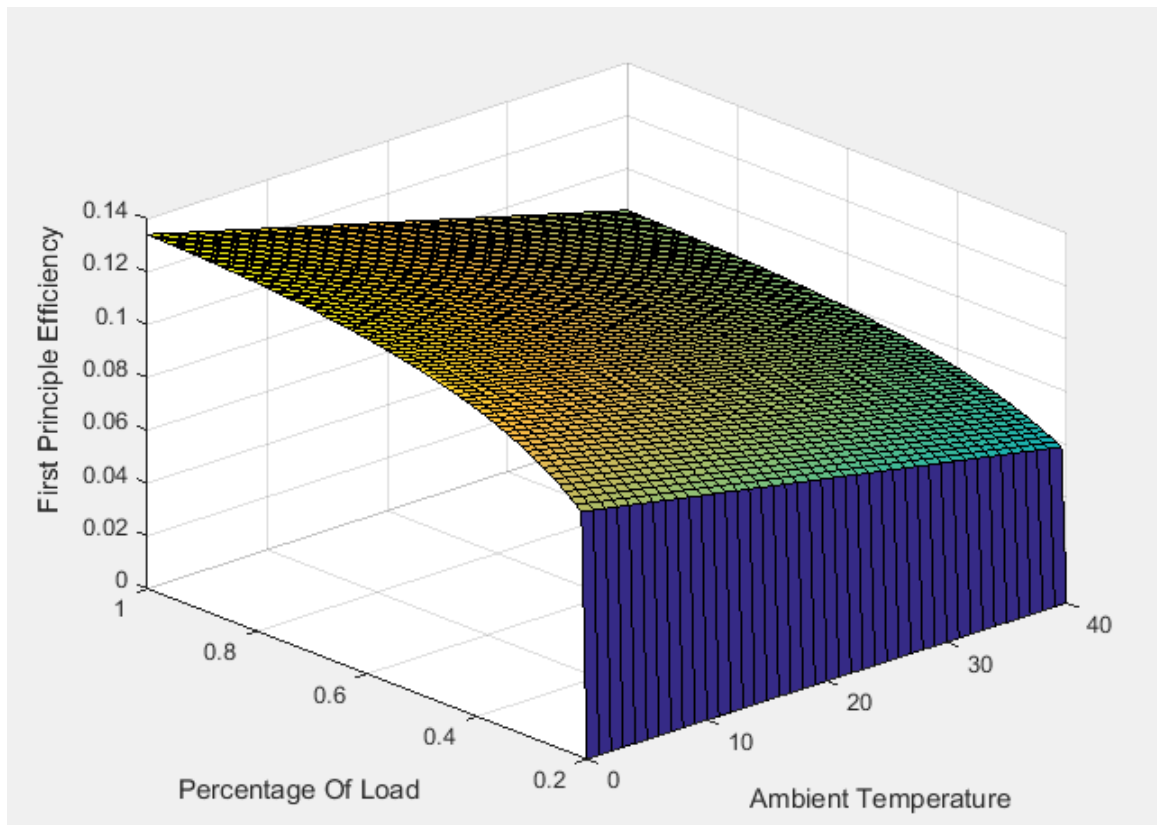
Figure 23 – First Principle Efficiency Chart

The heat input that must be provided to the cycle is computed according to the first principle efficiency definition and reversing the formula:

$$\eta_I = \frac{Pel_{required}}{\dot{Q}_{req,ORC}}$$

The mass flow rate required for power production, since the set of temperatures of the evaporator is fixed, is just:

$$\dot{m}_{req,ORC} = \frac{\dot{Q}_{req,ORC}}{c_p \cdot (Teva_{in,HTF} - Teva_{out,HTF})}$$

As previously mentioned the mass flow rate required at the evaporator is provided by different mix, according to the availability of solar collector, thermal storage and biomass boiler. The general equation is:

$$\dot{m}_{req,ORC} = \dot{m}_{ava} + \dot{m}_{storage} + \dot{m}_{boiler}$$

Evaporator

The evaporator of the ORC is modelled as a heat exchanger, which is the interface between the heat production loop and the ORC loop. The auxiliaries of the evaporator involve a pump that moves the hot stream across the evaporator. The work of the pump is computed as follows:

$$\dot{W}aux_{eva} = \frac{\dot{m}_{req,ORC} \cdot \Delta P_{eva}}{\rho \cdot \eta_{pump} \cdot \eta_{gen}}$$

Electricity dissipater

An electricity dissipater has been proposed as a safety measure, for those scenarios in which the batteries are completely full or not considered, and the ORC is operating at its minimum, leading to electric power rejection. Rejection is mandatory, because the plant is off-grid, meaning that no energy can be exchanged outside of the plant. This component has been modelled as a box in which a mass flow rate whitdrawn from the cold sink flows and get heated up thanks to a hot electric resistence. Then, is sent to the hot tank.

$$ORCmin - Pel_{required} = Pel_{diss}$$

The mass flow rate must be moved from the cold sink to the hot sink and heated up, hence a part of the surplus power is used to move it and another part to heat it up. The mass flow rate is computed reversing the formula:

$$Pel_{diss} = \dot{m}^{\leftarrow}{}_{storage} \cdot [c_p \cdot (T_{hot,storage} - T_{cold,storage}) + \frac{\Delta P_{dissipater}}{\rho \cdot \eta_{pump}}]$$

The ΔP of the dissipater is assumed 0.5 bar, the same of the evaporator, and the efficiency of the pump is assumed equal to 0.7.

Cost

The cost of the micro ORC has been estimated with a correlation [37]:

$$Cost_{ORC} = 5000 \cdot \left(\frac{Size_{ORC}}{1000}\right)^{0.7}$$

Where:

- Size ORC is the rated power output in nominal condition of the ORC.
- $5000 \frac{€}{kW}$ is the specific cost of the ORC.
- 0.7 is the scale factor.

The operating and maintenance cost are evaluated as follows, and they include insurance and maintenance. [39]

$$O\&M = 0.05 \cdot Cost_{ORC}$$

3.2.2 Biomass boiler

The biomass boiler is devoted to the production of the hot stream that flows in the evaporator of the Organic Rankine Cycle. The biomass boiler has been included in the case study because it is a crucial component that allows continuous operation, and, in peak load scenario, has a very low inertia with short response time. The selection of a biomass boiler is due to the access to biomass in a rural context, the purpose of running with pure renewables, and the compactness and easiness of installation of such component, which is experiencing year by year a process of standardization thanks to the increased demand for biomass worldwide. [40]

The nominal size of the boiler is assumed a priori, because it must be large enough to cover the energy demand in whatever situation. The nominal thermal power of the biomass boiler is selected based on the maximum energy demand:

$$\dot{Q}_{boiler,nom} = \max\left(\frac{\max(Pel_{VCC}) + \max(Load)}{\eta_{I,nom}}, \max\left(Heating_{load} + \frac{\max(Load)}{\eta_{I,nom}}\right)\right) = 35kW$$

Assuming a security factor of 10%, the closest size available on the market is $40kW$. After each simulation it is ensured that the maximum thermal power requirement is lower than the capacity of the boiler.

The biomass boiler has a range of operating conditions, as well as the Organic Rankine Cycle, meaning that there is a minimum and a maximum in terms of thermal Power output. The minimum can be set at the beginning of the simulation, while the maximum is the size of the boiler itself, because according to the off-grid nature of the plant, the boiler is sized on the peak value of thermal power required. The minimum of a biomass boiler is usually the 20-30% of the nominal capacity, hence it is not possible to set it with a lower value.

$$\dot{Q}_{boiler,min} = min_{boiler} * \dot{Q}_{boiler,nom}$$

The boiler must provide the hot stream required at the evaporator by the ORC and the one required by the heat-exchangeer for space heating, if present.

$$\dot{m}_{req} = \dot{m}_{heating} + \dot{m}_{req,ORC}$$

If ETCs are considered, it is considered as a back-up: in fact, the mass flow rate of the boiler is, in general given by:

$$\dot{m}_{boiler} = \dot{m}_{req} - \dot{m}_{ava} - \dot{m}_{storage}$$

Which means that first it is used the hot stream from the collectors, namely $\dot{m}_{ava}$, then the storage is emptied, and then is turned on the boiler.

If the solar field is not considered:

$$\dot{m}_{boiler} = \dot{m}_{req} - \dot{m}_{storage}$$

If also the storage is empty, the mass flow rate of the boiler is computed as:

$$\dot{m}_{boiler} = \dot{m}_{req}$$

Hence, it is switched on when the mass flow rate produced by the solar field – if present - and the mass stored in the hot tank is not enough to meet the demand. If this value is lower than the minimum set, the surplus is stored in the hot sink.

$$\dot{m}_{boiler,min} = \frac{\dot{Q}_{boiler,min}}{c_p \Delta T_{eva}}$$

$$\dot{m}_{surplus} = \dot{m}_{boiler,min} - \dot{m}_{boiler}$$

Assumptions

- $\eta_{boiler,nom} = 0.91$ [41]
- $LHV_{biomass} = 17\frac{MJ}{kg}$ [40]
- $\Delta P_{boiler} = 0.102 \ bar$, constant [42]
- $\eta_{pump} = 0.7$, constant
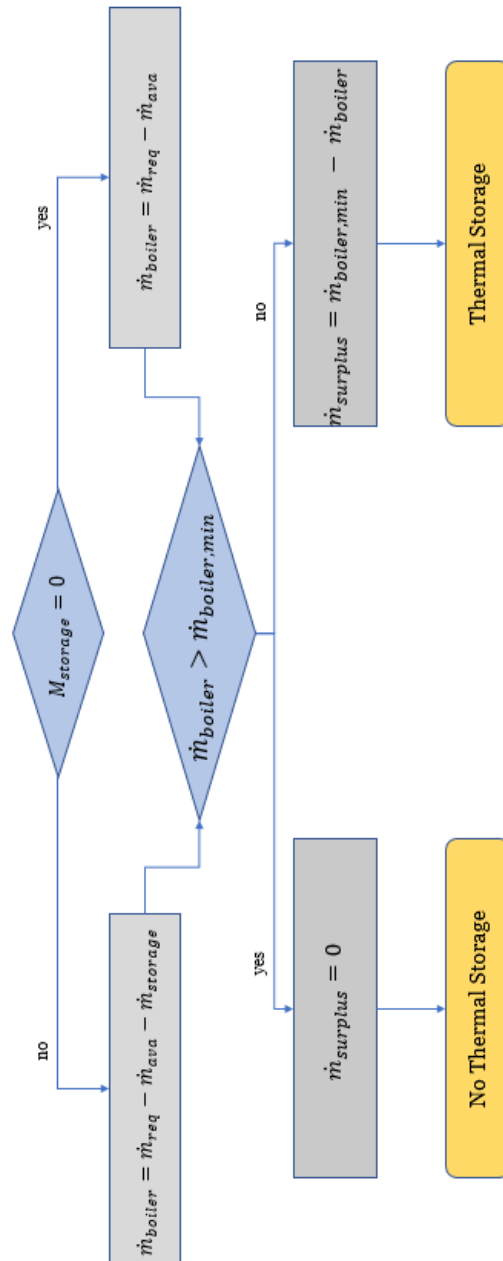
Figure 24 – The Flow Chart represents the control strategy of the component.

Equations

The thermal power is calculated starting from the mass flow rate computed, as shown in the flow chart of Figure 24.

$$\dot{Q}_{boiler} = \dot{m}_{boiler} \cdot c_p \cdot \Delta T_{eva}$$

Where ΔT_{eva} is the temperature difference across the evaporator.

Efficiency

The efficiency of the boiler is not considered constant, since it is well known that varies according to the thermal load and the inertia of the components. In particular, it is crucial to model this component in his off-design conditions because part load operations will happen often, since the thermal and electric load are highly fluctuating along both the day and the year. Moreover, because of the stand-alone nature of the plant, the size of the boiler would be set closer to peak load to avoid unmet thermal load, thus leading to yearly operating conditions closer to the lower bound. This operating conditions can result also in poor efficiency, based on fuel consumption, with values of 67%. [41]

The partial-load efficiency correlation has been interpolated with Matlab® from a test-case of a 12 kW biomass boiler [41], which belongs to the same order of magnitude of the size of the plant's boiler. The best fitting option results to be an exponential curve with two items (R-square=99%), as suggested by the shape and by the case study considered.

The interpolation is expressed by the formula:

$$\eta_{boiler} = a \cdot \exp(b \cdot B) + c \cdot \exp(d \cdot B)$$

Where:

- $a = 0.8952$
- $b = 0.1118$
- $c = -0.897$
- $d = -11,23$
- $B = \dfrac{\dot{Q}_{req}}{\dot{Q}_{boiler,nom}}$

Fuel Consumption

The fuel consumption is computed starting from the definition of efficiency of the boiler.

$$\dot{m}_{fuel} \cdot LHV_{biomass} \cdot \eta_{boiler} = \dot{Q}_{boiler}$$

Pressure Drop in the Boiler

The pressure drop in the boiler is assumed constant. The work of the pump that moves the hot stream is computed by:

$$\dot{W}_{aux,boiler} = \frac{\dot{m}_{boiler} \cdot \Delta P}{\rho \cdot \eta_{pump} \cdot \eta_{gen}}$$

Cost

The cost of the biomass boiler have been estimated with the IEA correlations for cooling and heating systems. [43]

$$Cost_{boiler,specific} = 2231 \cdot (size_{boiler})^{-0.488}$$

$$Cost_{boiler,auxiliaries} = 0.05 \cdot Cost_{boiler,specific}$$

$$Cost_{boiler,tot} = Cost_{boiler,specific} \cdot (size_{boiler}) + Cost_{boiler,auxiliaries}$$

In these correlations, there is a specific cost decreasing with the size of the boiler that must be multiplied for the size itself to obtain the cost of the item. The size is expressed in kW.

$$O\&M_{boiler} = 0.032 \cdot Cost_{boiler,specific} + 3.8 \cdot Energy_{boiler}$$

The Operating & Maintenance costs have a fixed part related to the size of the item, and a second one variable, that changes according to the energy produced by the boiler along the year. They include insurance and maintenance. The energy is expressed in MWh. [44]

The boiler employs biomass as a fuel, and the specific cost of biomass is:

$$Cost_{fuel,spec} = 0.2 \frac{€}{kg} \ [45]$$

While the yearly cost of fuel is computed starting from the mass flow rate of fuel consumed:

$$Cost_{fuel} = \sum_{i=1}^{8760} \dot{m}_{fuel,i} \cdot Cost_{fuel,spec} \cdot 3600$$

3.2.3 Evacuated Tube Collectors

Evacuated Tube Collector are investigated to evaluate the benefits they could carry on. Only ETCs have been considered in this study because of the already developed market

of solar collector in Greece, so, they have been preferred with respect to concentrated devices such as PTC because it is a well-known technologies and local manufacturers or technicians can be easily found, reducing the burden of maintenance. They have a very quick and easy installation procedure, even easier than that of Flat Plate Collectors (FPC), thanks to their lightness and plug-and-play design. Moreover, from a technical perspective, flat plate collectors are not suitable for power production purposes because of the low operating temperature, the typical maximum temperature of a FPC is up to 80°C. In fact, the cylindrical geometry of the evacuated tube allows them to collect more solar power at almost whatever angle of incidence thanks to their capability of self-tracking the sun guaranting a high yearly yield.

In the model proposed, the aperture area of the panel is a free parameter, i.e. the receiving surface, and it will be investigated if there is a trade-off between the biomass consuption and the area of the evacuated tube collectors.

The solar collectors are used to provide a hot stream, $\dot{m}_{ava}$, that will be immediately consumed by the utility if it is lower than the requirement, while it will be stored in the hot tank if it larger than the requirement, as in Figure 25.
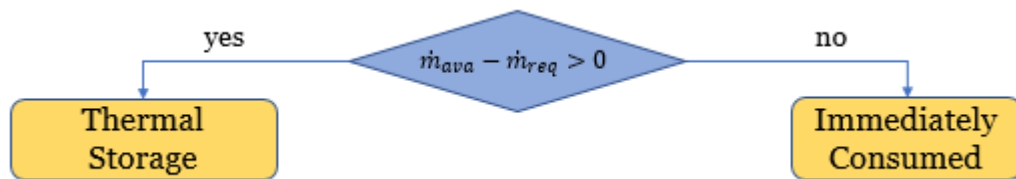
Figure 25 – The Flow Chart represents the simple control strategy of the collectors.

Assumptions

- No thermal losses in the pipeline, $Tcoll_{in} = 115°C, Tcoll_{out} = 140°C \rightarrow \Delta Tcoll = 25°C$, constant
- Pressure drop proportional to the mass flow rate
- No shadings are affecting the solar field
- Clear Sky Model
- Albedo, or ground reflectivity $\rho = 0.2$.
- Constant thermodynamic properties of the heat transfer fluid in the selected temperatures interval
- $\eta_{pump} = 0.7$, constant

Collector's Selection The ETC selected is the Thermomax DF100, thanks to its high efficiency range of performances and the high stagnation temperature, previously investigated by [30].

Here are briefly presented its main characteristics:

Table 2 - The efficiency's coefficient are referred to the Aperture Area [46]

Solar Collector	*Thermomax DF 100*
Aperture Area	3.23 m^2
Gross Area	4.25 m^2
η_0	0.781
a1	1.44 W/K/ m^2
a2	0.0062 W/K/ m^2
Nominal Flow Rate	250 l/h
Maximum Pressure	8 bar
Maximum Flow Rate	480 l/h
Heat Transfer Fluid	Water-Glycole Mixture

The efficiency of the collector is computed with the following formula:

$$\eta_{coll} = \eta_0 - a_1 \frac{\left(Tcoll_{average} - T_{amb}\right)}{G_i} - a_2 \frac{\left(Tcoll_{average} - T_{amb}\right)^2}{G_i}$$
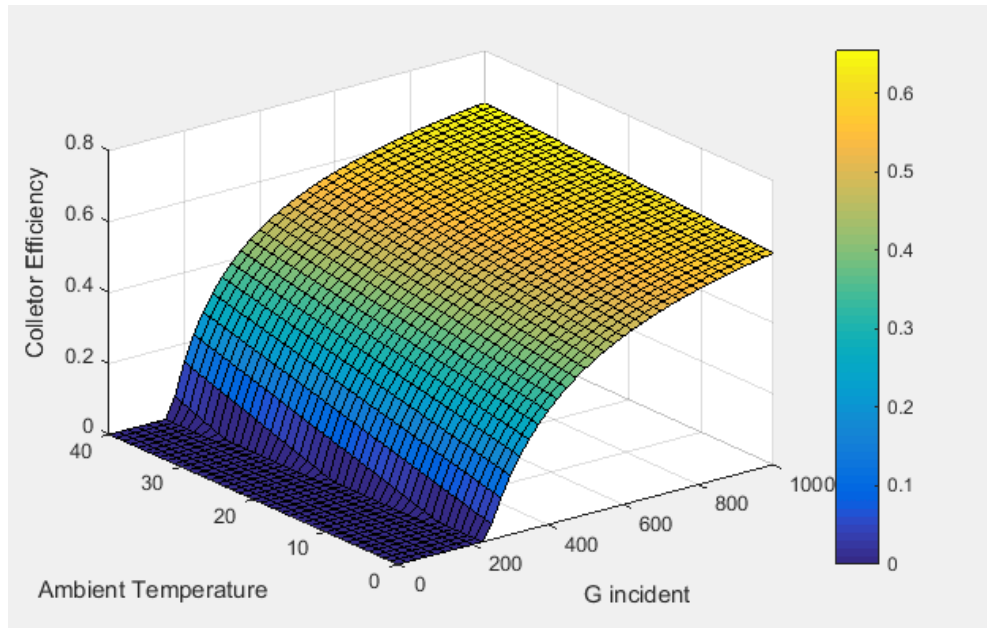
Figure 26 – Efficiency Curve of the solar Collector as a function of Ambient Temperature and incident Radiation

Where T_{af}, T_{amb} are the average temperature of the fluid in the collector, computed as a mathematical average, and the ambient temperature respectively; G_i is the incident radiation on the collector's surface. η_0 is the coefficient that includes optical losses, while a_1, a_2 are the coefficients that consider the thermal losses towards the ambient.

From the efficiency map of Figure 26, it is possible to notice that ETCs have a minimum radiation, approximately $200 \frac{W}{m^2}$, that activate them, leading to an efficiency larger than zero. Below that threshold thermal power is not produced.

Orientation The collector has been installed South-oriented with a tilt angle of 35°, namely β, which has been demonstrated to be the optimum in such climate region. In Greece in fact, the optimum tilt angle ranges between 35° to 39°, in the northern regions, such as Trace. [47] The zenith angle and the cosine of the angle of incidence, respectively $\theta_z, \cos\theta$, have been calculated on hour basis with the aid of SolPos online software [48], that requires as input:

Table 3 - Input parameters for the calculation of incidence angle's cosine

Latitude	37°44'
Longitude	23°44'
Time Zone	+2 UTC
Tilt Angle	35°
Azimuth Angle	0°

The incident solar power that the ETC is hourly experiencing is computed by the formula:

$$G_i = G_D \cdot \frac{1 + \cos\beta}{2} + \rho G \cdot \frac{1 - \cos\beta}{2} + (G - G_D) \cdot \frac{\cos\theta}{\cos\theta_z}$$

Where G_i is the incident radiation, G_D is the diffuse radiation, ρ is the albedo, that has been assumed equal to 0.2.

Operating Temperatures The operating temperatures of the solar array, the inlet and outlet temperatures, are fixed and no thermal losses are assumed in the pipeline. This two crucial parameters have been fixed according to a literature review, in particular it have been demonstrated that, in a climate zone such as the Greek one, the solar-to-electric peak efficiency for ETC that drive a small scale ORC is reached when the inlet temperature of the fluid belongs to the range [95-150] °C. [29] Hence, the set of temperature is assumed as the following:

Table 4 - Operating Temperatures of the collectors

Temperature Set of Solar Collectors	
T_{inlet}	115 °C
T_{outlet}	140 °C
$T_{average}$	127,5 °C

Heat Transfer Fluid The selected heat transfer fluid for the heat production loop is a water-glycole mixture, 20% of glycole and 80% of water. Although it is well-known and abundantly discussed how much is important the fluid selection for such applications, some considerations have been proposed in order to justify such choice:

- The manufacturer of the collectors suggests such heat transfer fluid.
- It shows good thermodynamic properties in the temperature range investigated, in particular a very high Cp compared to the other organic compounds thanks to the high presence of water.
- It is a very common heat transfer fluid for solar thermal collectors and can be easily replaced after its depletion.

Here are presented some thermodynamic properties of the selected fluid:

Table 5 - Thermodynamic Properties in the selected range of temperatures, source: Refprop

Thermodynamic Props in the [115-140]°C	
Vapour Pressure	0,53 - 2,29 bar
Cp	3970 - 4026 J/kg/K
ρ	994 - 982 kg/m^3
Cp$_{average}$	3998 J/kg/K
ρa$_{verage}$	988 kg/m^3

An average of this values is assumed to perform the calculations, those properties have been calculated at T_{ave}.

Moreover, since the maximum operating pressure of the collector is 8 bars, the fluid can be easily managed to avoid its vaporization and riskful operations.

Equations

Since no thermal losses are assumed in the pipeline, the governing equation of heat transfer in the solar field is

$$\dot{Q}_{ava} = G_i * A_{collectors} * \eta_{coll} = \dot{m}_{ava} * c_p * (Tcoll_{out} - Tcoll_{in})$$

The mass flow rate flowing in the solar field available from the solar radiation is calculated reversing the above-mentioned formula. A valve is put before the entering of the solar field in order to avoid reaching the maximum mass flow rate and also to provide the correct amount of mass flow rate.

The hot stream produced will cover the heat requirement of the ORC, if it is more than the required one, it is stored in the hot tank.

Pressure Drops in the Solar Field

A variable-speed pump is employed to move the mass flow rate flowing in the solar field. The pressure losses of the system are proportional to the flow rate of the collector, expressed in liter per minute. Once the calculation of the mass flow rate available has been performed, the mass flow rate in liters per minute is computed, and thanks to an interpolation of values it is possible to draw the pressure drop chart as a function of the mass flow rate. Since no pressure drop chart specific to the collector selected is available in literature, it has been interpolated from another evacuated tube collector datasheet with similar dimensions and same heat transfer fluid as in Figure 27. [49]
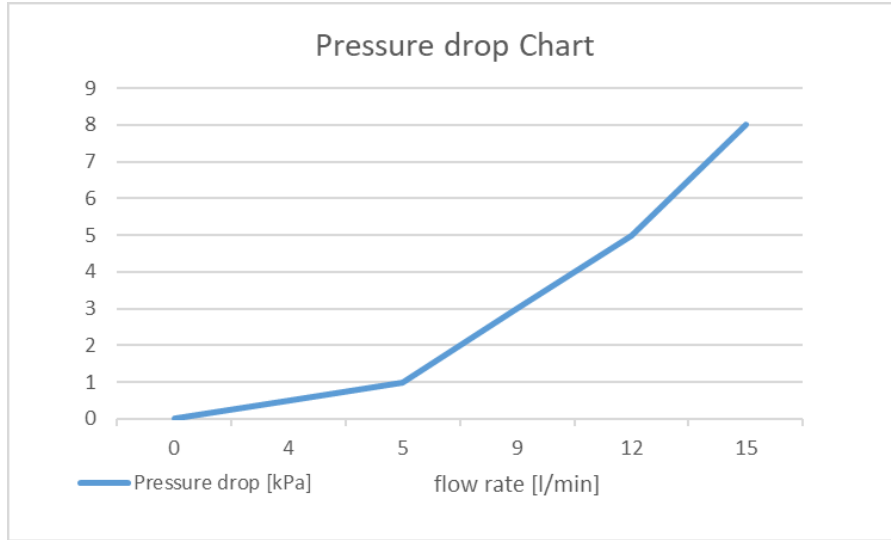
Figure 27 – Pressure Drop chart as a function of the volume flow rate.

Then, the work of the pump of the solar field is calculated as follows:

$$\dot{W}aux_{SF} = \frac{\dot{m}_{ava}}{\rho} \frac{\Delta P_{solar\ field}}{\eta_{pump} \cdot \eta_{gen}}$$

Cost

The cost of the evacuated tube collector is extremely variable according to literature and manufacturer datasheet. Some authors claim specific cost extremely low, for example in China, were the market is largely developed, others are more cautious. Two different correlations have been considered to take into account this discrepancy: the first one is given by IEA [43], and the second one is taken from a study that involve ETCs for power production purpose with a micro ORC. [50]

IEA correlation: $Cost_{ETC,specific} = 760.59 \cdot (Aperture_{area})^{-0.135}$

$$Cost_{ETC,auxiliaries,specific} = 5500 \cdot (Aperture_{area})^{-0.696}$$

$$Cost_{ETC,tot} = Cost_{ETC} \cdot Aperture_{area} + Cost_{ETC,auxiliaries} \cdot Aperture_{area}$$

Freeman Correlation: $Cost_{ETC,specific} = 146.25 \frac{€}{m^2}$, which includes auxiliaries' cost.

$$Cost_{ETC,tot} = Cost_{ETC} \cdot Aperture_{area}$$

As it is possible to see the two correlations are very different in terms of order of magnitude: $1m^2$ is evaluated approximately 1000 € according to IEA, on the other hand, the cost is approximately 150 €, according to the other case study. Moreover, the cost of

ETCs is very important because the energy gain given by them results in savings in terms of biomass: meaning that the higher the cost of the ETCs, the lower the chance that they get employed with respect to the biomass boiler, if the price of biomass is low.

The Operating and Maintenance cost, including insurance and maintenance are evaluated with the IEA correlation for both cases:

$$O\&M_{ETC} = 0.05 * Cost_{ETC,specific}$$

3.2.4   TES, Thermal Energy Storage

The thermal energy storage consists in two tanks, one for the low temperature fluid storage, the other for the hot temperature one. The volume of the tanks is as well a free paramenter, that must be carefully sized, considering not only the electric profile but also the heating load (If radiators are considered). The two thermal storages are modelled as black boxes with constant temperature and no thermal losses towards the ambient. The two reservoirs do not require auxiliaries for fluid pumping because pressure drop caused by them are not considered.

The hot storage fills up whenever there is an over production from the solar field, or, the boiler is working at its minimum, but the thermal input required is lower than its minimum. For sake of simplicity, $\dot{m}_{storage}^{\leftrightarrow}$ will refer only to the hot storage, as well as for the following expressions. In the meanwhile, the cold storage is experiencing the specular of the hot one.

$M(i)$ represents the actual capacity in kilograms of the storage, $M(i + 1)$ represents the level of the TES in the following hour of simulation.

$$\dot{m}_{storage}^{\leftarrow} = (\dot{m}_{ava} - \dot{m}_{req} - \dot{m}_{heating})$$

or, alternatively

$$\dot{m}_{storage}^{\leftarrow} = (\dot{m}_{surplus})$$

During the discharge phase, if it is full, or partially full, the storage release as much hot fluid as much is required at the evaporator.

$$\dot{m}_{storage}^{\rightarrow} = (\dot{m}_{ava} - \dot{m}_{req} - \dot{m}_{heating})$$

If ETCs are not considered the mass exiting the storage is:

$$\dot{m}_{storage}^{\rightarrow} = \dot{m}_{req} + \dot{m}_{heating}$$

Or, if the amount of hot fluid is not enough within the storage, it releases all the capacity:

$$\dot{m}_{storage}^{\rightarrow} = \frac{M(i)}{3600}$$

Mass flow rate of the storage is considered positive when entering and negative when exiting the storage.

Thuis equations can be visualised in the flow chart of the TES in Figure 28.
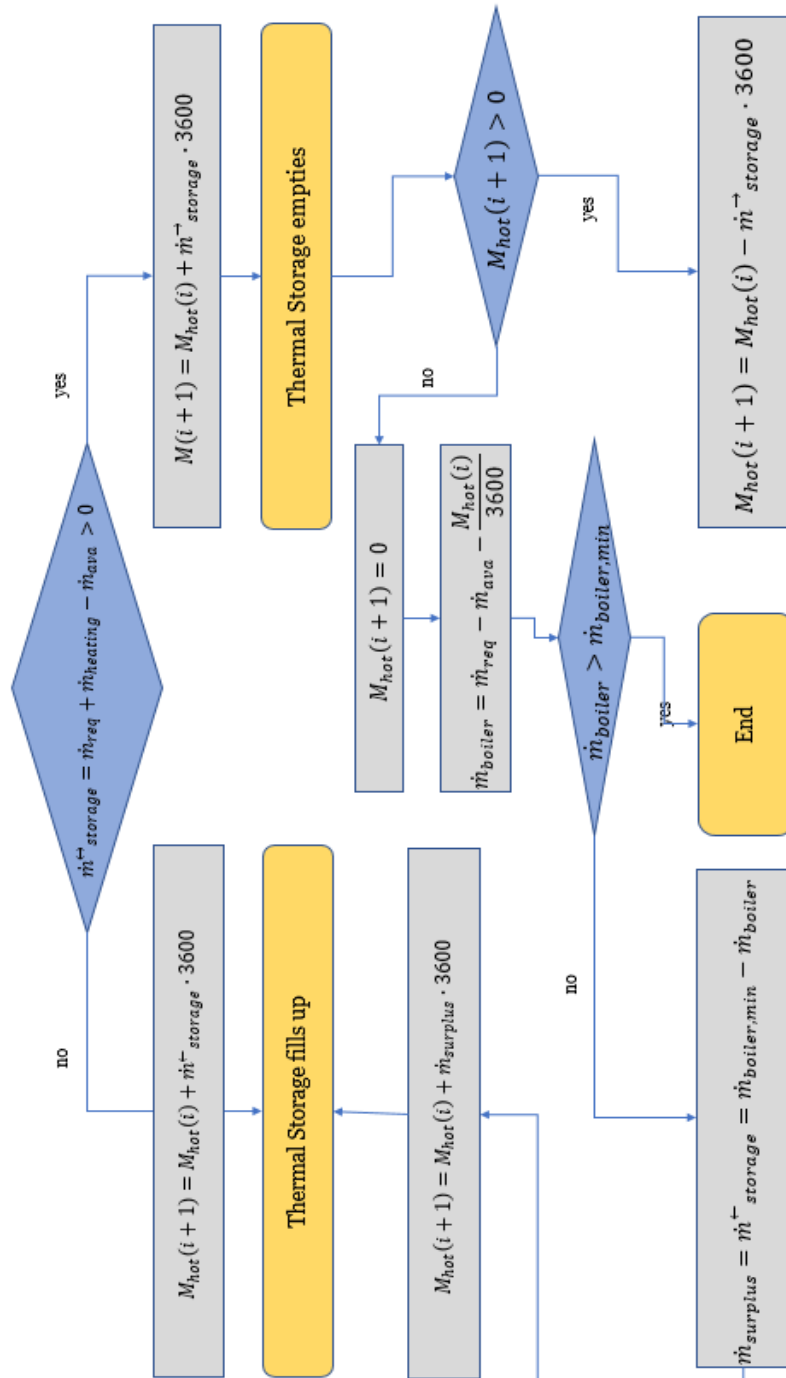
Figure 28 – The Flow Chart represents the control strategy of the TES. As it is possible to notice, two different ways of charging are set.

Assumptions

- No thermal losses towards the ambient, i.e. constant temperature profile within the storage
- No pressure drops introduced by the tanks
- $\Delta T_{air} = 25\,°C$, constant
- $\rho_{air} = 1.184\,\frac{kg}{m^3}$, constant
- $\Delta P_{air} = 0.05\,bar$, constant
- $\eta_{fan} = 0.8$, constant

Equations

The TES are modelled with a simple mass balance. A mass flow rate enters the hot storage when there is a surplus of heat production with respect to the heat input required by the ORC's evaporator, or, alternatively, when the boiler is working at its minimum. A mass flow rate gets out from the storage when it is required for heating purpose (in the case of radiator panels) and for power production.

$$M(i+1) = M(i) + \dot{m}^{\leftrightarrow}_{storage} \cdot 3600$$

It is calculated also the mass variation across two consequent hours to perform a global energy balance in the end.

$$\Delta M = M(i+1) - M(i) = \dot{m}^{\leftrightarrow}_{storage} \cdot 3600$$

$$\Delta Q_{storage} = \Delta M \cdot c_p \cdot (T_{sto,hot} - T_{sto,cold})$$

Where M is expressed in kilograms, and "i" is the time step, i.e. 1 hour.

Table 6- Temperature of the Thermal Storages, constant and with no thermal losses

Temperature Set of TES	
Tstorage_{hot}	140 °C
Tstorage_{cold}	115 °C

Heat Rejection

An air-cooled heat exchanger has been also modelled and included in the plant layout. Firstly, it is suggested by the manufacturer in the datasheet, also is a safety measure to prevent uncomfortable situation of over-production with a saturated hot tank. Hence, the heat exchanger is switched on whenever the tank is saturated and can not store more hot heat transfer fluid. Two different situations may arise: the first one is the over production of the solar field that leads to the need of rejecting a part of the hot stream. The second one arises when the boiler is switched on and works at its minimum, but the surplus mass flow rate can not be stored in the tank because it is saturated. The mass flow rate is cooled down and directly sent to the cold storage. The paragraph can be easily understood looking at the Figure 29.

The equations for heat rejection are:

$$\dot{m}_{rejected} = \dot{m}_{ava} - \dot{m}_{req} - \dot{m}^{\leftarrow}{}_{storage}$$

If there is an over production from the solar field.

$$\dot{m}_{rejected} = \dot{m}_{surplus} - \dot{m}^{\leftarrow}{}_{storage}$$

If there is a surplus given by the boiler working at its minimum.

$$\dot{Q}_{rej} = \dot{m}_{rejected} \cdot c_p \cdot (T_{sto,hot} - T_{sto,cold})$$

The auxiliary's consumption due to heat rejection is expressed by the formula:

$$\dot{W}_{aux,fan} = \frac{\dot{Q}_{rej}}{c_{p,air} \cdot \Delta T_{air}} \cdot \frac{\Delta P_{air}}{\eta_{fan} \cdot \eta_{gen} \cdot \rho_{air}}$$

The typical auxiliaries' consumption for air-cooled heat exchangers devoted to heat rejection is $0.045 \frac{kW_{el}}{kW_{th}}$, if the calculation neglects density and temperature effect on air.[51] According to the assumption made on the pressure loss of the air, the value computed is consistent with this value:

$$\frac{\dot{W}_{aux,fan}}{\dot{Q}_{rej}} = \frac{\Delta P_{air}}{\eta_{fan} \cdot \eta_{gen} \cdot \rho_{air}} \cdot \frac{1}{c_{p,air} \cdot \Delta T_{air}} = 0.05 \frac{kW_{el}}{kW_{th}}$$
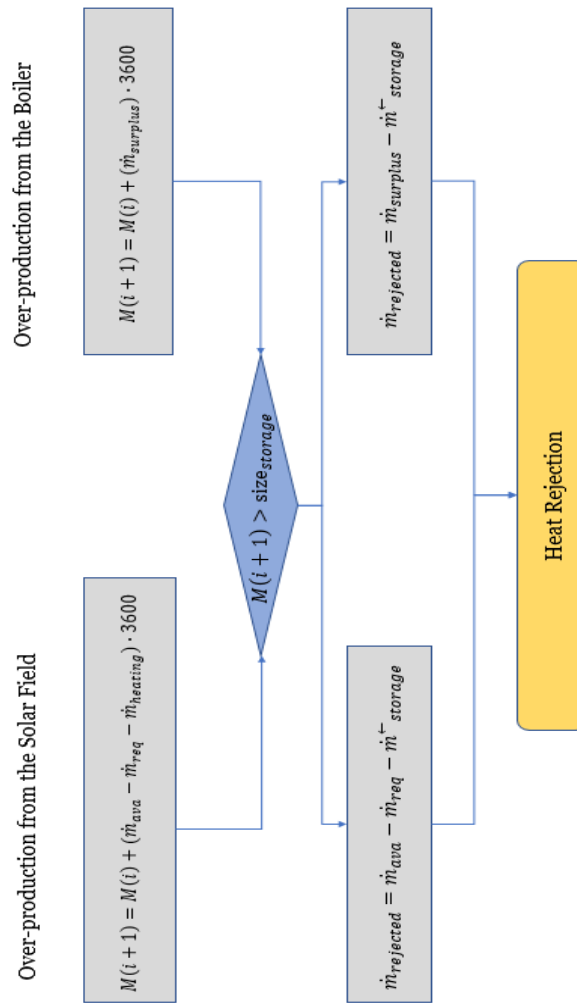
Figure 29 – Flow Chart of the Heat-Exchanger devoted to Heat rejection.

Cost

The IEA correlations for costs of items of cooling and heating for storage are different according to the nature of the storage: there is one for the cold storage and one for the hot storage.

$$Cost_{hot\ sto,specific} = 2500 \cdot \left(Size_{storage}\right)^{-0.28}$$

$$Cost_{cold\ sto,specifc} = 2135 \cdot \left(Size_{storage}\right)^{-0.299}$$

The cost of the storage includes auxiliaries. The total cost is.

$$Cost_{storage,tot} = Cost_{hot\ sto,specific} \cdot Size_{storage} + Cost_{cold\ sto,specific} \cdot Size_{storage}$$

Operating and maintenance are not considered in the IEA report, hence neither in this case study are considered.

3.2.5 BESS, Battery Energy Storage System

The battery energy storage has been considered because, as previously mentioned, for the 54.3% of the year it is just required the base load (occurring mainly during night time and equal to 80 W approximately), which is significantly lower compared to the operating minimum of the ORC. The batteries are supposed to cover mainly the night time base load, in fact, they discharge if there is no mass flow rate available from the solar field, and if the power required is lower than the ORC minimum. In such case, the micro ORC is switched off, and batteries should provide the electric load, the power for the compressor of the heat pump/VCC and, if present, the power for the auxiliaries of space heating.
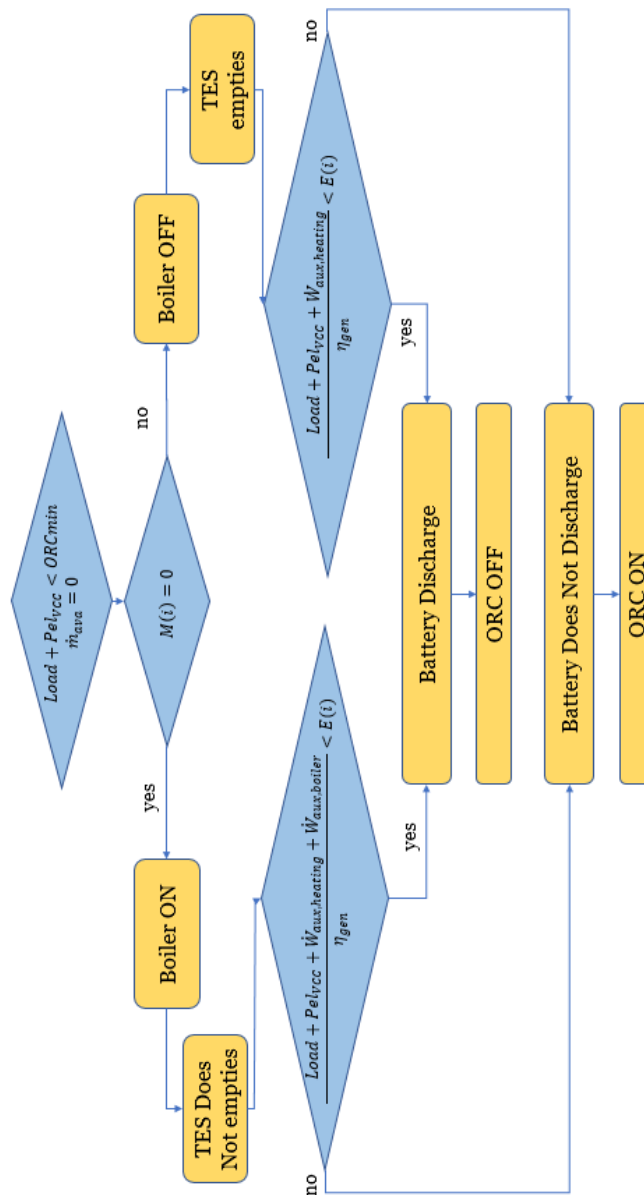
Figure 30 – Flow chart of BESS, $\dot{W}_{aux,heating}$ is present only if radiators are considered.

On the other hand, when the ORC is working at its maximum, but still is not able to provide the electric power required, batteries try to cover the unmet load, limiting the unmet load. On the other hand, they charge everytime there is a surplus of electric power coming from the ORC. This section is present in the flow-chart of the micro ORC previously shown.

The battery considered are Lithium-Ion because of their high energy and power density, their compactness and their well-known integration with renewables mini grid. The size of the battery is a free parameter in the simulation, because their size is a compromise based on the integration with the other plant's components.

Assumptions

- $\eta_{BESS,round-trip} = 0.8$, constant, round-trip efficiency includes the conversion losses in the battery and power electronics for the management. [52]
- No thermal model and temperature influence is considered on battery operations
- $\eta_{inverter} = 0.95$, constant

Efficiency

The round-trip efficiency of the battery is defined as:

$$\eta_{BESS,round-trip} = \frac{Discharged\ Energy}{Charged\ Energy}$$

Hence, the efficiency could be employed one time during charge or discharge phase, or, alternatively, two times, using the square root of the efficiency, both during charge and discharge phase. For sake of simplicity, the efficiency is applied only to the energy entering the storage.

Equations

The equations governing the BESS are simple energy balances, that changes according to the flow of energy, entering or exiting. The energy entering in the battery is the power surplus previously described, that occurs when the ORC is forced to operate at its minimum, but the load required is significantly lower.

$$Pel_{surplus} = ORC_{min} - Pel_{required}$$

The following equation represents the energy gain of the battery:

$$E_{batt}(i + 1) = E_{batt}(i) + Pel_{surplus} \cdot \eta_{BESS,round-trip} \cdot \eta_{inverter}$$

Where "E" is the energy of the battery, expressed in Wh. The variation of energy in the battery is described as:

$$\Delta E_{batt} = E_{batt}(i + 1) - E_{batt}(i)$$

The general form for the energy dissipated by the battery is:

$$E_{diss,batt} = \left(1 - \eta_{BESS,round-trip}\right) * \Delta E_{batt}$$

On the other hand, two macro scenarios occur when discharging, according to the heating device employed. If the heating is provided by the radiators, the battery should be able to power not only the electric load of the house, but also the auxiliaries for moving the hot stream from the storage to the heat exchanger, and eventually the auxiliaries of the boiler if the storage is empty. If the boiler is running at its minimum, but the storage is full, hence some heat must be rejected with the fan, it has been assumed that it will produce such amount of energy in a portion of the hour.

Viceversa, if the heating is provided by the heat pump, the battery should be able to power both the compressor and the house's appliances.

$$E_{batt}(i + 1) = E_{batt}(i) - \frac{Load + Pel_{heat\ pump}}{\eta_{inverter}}$$

or

$$E_{batt}(i + 1) = E_{batt}(i) - \frac{Load + \dot{W}_{aux,heating} + \dot{W}_{aux,boiler}}{\eta_{inverter}}$$

As previously mentioned, the batteries discharge also when the ORC is not able to provide the power required by the house. The unmet load is defined by:

$$(Pel_{VCC} + Load)_{max} + Pel_{auxiliaries} = ORCmax$$

$$Unmet_{load} = (Pel_{VCC} + Load)_{required} - (Pel_{VCC} + Load)_{max}$$

where $(Pel_{VCC} + Load)_{max}$ represents the peak power that the ORC can provide, considering the auxiliaries consumption when operating at its maximum conditions. The unmet load is defined as the difference between the real demand and maximum provided by the ORC. If the batteries are full, they will try to cover completely or partially the unmet load.

$$E_{batt}(i + 1) = E_{batt}(i) - \frac{Unmet_{load}}{\eta_{inverter}}$$

Cost

For Li-ion Batteries has been assumed a specific cost of $400 \frac{€}{kWh}$, thus the total cost is computed as follows:

$$Cost_{Batt,tot} = Cost_{batt,specific} \cdot Size_{BESS}$$

Where size of bess is evaluated in installed kWh. [53]

3.2.6   Notes

All the components of the first plant have been presented, and the most important equations too. Regarding the PV panels, their set of equations, and their assumptions, they will be explained in the next section, that will deepen the PV-BESS system. The control strategy of the PVs when integrated with the micro ORC will be deepened in the following chapter.

The term $Pel_{auxiliaries}$ is the summation of all the auxiliaries' consumption:

$$Pel_{auxiliaries} = \dot{W}_{aux,heating} + \dot{W}_{aux,eva} + \dot{W}_{aux,boiler} + \dot{W}_{aux,SF} + \dot{W}_{aux,fan}$$

Cost of components are introduced, because the case study aims also to provide a rough idea about the economic feasibility of such plant thanks to correlations that are size-related, and not taken from manufacturer data, which are not easy to obtain.

The investment cost (CI) will be calculated as the summation of all the investment cost of the components, as well as the total O&M. It is noteworthy that the CI is expressed in €, while the O&M are expressed in €/y.

$$CI = Cost_{Batt,tot} + Cost_{ETC,tot} + Cost_{storage,tot} + Cost_{boiler,tot} + Cost_{ORC,tot}$$

$$O\&M_{tot} = O\&M_{ETC} + O\&M_{boiler} + O\&M_{ORC}$$

The cost of the VCC and the HP, are not considered nor in the micro ORC, neither in the PV plant because it is considered as a sink cost.

3.3   PV-BESS

The photovoltaic panel coupled with bess has been investigated to provide a comparison with another system completely renewable. Moreover, photovoltaic and batteries have been deeply investigated for such purposes, resulting in a simpler mathematical model. Also, the number of components is significantly lower. The photovoltaic system is meant as a trigeneration system as well. The photovoltaic system powers a heat pump to provide the heating and cooling, no radiators are investigated. In such plant, no auxiliaries' consumption is assumed.
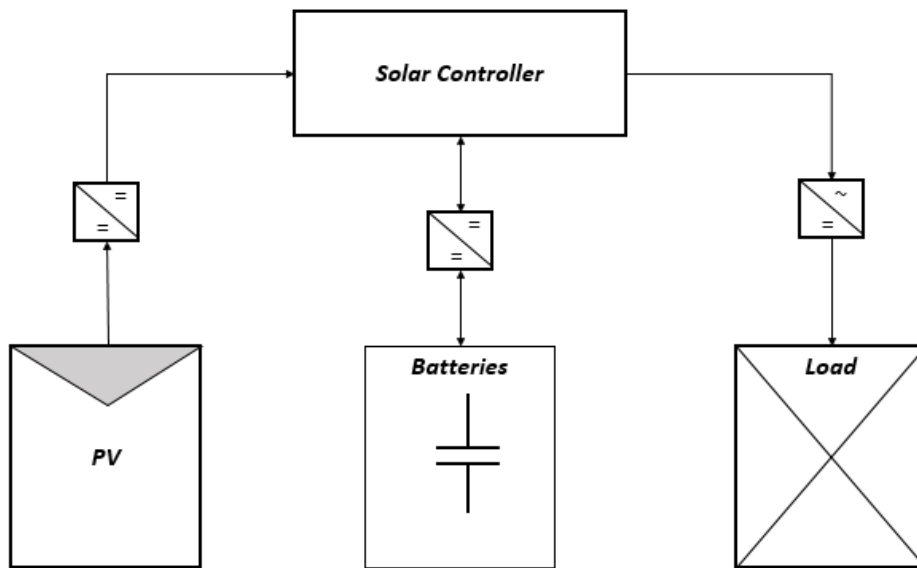
Figure 31 – Simple PV plant scheme, the arrows represent the directions of the power flows. The solar controller is the device devoted to make the demand met by PV or BESS. The Load includes HP and household consumption.

3.3.1   Photovoltaic Panels

Advantages of photovoltaic panels have been previously discussed: standardization, easiness of maintenance and installation, low specific cost per W installed, customization of the plant according to the needs, direct conversion of solar energy into electricity. On the other hand, the most important drawback of such plant is that while the micro ORC is dispatchable, the PV field has not a back-up engine when solar radiation is absent. Since the aim of the study is to investigate pure renewable solutions, the typical back up of a hybrid solar field, the diesel engine, has not been considered. Hence, the PV field should be oversized with respect to peak loads, because the driver of the sizing process would be the energy consumption and the reliability of the system, which should be the same of the

micro ORC, in order to provide a fair comparison. So, only solutions that are able to minimize the unmet load all over the year and with a good reliability of the system will be considered.

The PV panels are supposed to power both the electric appliances of the house and additionally the heat pump devoted to air-conditioning and space heating. The control strategy of power flows results to be very easy, in fact, when the PV field produces more power thant that is required by the heat pump and the appliances it is stored in the batteries. On the other hand, when there is no sun, or the power output of the PV field is not enough to cover the load deand, the batteries release energy to the utility. The aim would be to avoid unmet load all along the year. The unmet load is a condition in which nor the PV panels, neither the batteries are sufficiently charged to meet the energy demand, which is described by the equation:

$$Unmet_{load} = Pel_{required} - Pel_{PV,tot} - E_{batt}$$

Where $Pel_{required}$ is the power required by the utility, hence the sum of the electric load and the heat pump compressor power, $Pel_{PV,TOT}$ is the total power production from the PV field and E_{batt} is the energy stored in the BESS.

Assumptions

- Albedo, $\rho = 0.2$, Ground reflectivity
- $\beta = 35°$, optimum tilt angle [54]
- No shadings are affecting the solar field
- Clear Sky Model
- No auxiliaries' consumption
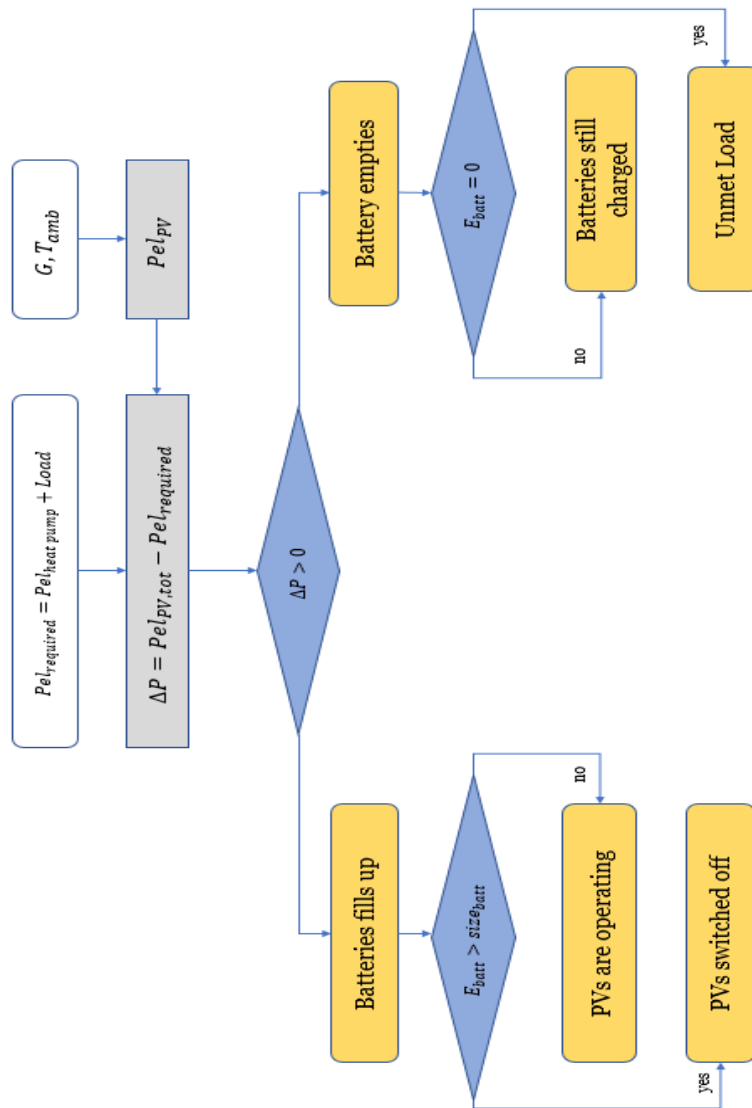
Figure 32 – Flow chart of the PV plant.

Panel's Selection

Since the market of photovoltaic panel is extremely wide it is very difficult to select a product. Regarding evacuated tube collectors the choice have been driven also by a literature review, while for PVs it is more difficult because the literature is more abundant and a wide span of products have been tested. Hence, after a review on the biggest companies of PV's producer, the selected panel for the test case has been chosen: a monocrystalline 60-cells high-power Peimar SG300M. [55] Although monocrystalline solar panels tend to be more expansive with respect to polycrystalline ones, they show better efficiencies of sunlight conversion, with a longer life span, and good performances in warm weather. The number of panel is one of the two free parameters of this

simulation: the goal is to find an optimum integration between them and the size of the BESS to provide continuous power to the utility with a reasonable reliability of the mini grid.

Solar Panel	*PEIMAR SG300M*	
α, Short Circuit Coefficient	0,047	%/°C
β, Open Circuit Voltage Coefficient	-0,32	%/°C
γ, Power Coefficient	-0,4	%/°C
Pel, STC	300	W
Voc, STC	39	V
Isc, STC	9,93	A
Gross Area	1.62	m2

Table 7 – Summarize Characteristics of the Monocrisytalline PV Panel. **STC**, Standard Test Conditions, i.e. T_{amb}=25°C, Radiation=1000W/m^2, Air Mass=1.5. **NOCT**, i.e. Normal Operating Cell Temperature, i.e T_{amb}=20°C, Radiation=800W/m^2, Wind velocity=1 m/s. **Voc**, Open Circuit Voltage. **Isc**, Short Circuit Current.

Orientation

The collector has been installed South-oriented with a tilt angle of 35°, namely β,which, according to several studies and different references, it has been demonstrated that for Athens' radiation, is in the range [35° -37°]. [47] [54]

The zenith angle and the cosine of the angle of incidence, respectively $\theta_z, cos\theta$, have been calculated on hour basis with the aid of SolPos online software [48], that requires as input:

Table 8 - Input parameters for the calculation of incidence angle's cosine

Latitude	37°44'
Longitude	23°44'
Time Zone	+2 UTC
Tilt Angle	35°
Azimuth Angle	0°

The incident solar power that the PV panel is hourly experiencing is computed by the formula:

$$G_i = G_D * \frac{1 + \cos\beta}{2} + \rho G * \frac{1 - \cos\beta}{2} + (G - G_D) * \frac{\cos\theta}{\cos\theta_z}$$

Where G_i is the incident radiation, G_d is the Diffuse radiation, ρ is the albedo, that has been assumed equal to 0.2.

Equations

The set of equations that describe the operating of the solar panel field on hourly basis are the following:

$$T_{cell} = T_{amb} + \frac{NOCT - 20}{G_{NOCT}} \cdot G_i$$

It is a linear empirical correlation to estimate the operating cell temperature in non-NOCT conditions widely employed. The operating cell temperature is a crucial parameter, since radiation and ambient temperature are the most affective parameter on rated power output, which is calculated as:

$$Pel_{PV} = \frac{G_i}{G_{stc}} \cdot Pel_{PV,STC} \cdot [1 + \frac{\gamma}{100} \cdot (T_{cell} - T_{amb,STC})]$$

The, the total power output of the solar field, assuming no shadings, and similar behaviour of the panels is:

$$Pel_{PV,TOT} = n_{panel} \cdot Pel_{PV}$$

Cost

The PV cost is evaluated as well by mean of a correlation, able to easily relate the size in temrs of installed W and the price. [56]

$$Cost_{PV,spec} = 2.38 \frac{€}{W}$$

$$Cost_{PV,tot} = Cost_{PV,spec} \cdot Pel_{PV,tot}$$

O&M costs are considered as well:

$$O\&M_{PV} = 40 \frac{€}{kW \, y}$$

3.3.2   BESS, Battery Energy Storage System

The capacity of the BESS is the other free parameter of this plant: their size must be large enough to store the energy produced by the PV panels and meet the energy demand with the lower unmet possible.

The battery energy system considerd is the same respectively to the one of the ORC, hence a Li-ion one. Moreover, in such way, the comparison results more similar. The batteries charge whenever there is an over-production of the PV field, while they discharge when they have to meet the load demand. As well as in the ORC case, a round trip efficiency have been considered, which affects the batteries during the charge phase only.

Assumptions

- $\eta_{Batt,round-trip} = 0.8$, constant, round-trip efficiency includes the conversion losses in the battery and power electronics for the management. [52]
- No thermal model and temperature influence is considered on battery operations

Equations

The equations governing the BESS are simple energy balances, that changes according to the flow of energy, entering or exiting, because the power flows are different according to their path, as it is possible to notice from the plant scheme.

The direction of energy, outgoing or ingoing the batteries, is given by the difference between the power production of the PVs and the power required. If it is a value larger than zero, the power is entering the batteries, if it is lower the batteries are discharging.

$$\Delta P = Pel_{PV,tot} - Pel_{required}$$

If the energy is entering the batteries, the equation is:

$$E_{batt}(i + 1) = E_{batt}(i) + \Delta P \cdot \eta_{trasformer} \cdot \eta_{BESS,round-trip}$$

Where $E_{batt}(i)$ is the energy inside the battery at the time-step "i", expressed in Wh. The energy entering is multiplied both by the efficiency of the batteries and transformer, since in the layout plant is included a transformer devoted to couple the voltage between the solar field and the BESS. The inverter efficiency is not included since the power production from the PVs is DC, as well as the power input of the batteries.

The energy lost during the charge process is

$$E_{diss,batt} = \Delta P \cdot (1 - \eta_{BESS,round-trip} \cdot \eta_{trasformer})$$

On the other hand, the equations governing the discharge phase is the following:

$$E_{batt}(i+1) = E_{batt}(i) - \frac{\Delta P}{\eta_{inverter} \cdot \eta_{trasformer}}$$

The discharged energy is divided by the efficiency of both the transformer and the inverter, since the power flowing out of the batteries must overcome the losses occurring in path to the load.

The energy lost in the discharging process is:

$$E_{diss,batt} = \Delta P \cdot (\frac{1}{\eta_{inverter} \cdot \eta_{trasformer}} - 1)$$

Cost

The cost of the batteries is considered the same of the ones employed in the micro ORC system.

3.3.3 Inverter

The PV panels and the batteries operate with DC current; hence, it is required the inverter which converts it into AC to supply the load of the house. The inverter is activated whenever power flows towards the house, while, for example when charging batteries is not activated. The inverter size is selected according to the maximum peak load of the utility. Thus, the maximum of the heat pump over the year is $2280.5\ W$ and the maximum of the appliances is $1885\ W$, that summed up result to be $4165.5\ W$, leading to a 5 kW inverter choice. The inverter is the interface between the production and storage loop, which is DC, and the utility, which is AC.

Assumptions

- $\eta_{inverter,nom} = 0.95$

Efficiency

The efficiency of the inverter is not considered constant because it is affected by partial load operations. The efficiency curve has been interpolated with Matlab® from typical curves that can be found in literature. Moreover, the efficiency curve as a function of the partial load are not significantly different changing the size of the inverter, they are very steep and reach the nominal conditions in the range [15-20] % of the load. The interpolated curve refers to a 5kW inverter.[57]

The efficiency formula turns to be the following:

$$\eta_{inverter} = \frac{a \cdot I + b}{I + c}$$

Where:

- $a = 0.9583$
- $b = 1.643 \cdot 10^{-7}$
- $c = 0.00624$
- $I = \frac{load}{load_{nom}}$

Cost

This component has a cost which is described by a correlation also: the cost is proportional to the installed W in AC current. [20] The specific cost of the inverter is:

$$Cost_{inverter,spec} = 0.1275 \frac{€}{W_{AC}}$$

As previously commented, the size of the inverter, in terms of W in AC current, is selected a priori and it is equivalent to $5\ kW$.

$$Cost_{inverter,tot} = size_{inverter} \cdot Cost_{inverter,spec}$$

3.3.4   Other Components

Transformer

The transformer is a device which receive as input current and voltage and "transform" them with another pair of current and voltage. In PV applications they are widely used to match the voltage between the components, expecially to match the voltage of PV output and the input of batteries that are usually 12,24,48 V. They are very compact and cheap components that allows better and more stable performances of the plant with a very modes expense. In the proposed plant, two transformers are employed: the first one at the output of the PV array, and one at the input/output of the BESS. The efficiency assumed for such component is $\eta_{transformer} = 0.95$ and is assumed constant. The power that they must be able to manage is equal to $max(Pel_{PV}), max(\Delta_{batt})$, which is actually their size. This power cannot be set a priori, and is dependent on the simulation performed because the power flowing through this component is dependent on the number of panels required to meet the electric demand and charge the batteries.

Cost

The specific cost of transformer is assumed:

$$Cost_{trasformers,spec} = 0.09 \frac{€}{W}$$

The total cost of the trasformers is thus:

$$Cost_{trasformers,tot} = (\max(Pel_{PV}) + \max(\Delta_{batt})) \cdot Cost_{trasformers,spec}$$

Solar Controller

A controller is assumed to be employed at the interface between batteries and PV panel to avoid over production of electric power and regulate the power flows as described in the flow chart. The device is not consuming power.

Cost

The cost of the solar charge controller is negligible compared to the order of magnitude of the investment cost of this plant.

3.3.5 Notes

No auxiliaries' consumption is considered in this simplified model that simulate the behaveiour of this plant.

The costs are computed as follows:

$$CI = Cost_{PV,tot} + Cost_{BESS,tot} + Cost_{inverter} + Cost_{trasformer,tot}$$

$$O\&M_{tot} = O\&M_{PV}$$

4 Simulation Code

4.1 Input of the micro ORC code

The simulation of the behaviour of the components in off-design conditions is the preliminary tool employed to visualize and understand how the system is performing, according to fluctuations of the load and weather. It is a crucial step to understand the performance of the system, that cannot be sized on-design, just looking to the nominal conditions. This is due to the off-grid nature of the plant: in fact, it must be able to meet the peak demand, but at the same time to perform with satisfying efficiency during base-load conditions, and the risk of designing such kind of plant at nominal conditions is to oversize each component. The simulation has been carried out with a code developed by the author in Matlab®, which, according to the assumptions previously discussed, simulate the interaction between the components of the plant in terms of energy fluxes.

The **free parameters** of the code are thus:

- The size of the storage, expressed in kilograms, $size_{storage}$
- The total aperture area of the ETCs, expressed in m^2, $Aperture_{area}$
- The nominal power of the micro ORC, expressed in W, Pel_{ORC}
- The capacity of the BESS, expressed in Wh, $size_{Batt}$
- The minimum operating thermal power output of the boiler, expressed in %, min_{boil}
- The number of photovoltaic panels, n

While, the **input parameters** are:

- Weather data
- Energy demand
- Electric Load
- Cooling Load
- Heating Load
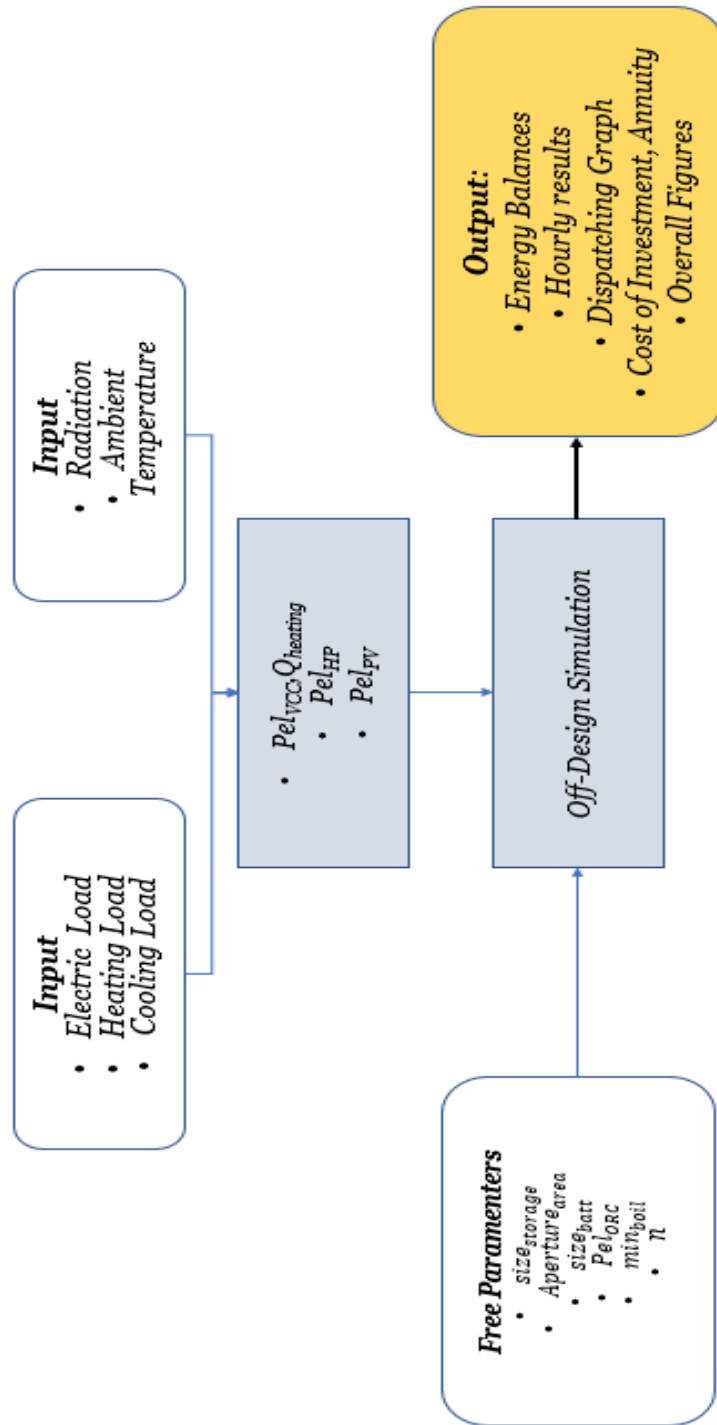
Figure 33 – The Flow Chart summarizes the general scheme of the simulating code

4.2 Output of the micro ORC code

The outputs of the code are several, and briefly summarized in the flow chart. Here they are listed and explained.

4.2.1 Energy Balances

First Principle Energy Balance is hourly computed to have an overall check on energy fluxes of the system and ensure the result.

$$G_i \cdot Aperture_{area} \cdot \eta_{coll} + \dot{Q}_{boiler} - \dot{Q}_{rej} - Pel_{ORC} - \dot{Q}_{cond,ORC} = \Delta Q_{storage}$$

Moreover, another energy balance is computed, to check not only the balance at the boarder of the system, but also the internal electric power flows.

$$\left(\frac{Load + Pel_{VCC} + Pel_{aux,tot} - unmet_{load}}{\eta_{gen}} + \frac{\Delta_{batt}}{\eta_{inv}} + E_{loss,batt} + Pel_{diss} \right) = Pel_{ORC} + Pel_{PV}$$

4.2.2 Hourly results

All the heat and power fluxes of each component are hourly computed to check the enegy balances, and to understand the behaviour of the components. All the mass flow rates, state of charge of batteries and level of the TES are hourly computed. At the end of the simulation is checked if the size of batteries and thermal storage have not been exceeded. They are given as output in two different formats: as a row-array of 8760 values, or as a matrix with 24 rows, i.e. the hours of a day, and 365 columns, i.e. the days of the year.

Practically speaking, all the equations that have been presented in the previous chapter are solved.

4.2.3 Dispatching Graph

The code provides also charts that illustrate the logic of dispatching both thermal and electric energy. They are very useful since give an instantaneous picture of how the system is responding to the input given. They allow to analyse the thermal production of the boiler and ETCs, or the electric production of the micro ORC and the role of the batteries.

4.2.4 Cost of Investment, Annuity

The cost of investment has been discussed in the previous chapter, and is the summation of all the equipment cost.

The annuity is calculated to have an economic term of comparison. The annuity is the cost of investment multiplied by the CRF (Capital Recovery Factor), which is the ratio of a constant annuity to the present value of receiving that annuity for a given length of time. Practically, it includes the interest rate, the inflation and the lifetime of the component, and makes the investment cost a yearly cost. Keeping fixed the interest rate, it depends mostly on the lifetime of the component: it has been assumed a $CRF = 0.11$ for all the components, except for batteries that usually have a lower life span, thus $CRF_{batt} = 0.34$ has been assumed. Then, it is summed up with the operating and maintenance cost, which includes maintenance and insurance and finally with the cost of fuel.

The annuity is computed because it was unfair to compare the LCOE of the two systems, since the ORC-HP would take advantage because it would have a higher denominator due to the higher electric load induced by the HP.

$$Annuity = CI \cdot CRF - (CRF - CRF_{batt}) \cdot Cost_{tot,batt} + O\&M_{tot} + Cost_{fuel}$$

4.2.5 Overall Figures

With Overall Figures, it is meant a list of parameters of merit of the system: they are based on the hourly calculations and try to depict with a value the behaviour of a single component or the system one. They are organised as a table, the rows 13, i.e. the month of the year plus the yearly value, while the column are the overall figures itself.

Overall Figures	h unmet	% unmet	h full	h full batt	LF	SF	MF	Q rej	Solar diss
Month	-	-	-	-	-	-	-	-	-
Yearly	-	-	-	-	-	-	-	-	-

h unmet, % unmet

h unmet are the hours in which the unmet load has a value different from zero, while **% unmet** is the ratio between al the unmet demand of energy of the month over the total energy demand. The first parameter is expressed in hours, the second one is a percentage.

$$h_{unmet,month} = \sum_{i=1}^{hours\ of\ month} h_i\ (unmet_{load} \neq 0)$$

$$\%_{unmet,month} = \frac{\sum_{i=1}^{hours\ of\ month} unmet_{load},i}{\sum_{i=1}^{hours\ of\ month} Load_i + Pel_{VCC},i}$$

The yearly values are computed in the same way, summing up throughout the whole year.

These two parameters are important to estimate the the unmet energy demand, if present, from two different perspectives: thanks to the number of hours, we can understand if it is an isolated phenomenon or a recurrent one, while with the percentage it is possible to estimate the intensity. For instance, if the percentage is very high, but it happened in just one hour is less important than having a discomfortable situation of small unmet energy demand every day, that means that the system is not the most suitable one.

h full, h full batt

h full is the ratio between the hours in which the TES is saturatered with hot fluid, and the hours of the month; it is a percentage. **h full batt**, is the same ratio of the former, but considering the hours of batteries at full charge on the numerator. It is expressed as a percentage.

$$h_{full} = \frac{\sum_{i=1}^{hours\ of\ month} h_i (M == size_{sto})}{\sum_{i=1}^{hours\ of\ month} h_i}$$

$$h_{full,batt} = \frac{\sum_{i=1}^{hours\ of\ month} h_i (E_{batt} == size_{batt})}{\sum_{i=1}^{hours\ of\ month} h_i}$$

These two parameters have been considered to easily understand if the storages are over or underestimated: for instance, a value close to one means for the TES that the storage is full almost all the month, leading to heat rejection with the fan and to a high energy consumption of auxiliaries and also that its size is not coupled with the boiler minimum nor with the total area of collectors.

LF (Load Factor)

LF is the Load Factor of the micro ORC, i.e. the ratio between the energy production of the engine and its nominal power times the functioning hours. The functioning hours are those hours in which the micro ORC is operating. It is expressed as a percentage.

$$LF = \frac{\sum_{i=1}^{hours\ of\ month} Pel_{ORC},i}{Pel_{ORC,nom} \cdot h_{functioning}}$$

This parameter is crucial to understand the utilization of the micro ORC: since it is a dispatchable engine, that can operate whenever thanks to the boiler, it is interesting to highlight how, on average, is working close to its nominal conditions. For instance, a ratio close to one means that the Organic Rankine Cycle often operates close to its nominal conditions, i.e. with a higher efficiency.

SF (Solar Fraction)

SF is the solar fraction, i.e. the fraction of heat input required by the utility provided by solar collectors. It is expressed as a percentage.

$$SF = \frac{\sum_{i=1}^{hours\ of\ month} \dot{Q}_{ava}}{\sum_{i=1}^{hours\ of\ month} \dot{Q}_{req}}$$

This parameter is used to estimate how much the production of thermal energy of the ETCs is covering the total heat demand and the eventual benefit of employing the collectors.

MF

MF is the mass of biofuel consumed by the system, expressed in kilograms.

$$MF = \sum_{i=1}^{hours\ of\ month} \dot{m}_{fuel} \cdot 3600$$

It is used to evaluate the system from different standpoints: it is crucial because is proportional to a portion of annuity, and at the same time provides suggestions to understand the benefit introduced by the different components.

Q rej, Solar diss

These two parameters are considered to take into account the energy that is rejected by the fan auxiliary, to estimate the wasted heat by the solution considered. **Q rej** represents the heat rejected by the fan, that can come both by a hot stream provided by the collectors' field and the boiler when is working at the minimum, as previously explained. It is expressed in Wh. **Solar diss** is the ratio between the heat rejected coming from the ETCs' field and the total amount of heat rejected by the fan. It is expressed as a percentage.

$$Q_{rej} = \sum_{i=1}^{hours\ of\ month} \dot{m}_{rej} \cdot c_p \cdot \Delta T_{storage}$$

$$Solar_{diss} = \frac{\sum_{i=1}^{hours\ of\ month} \dot{Q}_{rej}(\dot{Q}_{ava})}{\sum_{i=1}^{hours\ of\ month} \dot{Q}_{rej}}$$

With these two values it is possible as first to see the heat waste of the system, then to understand by which component is given: the boiler, or the collector field. For instance, if Solar diss has a value close to one, it means that the area of ETCs is too large with respect to the capacity of the TES, or either the capacity of the storage is too small.

4.3   Off-design Code

The off-design code is based on the control strategies of the components previously discussed: in the simulation they are summed up, constituting the core. The control strategy that is missing is the PV's one, which are considered only with the micro ORC-HP. The Photovoltaic panels produce electric power which, if it is larger than the electric load, it is used to cover it, the ORC does not operate, and the surplus is stored in the batteries. If the power production from the PV is lower than the energy demand, the energy is stored directly in the BESS and the ORC is switched on. The power production from the PV panels is known a priori, since it is dependent only on radiation and ambient temperature. This is the reason by which it is estimated if they can cover the load before the ORC, that involves calculations that depends not only by the input, but also on the relationships between components.
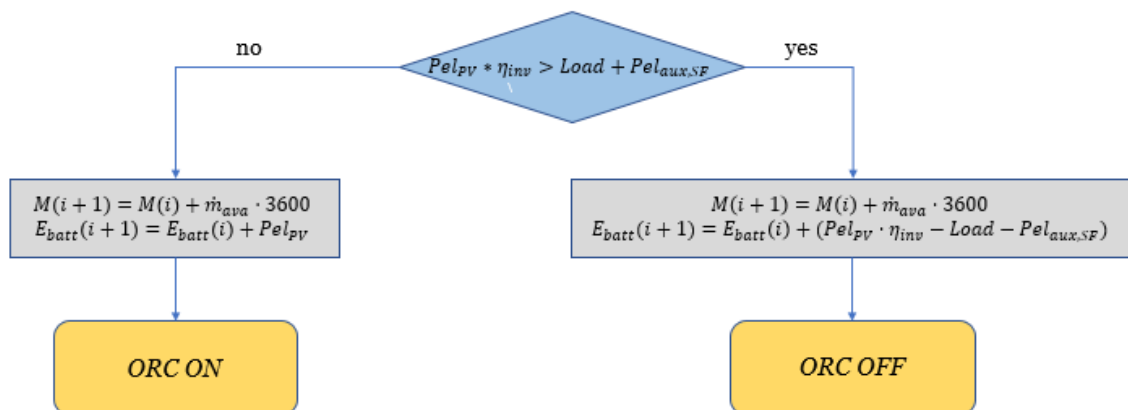
Figure 34 – The Flow Chart represents the control strategy of the PV, when present.

When the Organic Rankine Cycle is switched on, a while loop ensure the convergence of the solution: the convergence is reached on the electric power required, as shown in the flow chart of the micro ORC. If the power required is lower than the minimum of the ORC, a "fake load" equal to its minimum is introduced, the auxiliaries are computed again, but at that power output. The convergence is reached again with a loop cycle, based on the minimum load.

Figure 35 – Functioning of the ORC when is switched on, convergence is accepted with a tolerance lower than 10^{-12}

4.4   Input of the PV-BESS code

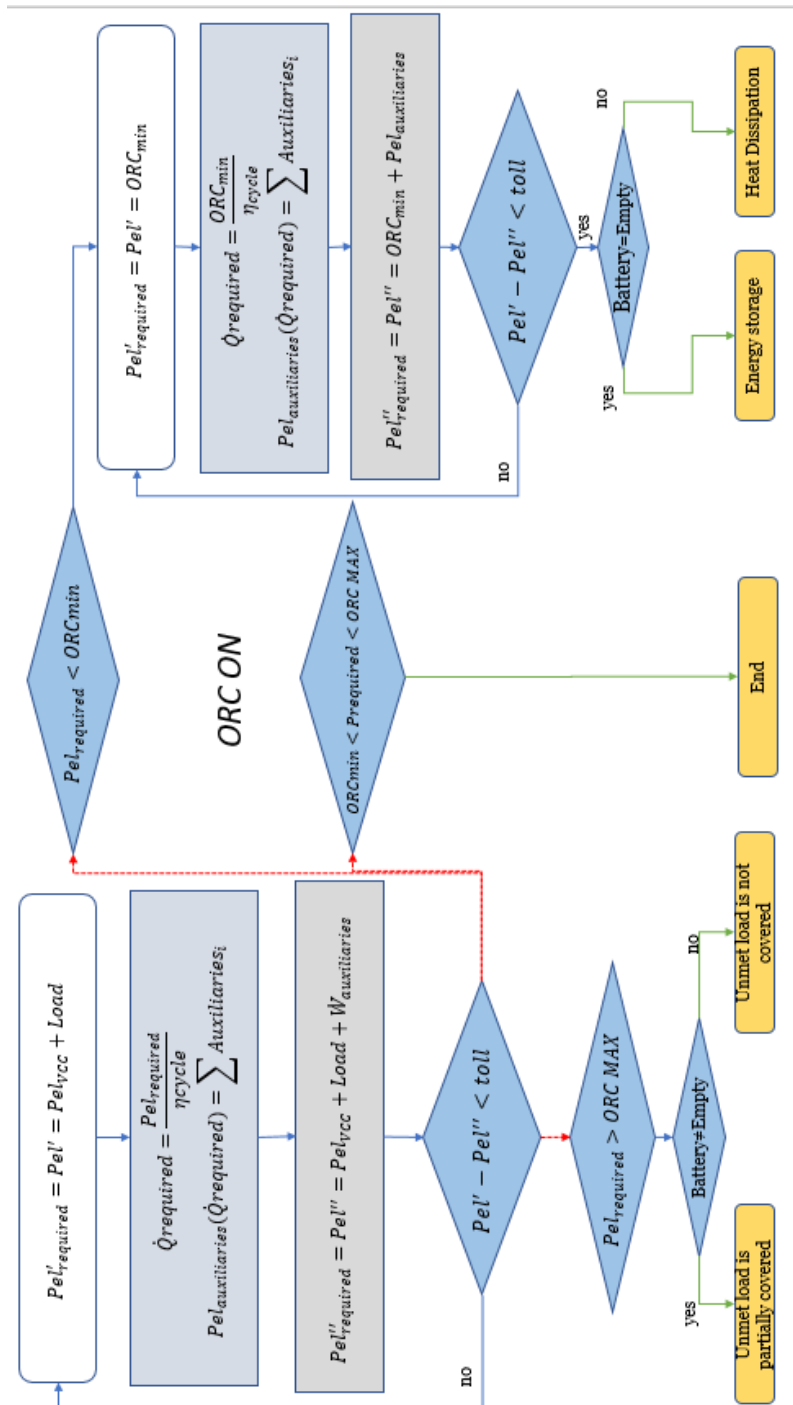The PV-BESS code is lighter than the ORC one, and it has been developed to assess a competitor, and benchmark the dimensions, the costs and the reliability of fully renewable plants. The free parameters of this code are the number of the panels and the size of the batteries. The inputs are obviously the same of the micro ORC, to have a fair comparison.
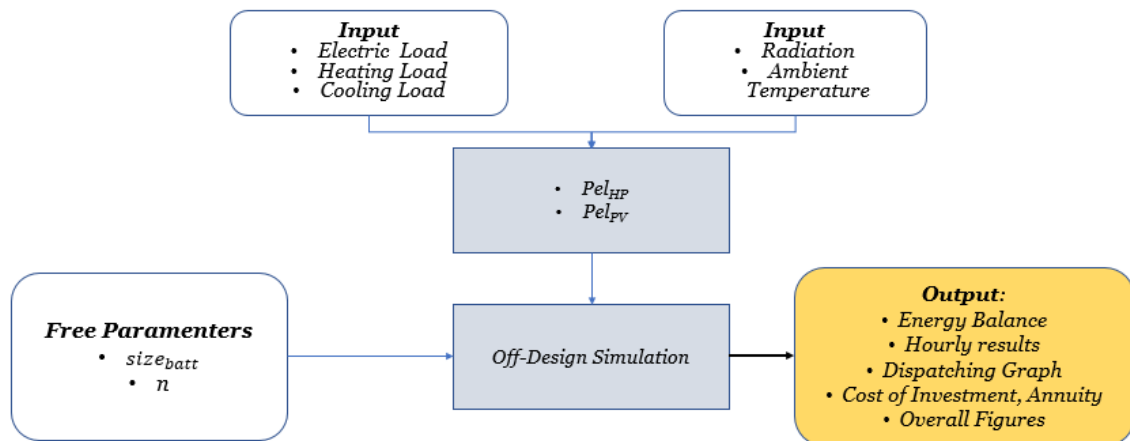
Figure 36 – Structure of the code

4.5   Output of the PV-BESS Code

The outputs are meant with the same logic of the micro ORC code.

4.5.1   Energy Balances

The Energy Balance is verified per each our, and it is written as follows:

$$Pel_{PV} \cdot \eta_{inv}\eta_{trasf} - Load + unmet_{load} - E_{diss,batt} = \Delta E_{Batt}$$

The balance is checked each simulation, and has usually a tolerance lower than 10^{-12}.

4.5.2   Hourly Results

All the power fluxes are hourly computed to check the enegy balances, and to understand the behaviour of the components. The state of charge of batteries are hourly computed and at the end of the simulation is checked if the size of batteries has not been exceeded.

4.5.3 Dispatching Graph

The dispatching graphs in this case are meant only for electric production, because there is not a thermal loop.

4.5.4 Cost of Investment and Annuity

Cost of investment have been previously introduced, while annuity is calculated as well as micro ORC system. The same assumption about CRF has been made also in this case.

$$Annuity = CI \cdot CRF - (CRF - CRF_{batt}) \cdot Cost_{tot,batt} + O\&M_{tot}$$

4.5.5 Overall Figures

Some overall figures have been introduced also in this code, to have quick values able to capture the operating conditions of the system. They are mainly the same of the micro ORC: unmet load, percentage of unmet load and hour full of batteries, the calculation procedure is the same. The only new one that have been introduced is called **PV.**

PV is the ratio between the total energy produced by the photovoltaic panels over the total electric load. It has been introduced to see how much large should be a fully renewable PV field, that, although the favourable weather conditions and the good radiation, to cover the yearly energy demand. It is important because is also a figure that involves the dimensions of the plant.

$$PV = \frac{\sum_{i=1}^{8760} Pel_{PV}}{\sum_{i=1}^{8760}(load + Pel_{HP})}$$

4.6 Off-design Code

The off-design code is implemented following the control strategy previously discussed in the section about the PVs.

5 Results

Results of the simulations of the μORC will be presented following the order of integration of renewable, from the simplest to the most complex.

5.1 μORC + TES + Boiler

The aim of each chapter is to find a reasonable preliminary sizing of the system with the aid of the outputs of the simulation.

5.1.1 Preliminary Sizing

The first overall figures analysed is the yearly unmet load: thanks to this parameter it is possible to understand the minimum size of the μORC able to cover the energy demand without unmet load.

The following two charts, Figure 37 and Figure 38, the first refers to the ORC-radiators-VCC plant, the second to the ORC-HP. From now on they will be named as ORC-VCC and ORC-HP for sake of simplicity. The two graphs are parametric with respect to the minimum of the boiler. We can notice four main aspect:

- At 2500 W of nominal power of the ORC-VCC the unmet load approaches the zero, and it is a trend independent from the size of the storage. Meaning that, the size of the micro ORC should be this one.
- At 2500W of nominal power of ORC-HP system the unmet load approaches the zero, and as well as the other case, is independent from the size of the storage. Meaning that the size of the micro ORC should be approximately this one.
- The unmet load increases with the minimum of the boiler, at constant rated power and constant TES capacity. This is due to the fan devoted to heat rejection: a high minimum of the boiler leads to higher mass flow rate in excess entering the TES, which if saturated, must reject it: the higher the minimum, the higher the rejection if the TES size is not properly dimensioned.
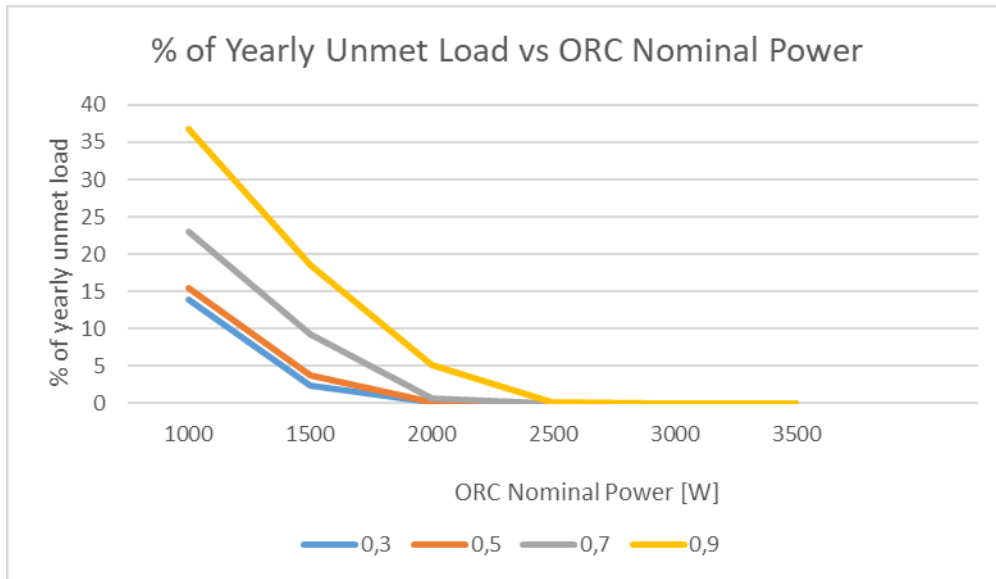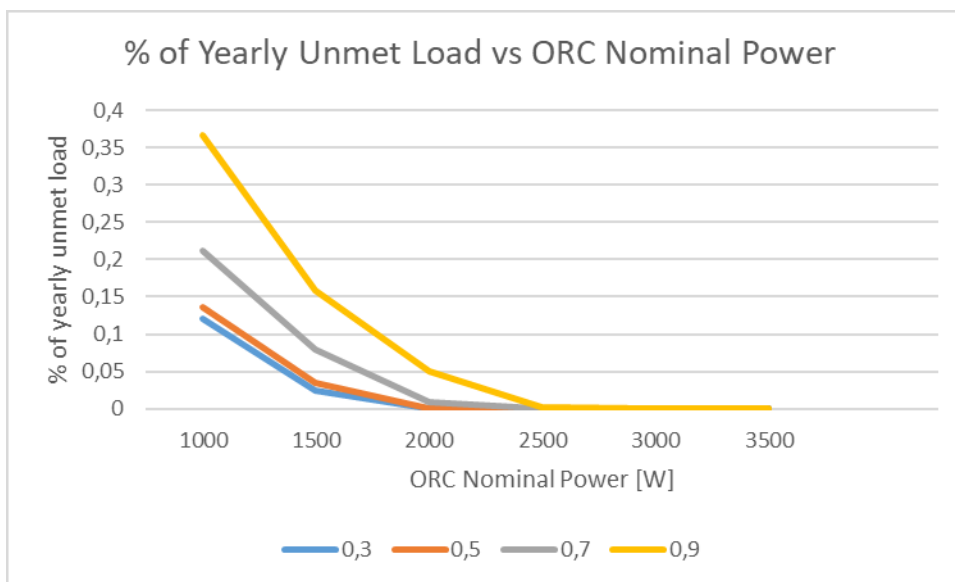
Figure 37 – ORC-VCC plant, preliminary design of µORC

Figure 38 – ORC-HP plant, preliminary design of µORC

The size of the storage is crucial: because if wisely chosen allows to save fuel, but, on the other hand, if it is too small leads to higher fuel consumption for heat rejection, a waste of energy. So, the next charts will show the heat rejection as a function of the storage size, at fixed ORC power output, parametric on the minimum of the boiler.

As previously said, the higher the minimum of the boiler, the higher the excess mass flow rate, the higher the heat rejection. According to the following chart, Figure 39, it is possible to notice that after 1500 kg, there is no heat rejection anymore. This trend is valid for both the plant.
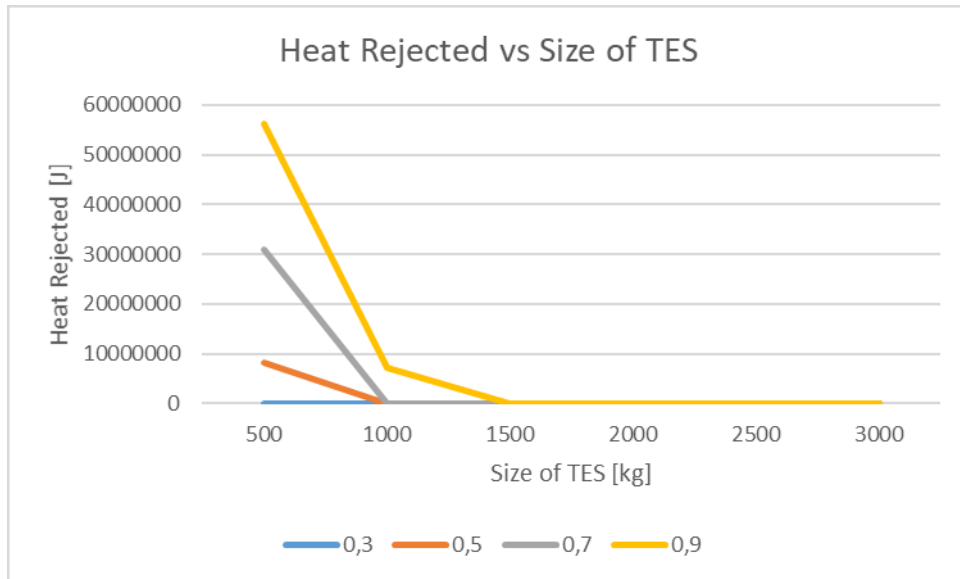
Figure 39 – Heat rejection at the selected ORC nominal power for ORC-VCC system.

Now, we want to investigate if there is a minimum of the boiler that minimizes the biomass consumption at the selected power output and evaluate if there is such evidence. The following surface highlights that the higher the minimum of the boiler, the lower the biomass consumption if the storage is properly designed, although for the selected size of TES the decrease is not impressive. This is mainly due to the boiler operations at 90% of its nominal power that leads to higher efficiency, decreasing the fuel consumption. Moreover, in Figure 40 it is possible to notice that the threshold is 1500 kg as well.
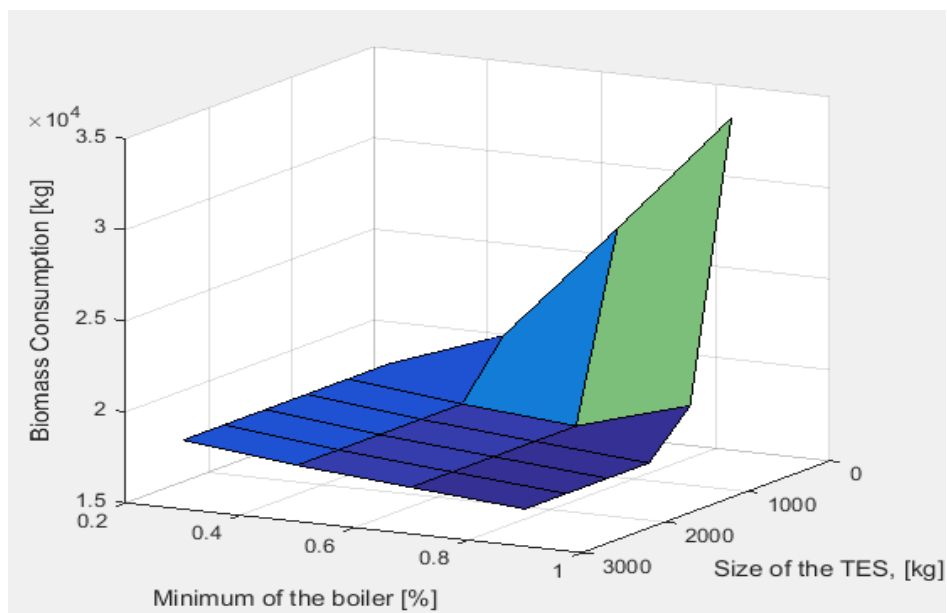

Figure 40 – Surface that shows the biomass consumption. The worst case is obviously a high boiler minimum coupled with a small storage.

This trend is valid for both the plant, the only difference is related to the lower biomass consumption of the ORC-HP system with respect to the ORC-VCC one, but it is a very small difference. This is mainly due to the average electric load of the ORC-HP system, which is higher, that leads to higher Load Factors (LF=0.2850) and thus higher first principle efficiency, which are 8.57% and 8.39%.

The annuity of the ORC-HP is lower due to the lower biomass consumption.

Results are summarized in Table 9

Table 9 – Results of the Preliminary Sizing

	Size Storage [kg]	Minimum of Boiler [%]	ORC Nominal Power [W]	η_I	Annuity [€]	Biomass Consuption [kg]
ORC-VCC	1500	0.9	2500	0.0839	8,064	$1.7059 \cdot 10^4$
ORC_HP	1500	0.9	2500	0.0857	7,995	$1.6739 \cdot 10^4$

5.1.2 Check of the Results

Table 10 – Tollerances on Energy Balances and Check on the Maximum of the Boiler

Check	1st Principle Energy Balance	Electric Balance	Q boiler max
Value	$<10^{-7}$	$<10^{-12}$	< 40 kW

5.1.3 Dispatching Graph

To have a picture on how the system is responding to the input, dispatching graphs are presented.

Electricity

ORC-VCC

The Figure 41 and Figure 42 refers to the electric production/consumption of the ORC-VCC system, summer and winter typical days. It is immediately clear that a lot of the

power production of the ORC is wasted in heat with the heat dissipater, due to the minimum of operating condition of the engine, which is much larger with respect to the base load. So, this leads clearly to an eventual integration with batteries that would be able to operate when the load is low compared to the minimum and charged when the ORC is switched on at the minimum to safe the power dissipated. During both winter and summer, the dissipation is more evident during night time. During summer it is possible to notice the larger consumption with the peak in the mid of the day due to VCC operations for cooling. Moreover, the summer chart is the same for both ORC-VCC and ORC-HP systems because they are employing the same heat pump, thus the summer chart will be presented only for the ORC-VCC.
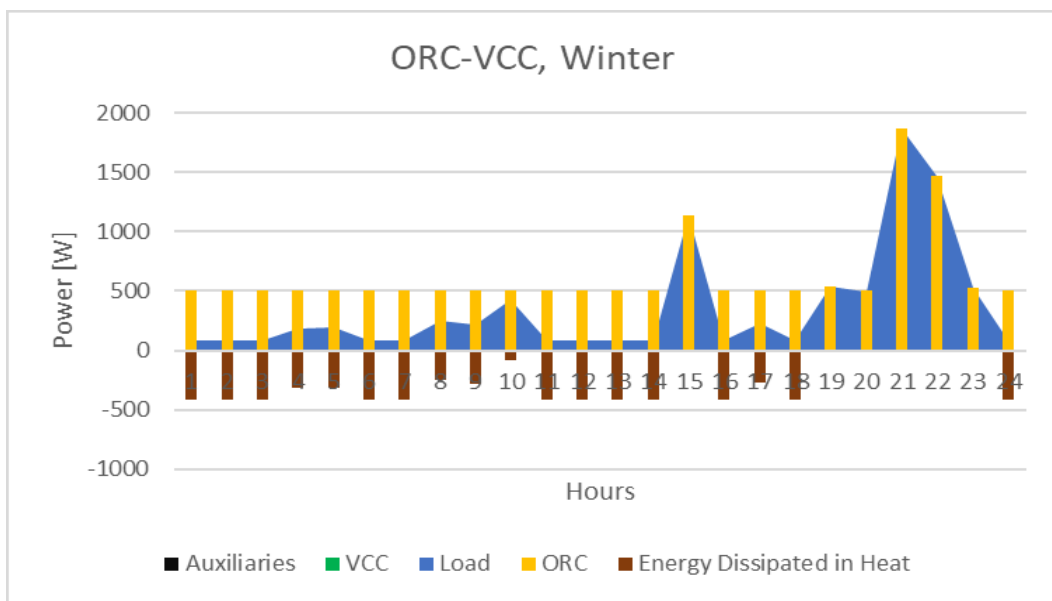

Figure 41 – Dispatching Graph of the ORC-VCC.
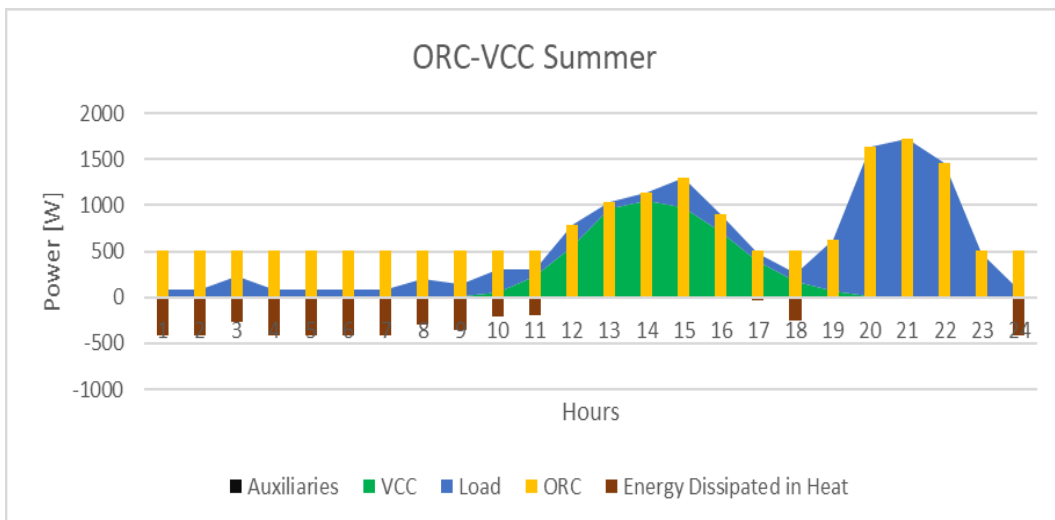
Figure 42 – Dispatching Graph of the ORC-VCC

ORC-HP

ORC-HP dispatching of summer is the same of the ORC-VCC system, while in the winter case it is noteworthy that during night there is a larger consumption due to the HP operations in heating mode, hence the energy dissipation is concentrated in the mid day, which is a specular behaviour with respect to the summer period. Moreover, this will have consequences on the functioning of batteries, that are meant to cover the night time base load.

Figure 43 – Dispatching graph of the ORC-HP system

Thermal

The thermal dispatching graphs will be presented together, because the functioning is very similar, Figure 44 and Figure 45. It is noteworthy to highlight the functioning of the boiler, that, coupled with a large TES, works at its maximum and is switched on few times per day. Moreover, the red area is the heat provided for space-heating purposes, and it is a small fraction with respect to the one required by the ORC to operate. On the other hand, the ORC-HP requires more heat to operate due to the heat pump operations. In the end, the consumption of biomass is confirmed as very similar (Just 320 kg of difference), as it is possible to notice looking at the values of the heat output of the boiler. Summer period shows the same trend, Figure 46, because they are using the same engine, with same operating conditions. Hence summer graph is presented once.

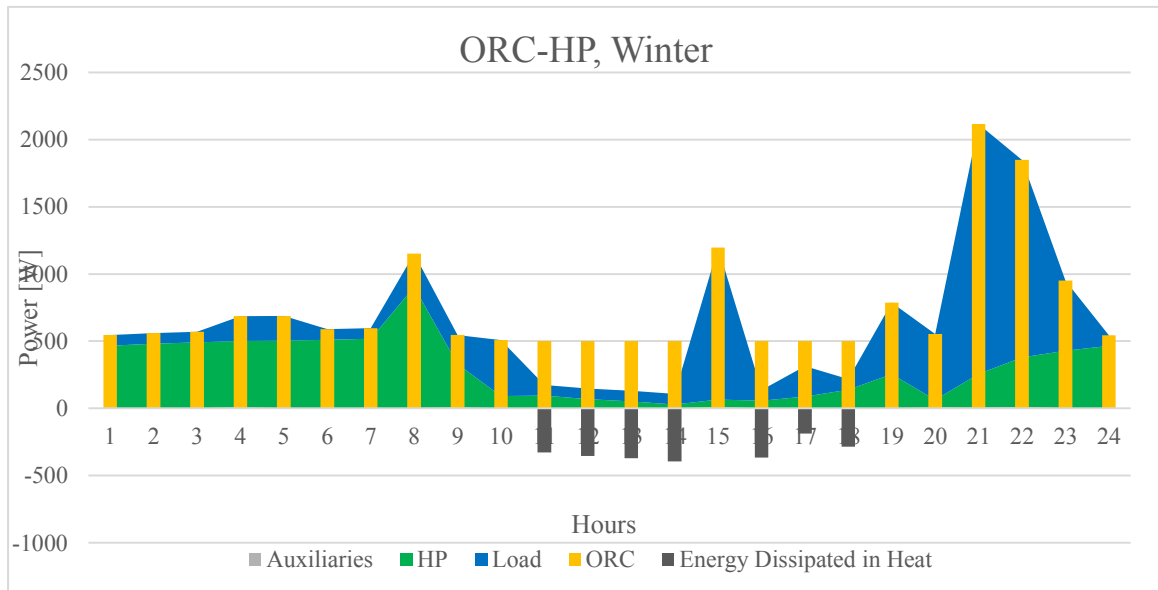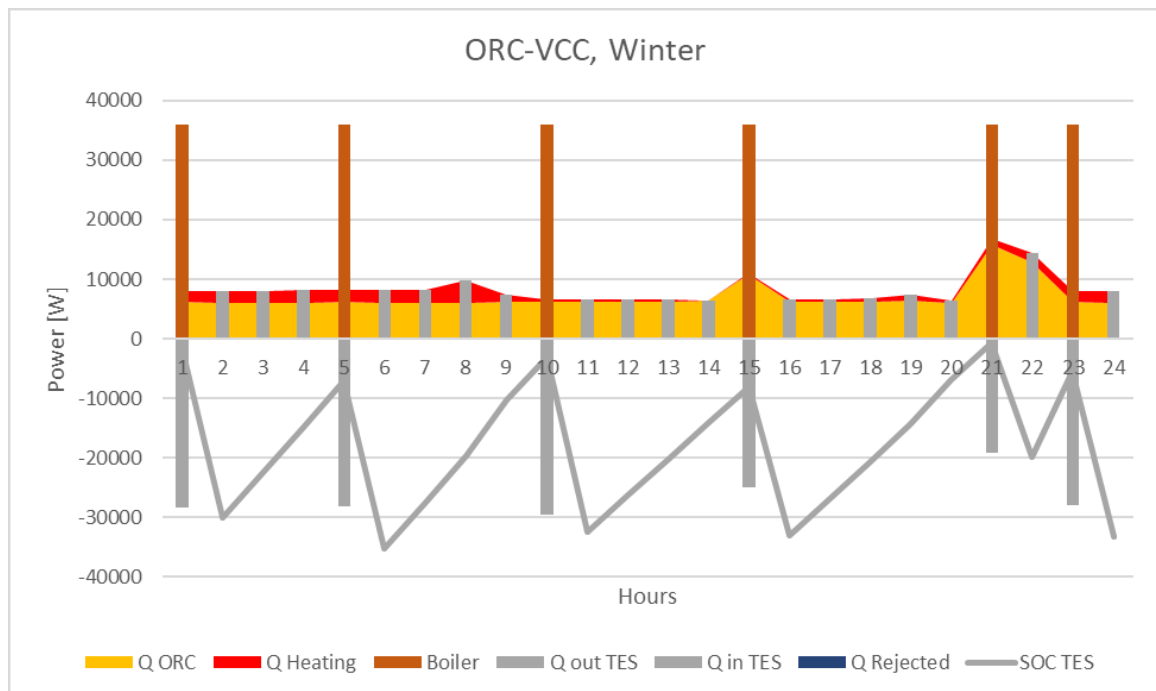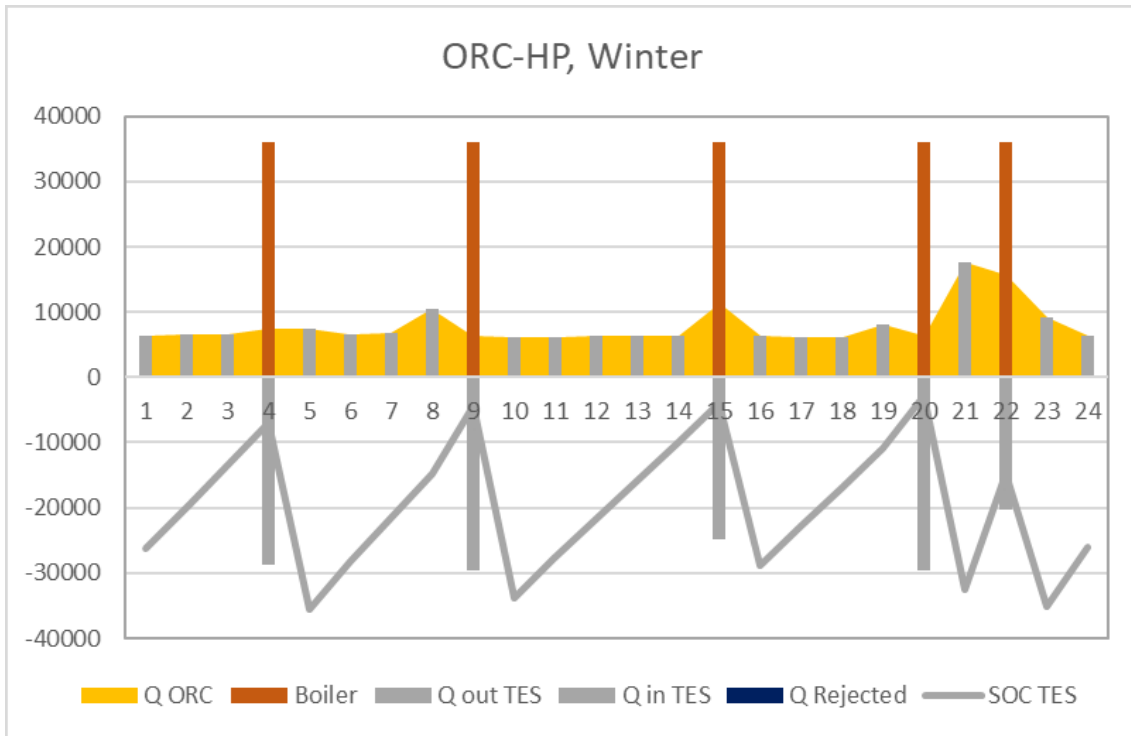Figure 44 – Dispatching Graph of the ORC-VCC System.
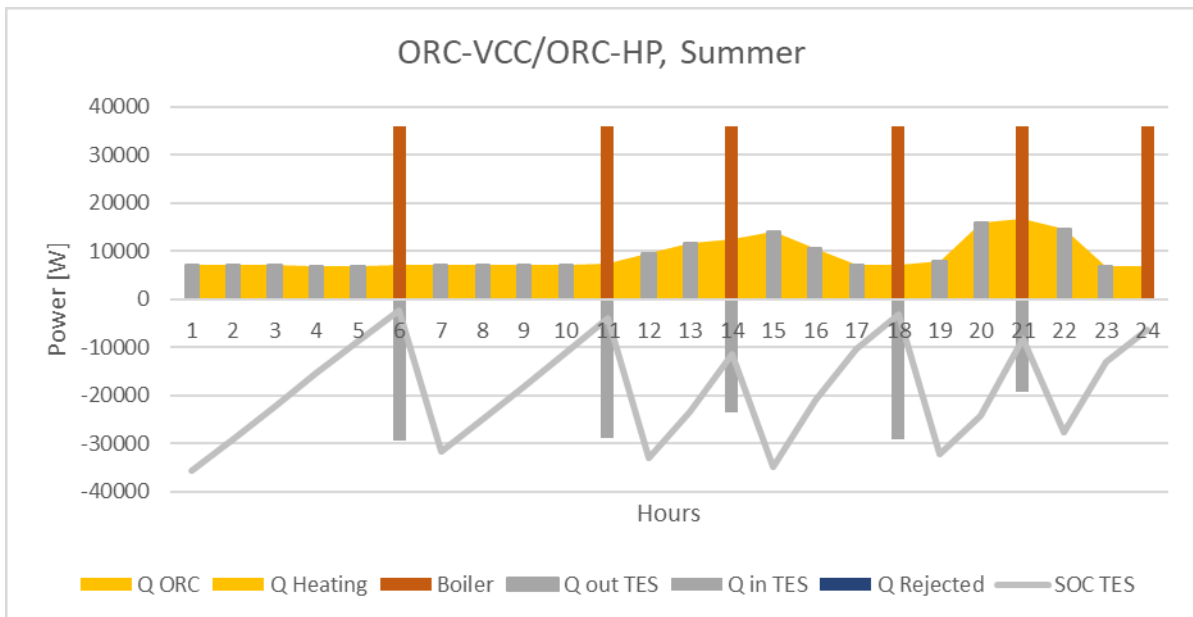
Figure 45 – Dispatching Graph for the ORC-HP System

Figure 46 – Dispatching Graph of the ORC-VCC and ORC-HP Systems.

5.2 μORC + TES + Boiler + BESS

Batteries, according to the data presented, should be a device that improve the systems, decreasing the biomass consumption, allow less part load operation of the ORC, and decrease the amount of electricity dissipated in heat. The surplus power produced and dissipated in heat are 1.43 MWh/y for the ORC-HP and 2.15 MWh/y for the ORC-VCC, which are a remarkable potential that can be stored inside the batteries.

The control strategy imposed to the battery, as previously presented in the flow chart, is the following:

- They charge whenever the ORC is working at its minimum, but the load is smaller, and, only if they are saturated, electric power is dissipated in heat.
- They discharge when they are sufficiently charged to cover the load requested, if it is lower than the minimum of the ORC preventing its operations, and when there is no radiation available. The last condition has been imposed because during night time and morning there are the lowest load requests; moreover, dispatching graphs shows that is the most dissipating period for ORC-VCC, and it is true also for the ORC-HP in winter conditions. Batteries discharge also during peak periods if the maximum power of the ORC is not enough to cover the load.

5.2.1 Preliminary Sizing

As first, we want to investigate if it is possible to reduce the nominal power of the micro ORC with the introduction of batteries.

The percentage of yearly unmet load is slightly affected by the size of the battery, keeping fixed the nominal power of the engine. This is due to the charge phase of the batteries: they charge according to the surplus of electric production which is directly proportional to the nominal power of the ORC.

From Figure 47 it is possible to see how the two systems can benefit from the introduction of the batteries: the percentage of unmet load is equal to zero for 2500W for both systems, but they can be undersized even more: the percentage of unmet load at 2000 W is lower than 0.01%, equal to 400Wh lost in august over the whole year. But the aim of the case study is to avoid as much as it is possible the unmet load, and, moreover, since energy consuming devices are present (electric stove and air-conditioning), it is better to have a reliable engine able to operate simultaneously at least a couple of devices and able to cover peak demand as well.
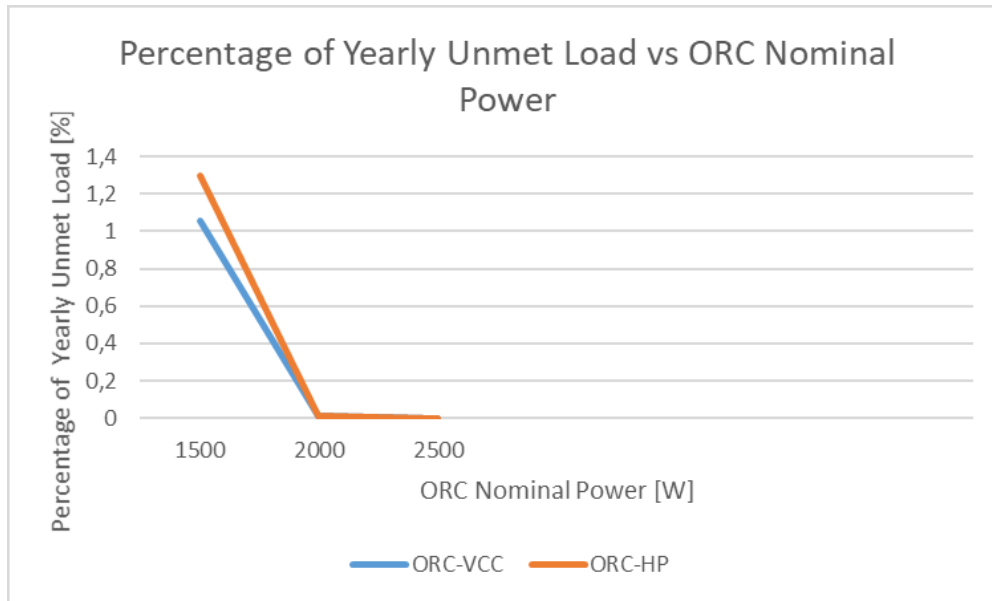
Figure 47 – Percentage of Yearly Unmet Load as function of the ORC power output.

ORC-HP

The ORC-HP has a nominal power of 2500 W. Now we want to understand if the minimum of the boiler set at 0.9 is still an advantage for the system. According to the biomass consumption chart, Figure 48, the employment of BESS introduces benefits: the biomass consumption decreases with an increase of BESS capacity. We can notice two important trends:

- After a certain threshold the biomass consumption is not dependent anymore on the size of batteries, meaning that an eventual increase of the BESS is useless. This threshold is in the interval [2000-2500] Wh of capacity.
- The minimum of the boiler set at 0.9 is still the less consuming.

Figure 48 – Biomass Consumption vs Size of BESS and Minimum of the Boiler.

But, on the other hand, the annuity gives different hints, according to Figure 49: there is a minimum for BESS' capacity equal to 1 kWh for every minimum of the boiler, at the selected TES capacity.
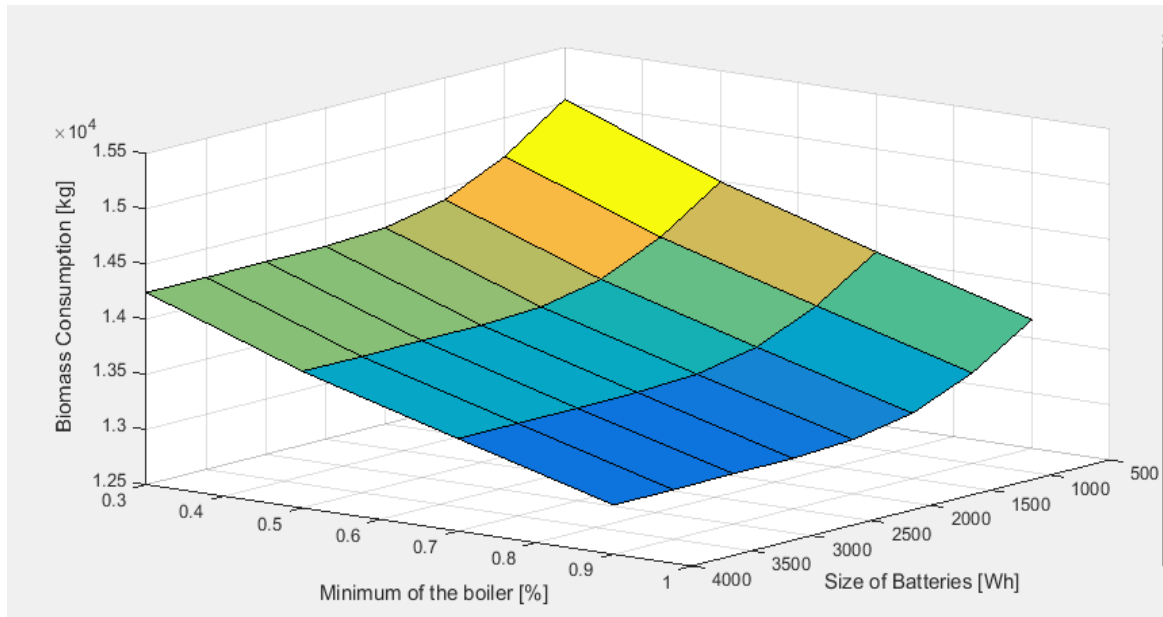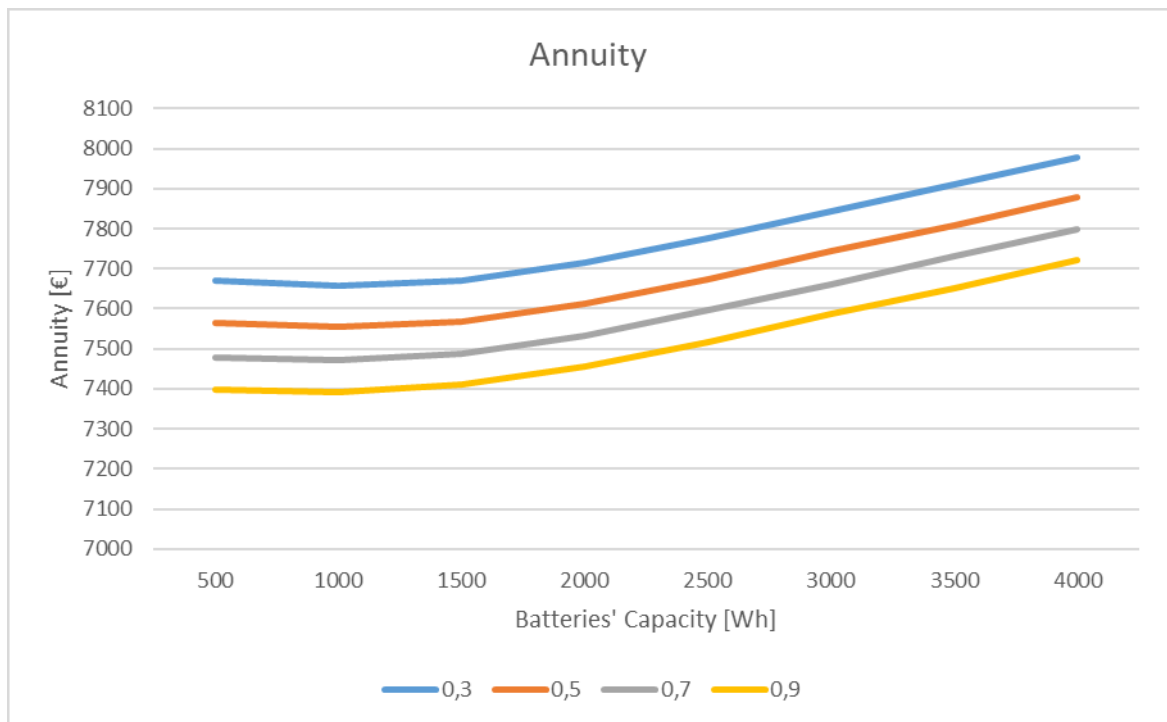

Figure 49 – Annuity vs Size of Batteries and Minimum of the Boiler

This minimum is reflecting the trade-off between the biomass consumption and the cost of the batteries and can be explained with a simple calculation. The energy dissipated in heat is $6.65 \cdot 10^5$ Wh, for the system with 2500 of nominal Power, 0.9 of minimum and 1 kWh of batteries. The average efficiency of the ORC is 0.0888 and the average boiler efficiency is 0.9014 both on a yearly basis. The biomass consumption to produce this energy can be computed as:

$$M_{biomass} = \frac{\sum_{i=1}^{8760} Pel_{diss} \cdot 3600}{\eta_I \cdot \eta_{boiler} \cdot LHV_{biomass}} \sim 1900 \; kg$$

The related cost is:

$$Cost_{biomass} = M_{biomass} \cdot Cost_{specific,biomass} \sim 350€$$

Which is lower than the cost of an additional 1 kWh of BESS, so, it is more convenient to burn the biomass and dissipate electric energy into heat. Installing 1 kWh to minimize the annuity means that still a portion of energy is dissipated in heat although the employment of batteries (24% of the surplus energy produced), due to the specific cost of these two items that makes it more favourable.

Introducing the batteries, there would be the chance to lower the size of the storage, thanks to the less amount of energy dissipated in heat, although heat rejection would be eventually present. If the TES capacity is lowered down, still the percentage of unmet load is equal to zero, but the biomass consumption decrease, in particular, for 1000 kg of capacity, there is a minimum for annuity, even lower than the case with 1500 kg, at the same BESS capacity. The minimum is for 0.7 of boiler. This result is provided in Figure 50.
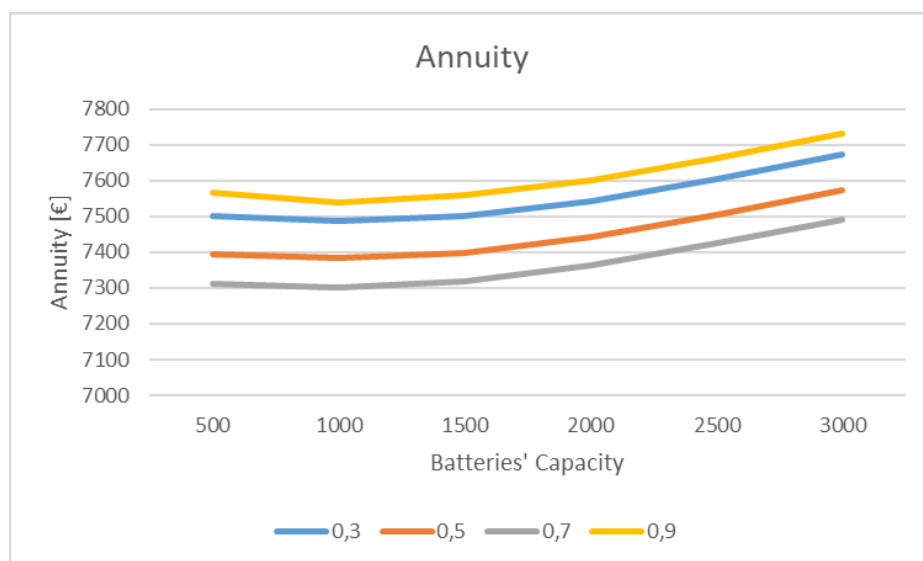

Figure 50 – Annuity chart with a lower TES capacity, the minimum set of 0.7 allows a reduction in terms of costs.

This is due to the very small amount of heat rejected: in the previous chapter it was showed that for a 1000 kg TES capacity heat rejection at 0.7 boiler set would have been very small. In fact, it represents the 0.006% of the total heat input provided by the boiler, which is a meaningless amount of biomass wasted, but a significant cost saving in terms of storage capacity.

Table 11 - Results of the Preliminary Sizing

	Size Storage [kg]	Minimum of Boiler [%]	ORC Nominal Power [W]	η_I	Annuity [€]	Biomass Consuption [kg]	BESS Capacity [kWh]
ORC-HP	1000	0.7	2500	0.0888	7,3011	$1.3717 \cdot 10^4$	1

ORC-VCC

Since ORC-HP system shows improvement with a decrease of the TES capacity, we will start the analysis looking if it is true also for the ORC-VCC.

The Figure 51 is a surface, function of the minimum of boiler and of the size of the batteries and shows two main trends, for a TES capacity equal to 1000 kg:

- The first one is related to the minimum of the boiler: Biomass consumption has a minimum as a function of it, if the storage size is decreased.
- The second one is that, at 0.7 of minimum boiler set, the biomass consumption is approximately constant in the range of batteries [1000-2000] Wh, meaning that an eventual increase of the size of the BESS would not lead to a significant saving of biomass. Hence, the cost of fuel in that region is contant, and thus the annuity would be minimized with the minimum BESS capacity (1000 Wh).
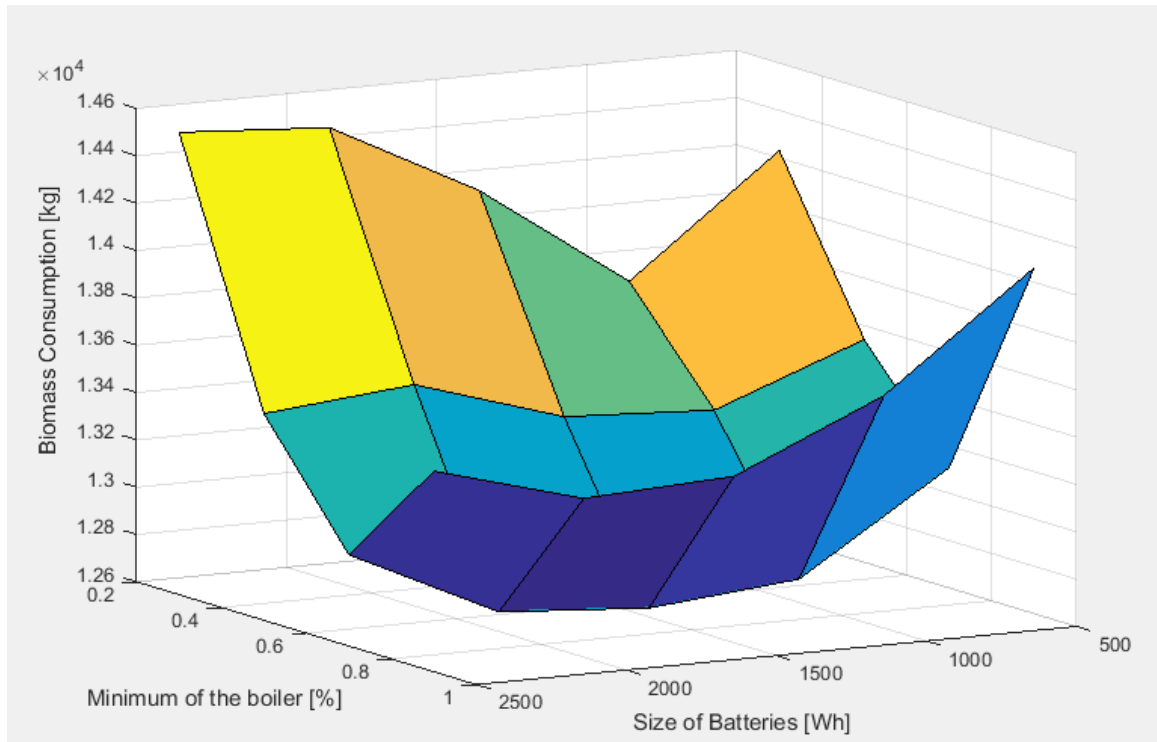
Figure 51 - Biomass consumption of the system as a function of minimum of the boiler and size of batteries. TES capacity=1000 kg

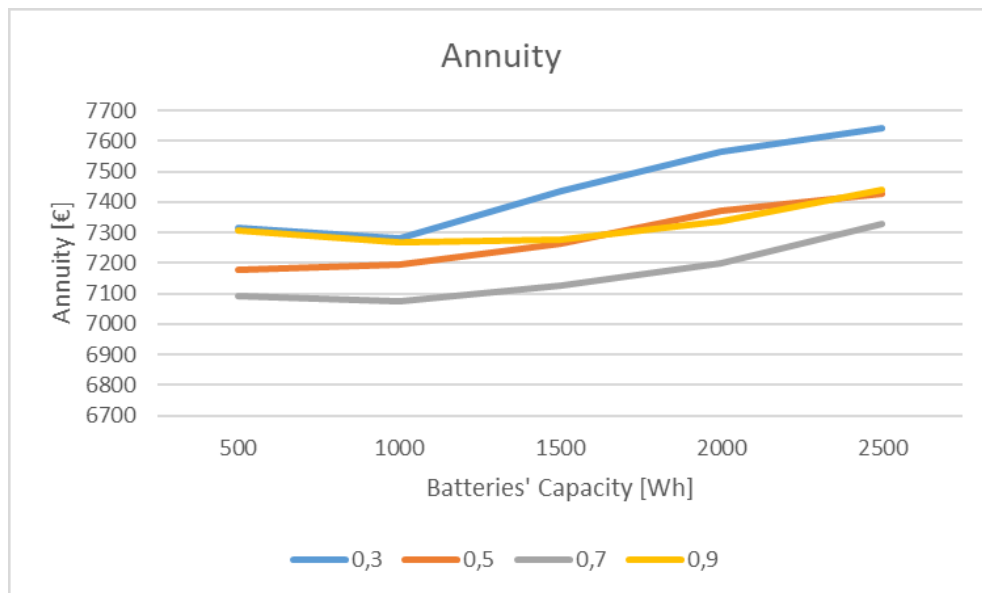These two features can be noticed in Figure 52:

Figure 52 – Annuity trends as a function of the size of the BESS and minimum of the boiler. The minimum at 0.7 agrees with the trends highlighted by Biomasss consumption.

The energy dissipated in heat is the 22% of the total energy surplus.

An average capacity of BESS that would be able to store all the energy dissipated, can be calculated as:

$$Size_{batt} = \frac{\sum_{i=1}^{8760} Pel_{diss}}{365} \sim 5500 \, Wh$$

But this capacity would cost 2200€ approximately, hence also here, from an economical standpoint, it is better to consume biomass instead of having a higher battery capacity, because the low specific cost of biomass lead to this solution. ORC-VCC system will have 1 kWh of BESS installed and a minimum of the boiler set at 0.7. The different set of the minimum, lead to an investigation on the capacity of the TES, if it the trends analysed are confirmed.

According to the biomass surface in Figure 53, it is possible to notice that biomass consumption is quite the same between the point (0.7;1000) and (0.9;1500), and therefore the minimum of annuity is at the first point: because there is not a significant decrease of biomass consumption, but there is a saving thanks to the decrease of the TES capacity.
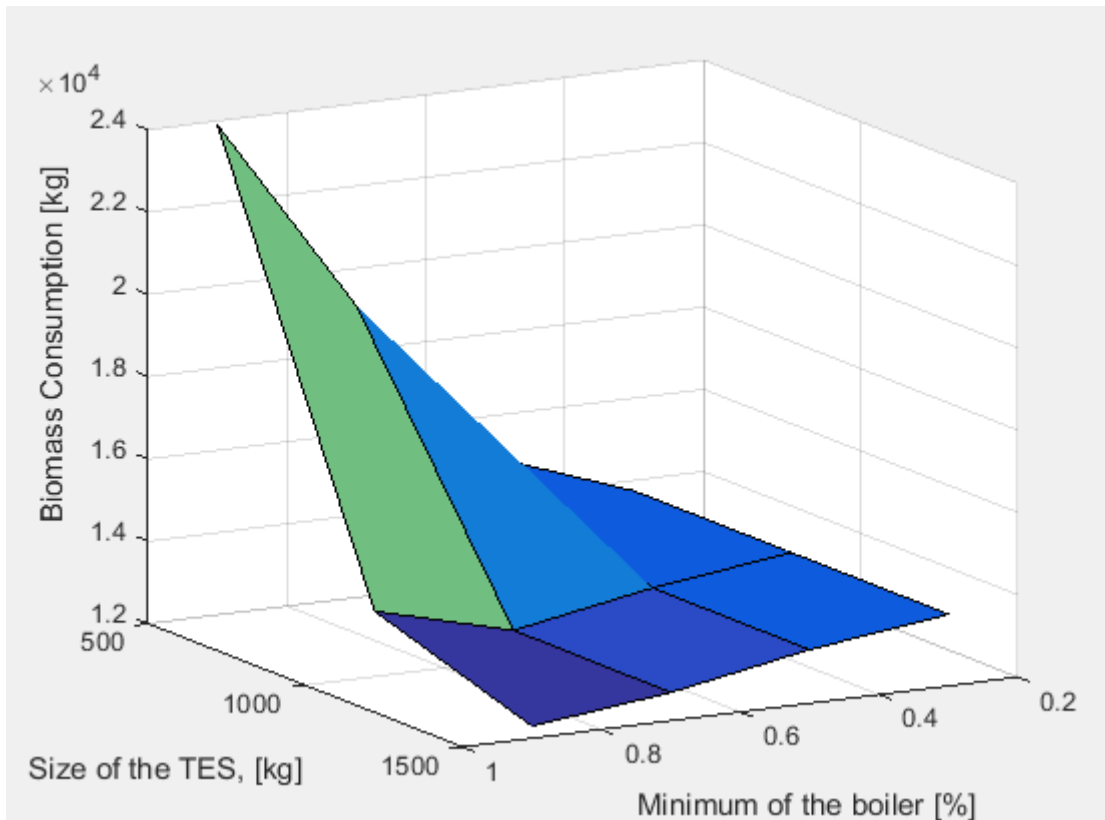

Figure 53 – Biomass consumption as a function of TES capacity and minimum of the boiler. It is interesting that the minimum is highlighted also here, and it is noticeable the small benefit introduced by a larger TES and a higher minimum set.

Thanks to batteries, the micro ORC operates closer to its nominal conditions, avoiding less efficient part load conditions. In fact, also here we have an increase in the Load Factor for the selected system (LF = 0.32), which corresponds to an increase of the efficiency.

Heat rejection represents here as well a small portion of the heat input (0.005%), meaning that there is a good impairment between the hot storage and the minimum set of the boiler.

Table 12 - Results of the Preliminary Sizing

	Size Storage [kg]	Minimum of Boiler [%]	ORC Nominal Power [W]	η_I	Annuity [€]	Biomass Consuption [kg]	BESS Capacity [kWh]
ORC-VCC	1000	0.7	2500	0.0875	7,073	$12,699 \cdot 10^3$	1

5.2.2   Check of the Results

Table 13 - Tollerances on Energy Balances and Check on the Maximum of the Boiler

Check	1st Principle Energy Balance	Electric Balance	Q boiler max
Value	$<10^{-6}$	$<10^{-13}$	< 40 kW

5.2.3   Dispatching Graphs

Electricity

ORC-HP

From the dispatching graph in Figure 54 and Figure 55, some outcomes can be visualized:

- The BESS during winter are not largely employed during night time, this is because it is the peak period for the heat pump during such season, hence the micro ORC is not working under its minimum operating conditions and they are not activated. Moreover, some electric energy is dissipated in heat as well. On the other hand, batteries seem to fit the demand properly during summer time: their

limit is slightly overcome and they discharge during night time base load conditions.

- ORC operates more during winter time because the control strategy of the BESS fits better with the ORC-VCC system and during summer period. Despite of that, the performances of the system are increased and costs are reduced.

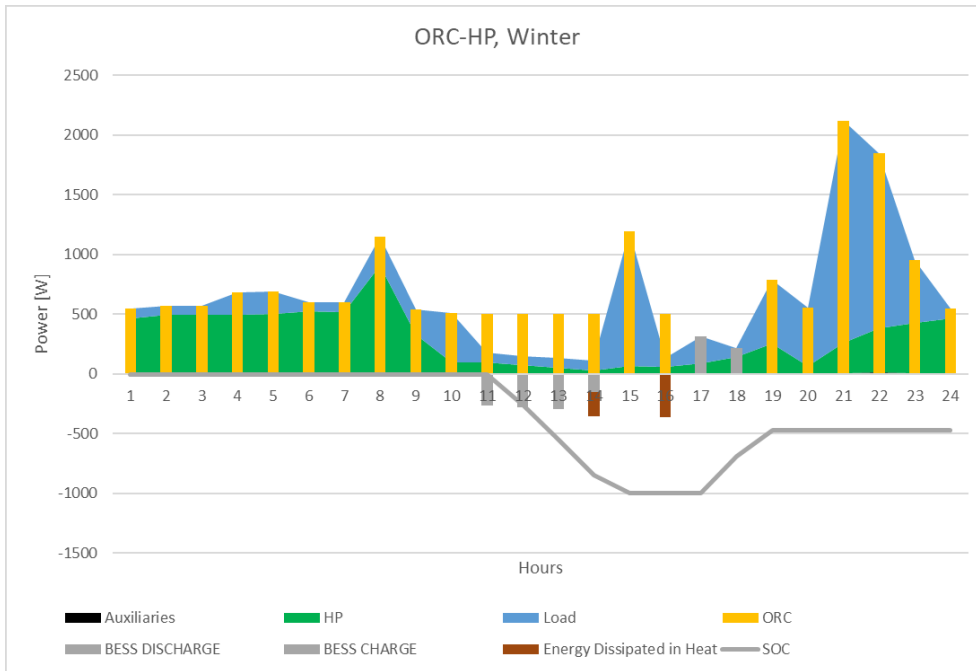- Summer chart is the same as well for both the system.

Figure 54 – Dispatching Graph of the ORC-HP system
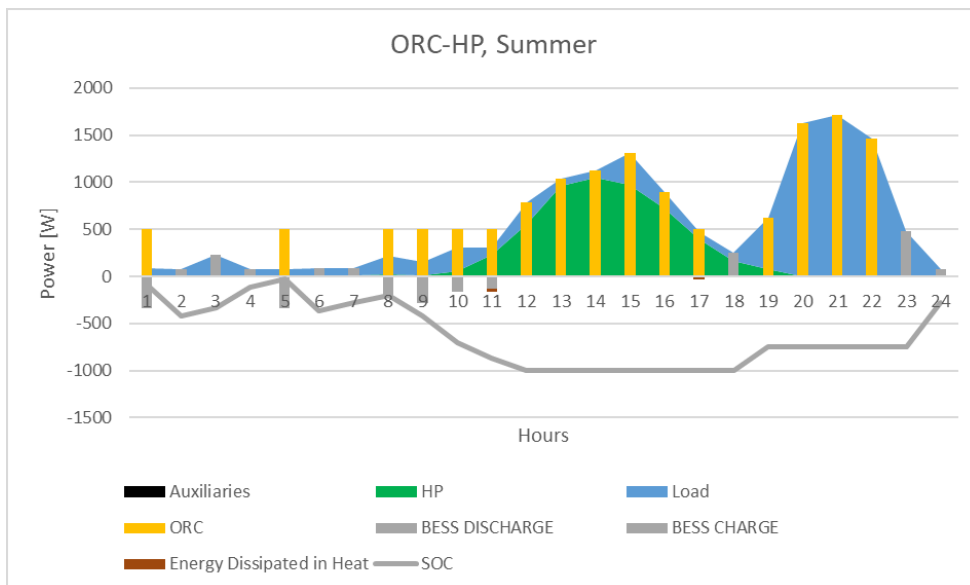
Figure 55 - Dispatching Graph of the ORC-HP system

ORC-VCC

From the Figure 56, some outcomes can be visualized:

- Electric energy dissipated in heat is largely diminished, for the winter case it is still present because of the control strategy of batteries, that should operate during morning and night time, although there is a very small load. In the winter case this is factor of penalization. This outcome highlights another time how much the seasonal load impacts on the design of the components, which is definitely a compromise between many factors.

- The batteries reduce the operations of the ORC: in terms of hours, the ORC does not operate for 4173 hours over the 8760 of the year, approximately half of the year.

- Summer graph is the same of the previous case.

Figure 56 – Dispatching Graph of the ORC-VCC system.

Thermal

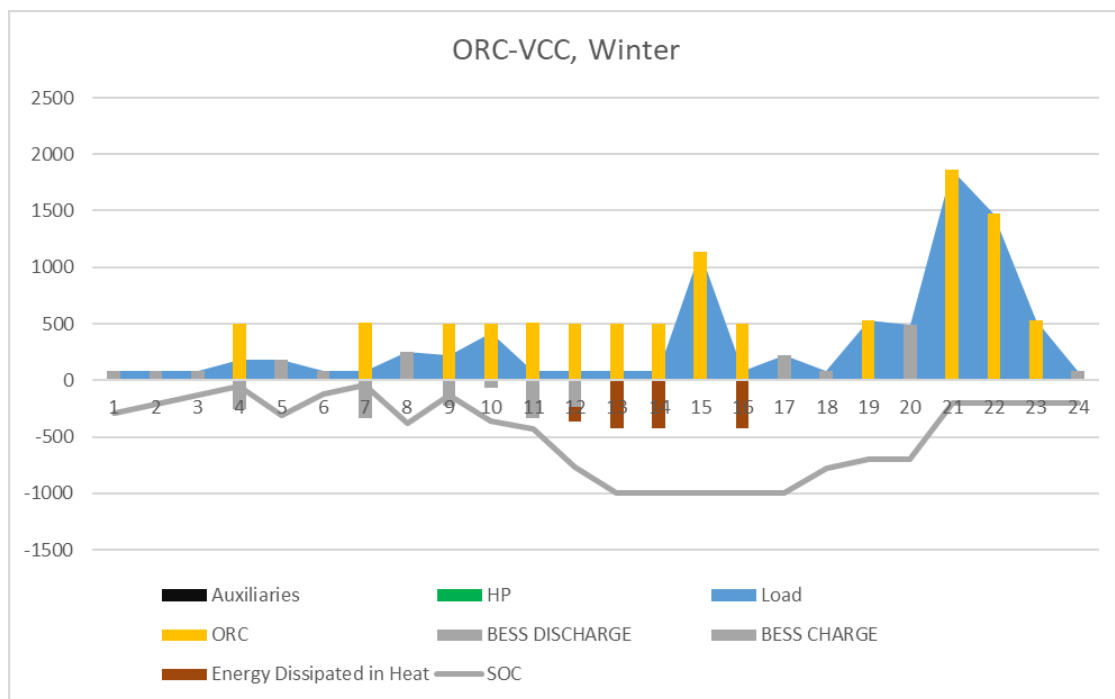Regarding the thermal dispatching graph, the same differences between space heating provided by radiators and heat pump can be noticed. The functioning of the boiler is the same, but working at a lower rated heat output.
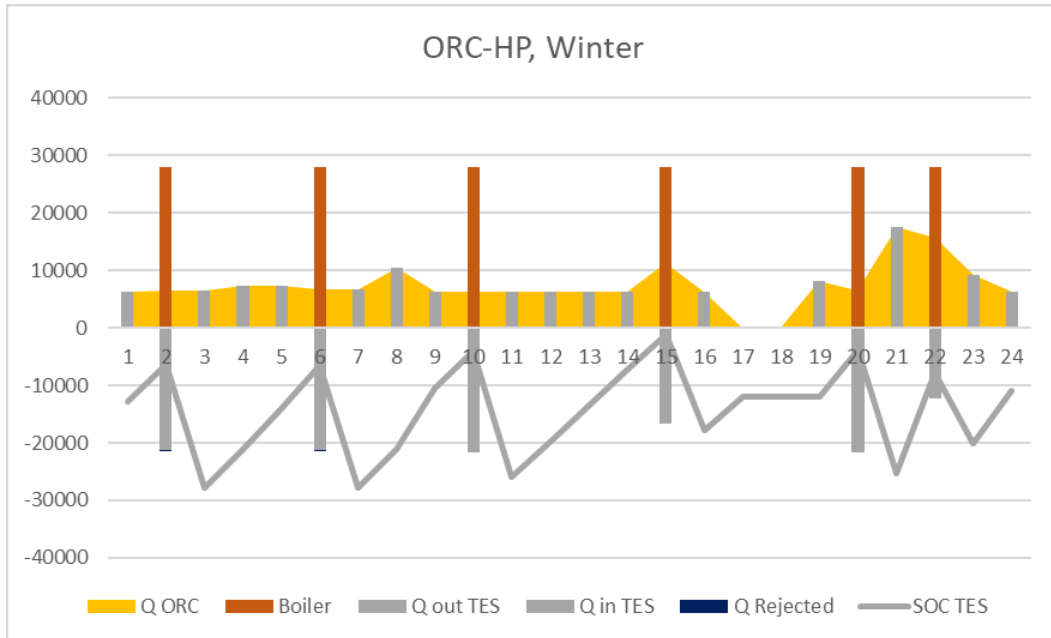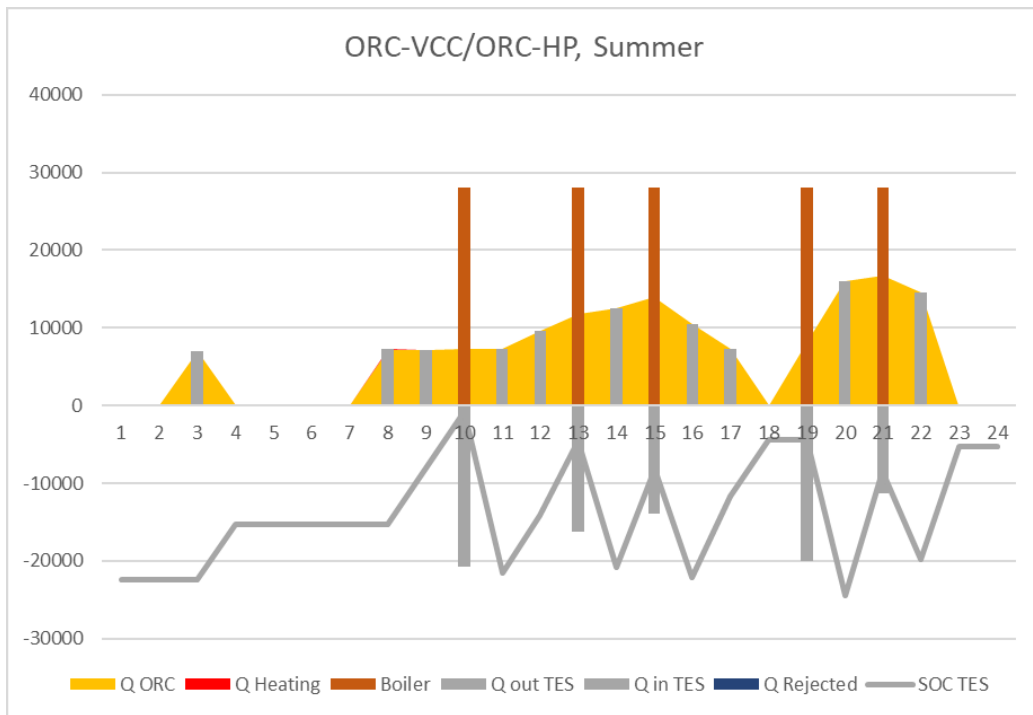

Figure 57 – Dispatching Graph of the ORC-HP system.

Figure 58 – Dispatching Graph of both the systems ORC-HP and ORC-VCC.

It is possible to notice the main innovations with respect to the previous case, without the bess in the Figure 57 and Figure 58:

- Boiler is switched off not only when the TES can cover the energy demand, but also when batteries are operating. In such case, it is possible to see that the level of the TES keeps constant because the ORC is not operating and the heat required is thus zero.
- The control strategy of the BESS is reflected also on thermal management: while it seems to fit for the summer period, allowing less functioning of the boiler, during winter it seems less appropriate, for the ORC-HP system.

ORC-VCC
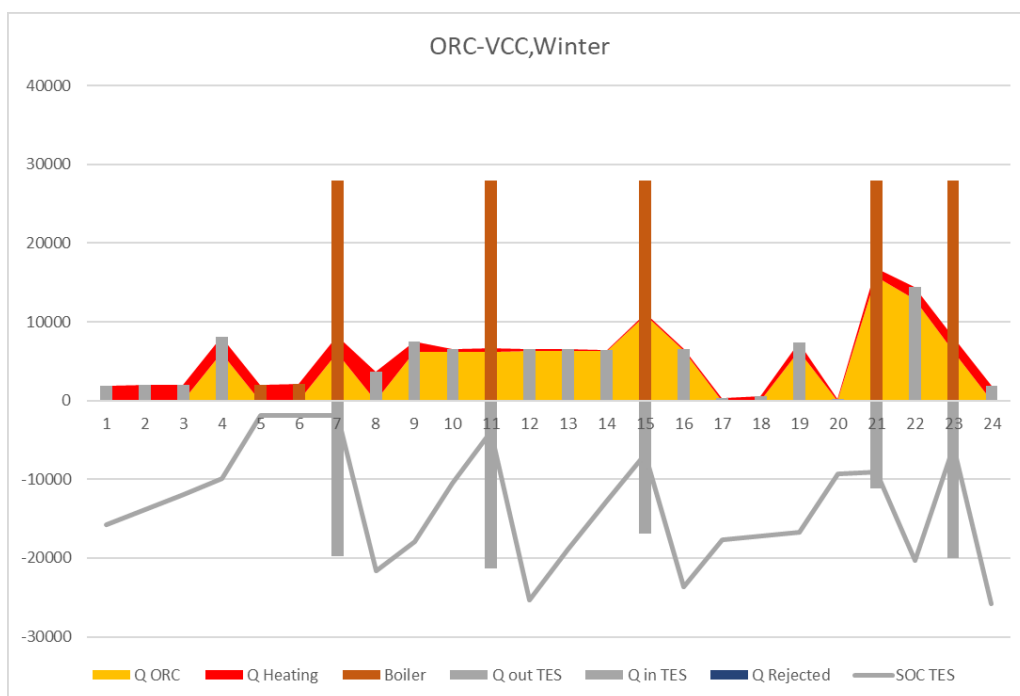
Figure 59 – Dispatching Graph of the ORC-VCC system.

- While batteries cover the electric energy demand, the TES covers the thermal energy requirement, allowing less boiler utilisation.
- It is possible to see the assumption made on the boiler operations when batteries are discharging. In fact, in such periods, the boiler can operate at lower conditions with respect to the minimum: it provides the same amount of energy, but in a smaller interval of time. This assumption is made because otherwise it would occur that the TES is saturated and fan for heat rejection must be switched on, leading to an overconsumption of BESS or, even worse, to switch on the micro ORC.

5.3 μORC + TES + Boiler + BESS + ETCs

Another way to reduce the consumption of biomass is to provide the heat input of the micro ORC with the aid of ETCs. So, it is investigated the benefits, if present, introduced by this technology if integrated with the system.

ETCs run whenever the sun radiation allows it, and try to cover the heat required both by the ORC and by the radiators. If the hot stream overcome the requirement, the surplus is stored in the hot tank.

5.3.1 Preliminary sizing

As it can be easily imagined, the introduction of evacuated tube collectors is not affecting the size of the μORC, like batteries did before. This is because they are covering the heat demand, while the electricity demand is not directly affected by their introduction. Hence the size of the two ORC is kept fixed, and for the following analysis also the battery's capacity will be kept constant, since its level of charge is directly proportional to the nominal power of the ORC.

In the cost section of the ETCs, we have presented two different specific cost of this technology, which are significantly different, approximately one order of magnitude of difference. This is reflected on the annuity, that, if calculated with the "expensive" correlation, is not experiencing any advantage, because of the extremely high specific cost (1000 €/m^2, which in nominal conditions can produce 700 Wh, while with 1000 € of biomass the production in nominal conditions is 20 MWh). So, if the specific cost of the technology is the one suggested by the IEA, it is not worthy to employ it, because no economic benefits are obtained. On the other hand, if the "cheap" specific cost is employed, the system takes advantage from the introduction of the solar panels.

As previously done, the analysis will be carried out separately for the ORC-VCC system and ORC-HP system.

ORC-HP

The first graph, Figure 60, is the biomass as a function of collectors' area and minimum of the boiler, with fixed size of the storage. The data reveal that, independently from the size of the storage, the minimum of the boiler has a very small influence on biomass consumption, while adding ETCs allow considerable savings. According to that chart, if the minimum of boiler set is not affecting significantly the biomass consumption, this could be made by different size of the storage, meaning that there could be a trade-off between the capacity of the TES, the area of collectors, and the biomass consumption.
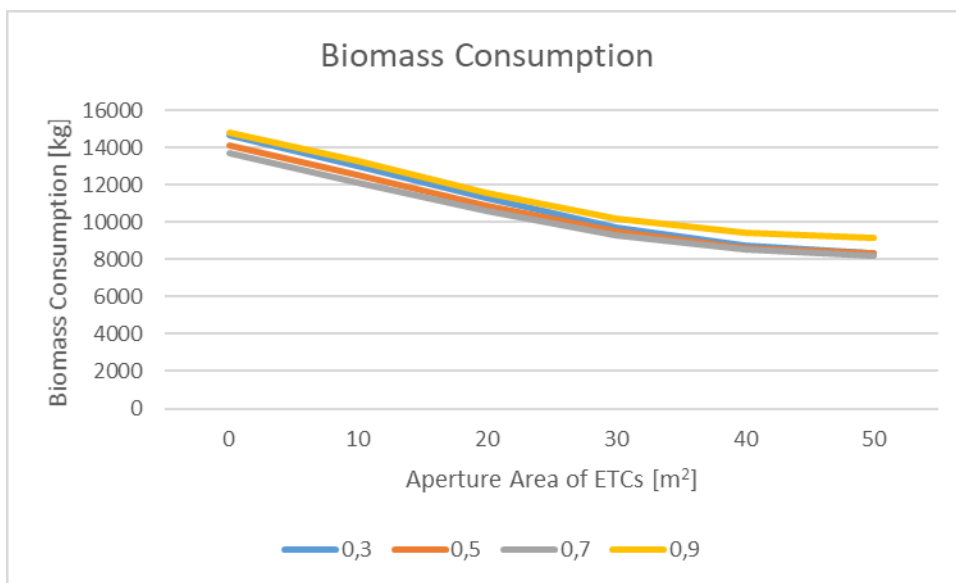
Figure 60 – Biomass consumption vs Boiler minimum and Collector Aperture Area. It is possible to notice that the influence of the minimum of the boiler is limited.

If we have a look at the annuity plotted as a function of TES capacity and area of collector, Figure 61, we could notice that the trade-off is showed, independently from the minimum set of the boiler.
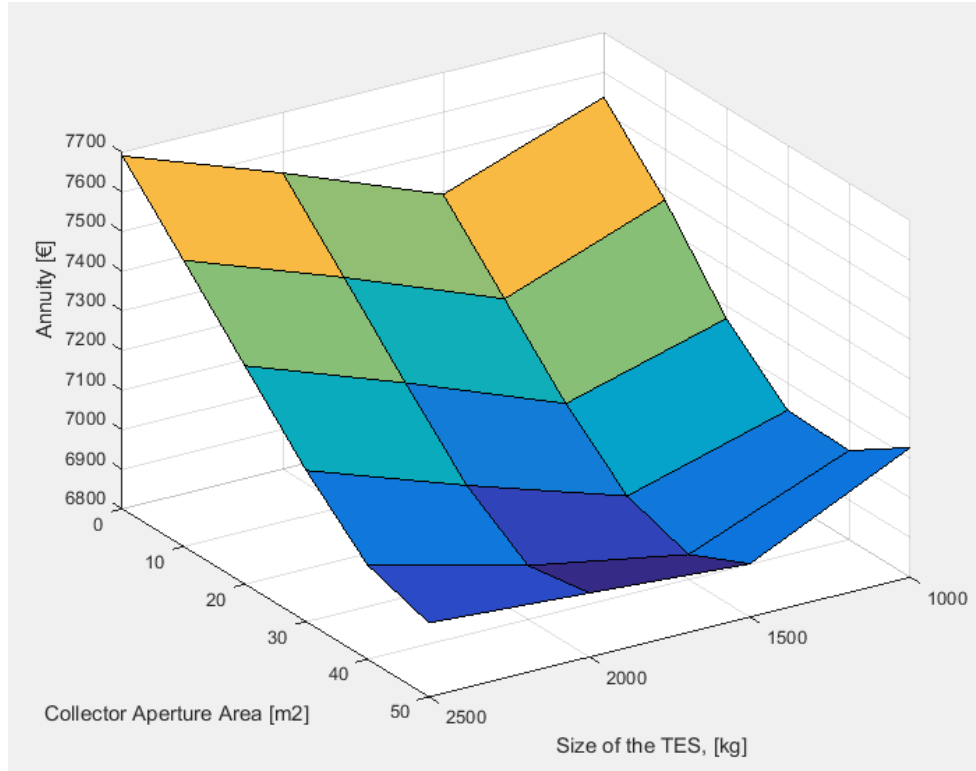
Figure 61 – Annuity map as a function of the collector's aperture area and the TES capacity. The minimum highlighted is for 1500 kg of capacity and 40 m^2 of collector's aperture area.

As it is possible to see in the next figure, once the size of the TES is selected equal to 1500, the influence of the minimum of the boiler is not very significant, and it is even lower in the minimum highlighted where all the curves collapse, Figure 62.
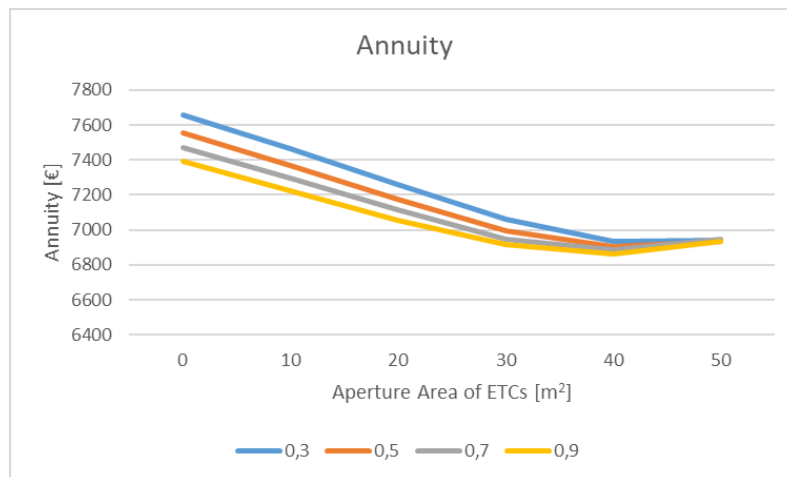
Figure 62 - Influence of minimum of the boiler on the annuity: it is noteworthy that it is not affecting significantly the annuity, expecially on the minimum at 40 m^2.

This small influence can be explained again with the heat rejection-minimum of the boiler chart: 1500 kg of TES capacity is the threshold after which there is no heat rejection.

So, the new parameters of the system are 1500 kg of TES capacity, 40 m² of collector's aperture area and a minimum of the boiler equal to 0.9. BESS capacity will not be changed, also because the electric energy dissipated in heat has decreased (20% of the surplus, -4% with respect to the previous case).

Heat rejection is increased with respect to the previous case (3,9 % of the total heat input), but is only due to the solar collectors, but still the total auxiliaries' consumption is low compared to the total energy output of the micro ORC (2,53%).

Biomass consumption is approximately halved, thanks to the high solar fraction achieved by the system: 43,6%. The annuity has been decreased by a 7%.

Table 14 – Results of the Preliminary Sizing

	Size Storage [kg]	Minimum of Boiler [%]	ORC Nominal Power [W]	η_I	Annuity [€]	Biomass Consuption [kg]	BESS Capacity [kWh]	ETCs Gross Area [m²]
ORC-HP	1500	0.9	2500	0.0891	6,863	$7.8923 \cdot 10^3$	1	54.90

The table resume the results obtained by introducing ETCs, if the cost correlation employed is the "cheap" one, in the other case it is not worthy to integrate them in the system. Moreover, the table highlights the gross area of the collectors, which is value consistent with the dimensions of the utility: for instance, the solar field could be installed also on the rooftop of the house.

ORC-VCC

The ORC-VCC shows the same results with respect to the ORC-HP system, with a minimum of the annuity in the same position, for the same hot storage capacity. So, for this system, new values for the minimum boiler set and storage size are introduced.

The system rejects approximately the 3,4% of the total heat input, the value has increased due to the introduction of collectors, but is a value close to the the other system, meaning the the preliminary sizing has led to shared results. Auxiliaries consumption is 2.8% of the energy produced by the ORC. It is higher with respect to ORC-HP although heat

rejection is less because the total energy produced by the ORC of this system is lower, since heating is provided by radiators.
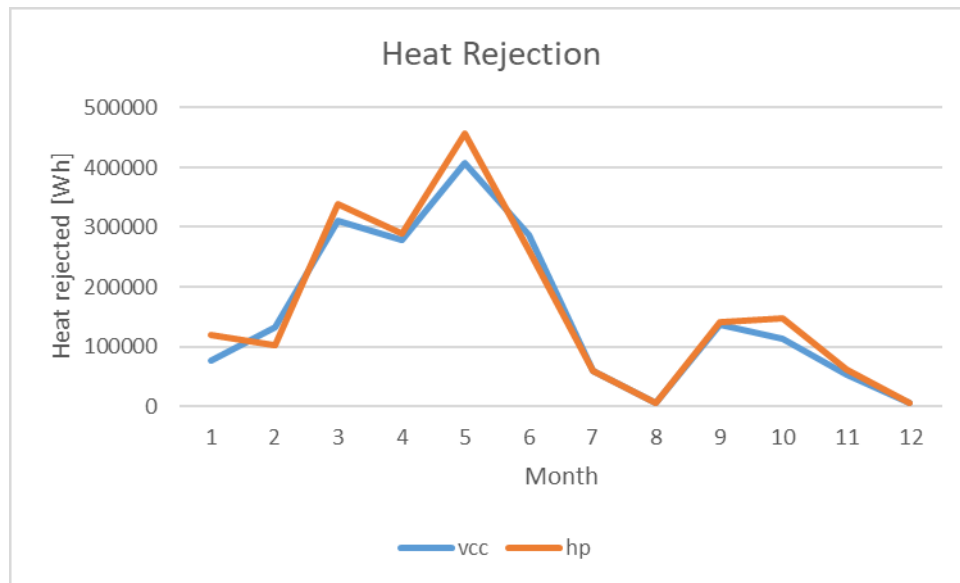
Figure 63 – Heat Rejection of the Two systems: values are approximately the same, as a confirm of the similar size of area and storage capacity.

Table 15 – Results of the Preliminary Sizing

	Size Storage [kg]	Minimum of Boiler [%]	ORC Nominal Power [W]	η_I	Annuity [€]	Biomass Consuption [kg]	BESS Capacity [kWh]	ETCs Gross Area [m²]
ORC-VCC	1500	0.9	2500	0.0879	6,595	$6.784 \cdot 10^3$	1	54.90

The annuity of the system is lower with respect to the ORC-HP due to the lower biomass consumption. With respect to the previous case, it has not experienced a significative decrease in terms of annuity, but the biomass consumption is approximately halved thanks to the high solar fraction (49.3%). The first principle efficiency has not particularly improved, because the ETCs have an impact mainly on the thermal production, and because the size of the ORC has not been changed.

5.3.2 Check of the Results

Table 16 - Tollerances on Energy Balances and Check on the Maximum of the Boiler

Check	1st Principle Energy Balance	Electric Balance	Q boiler max
Value	$<10^{-7}$	$<10^{-13}$	< 40 kW

5.3.3 Dispatching Graphs

Electricity
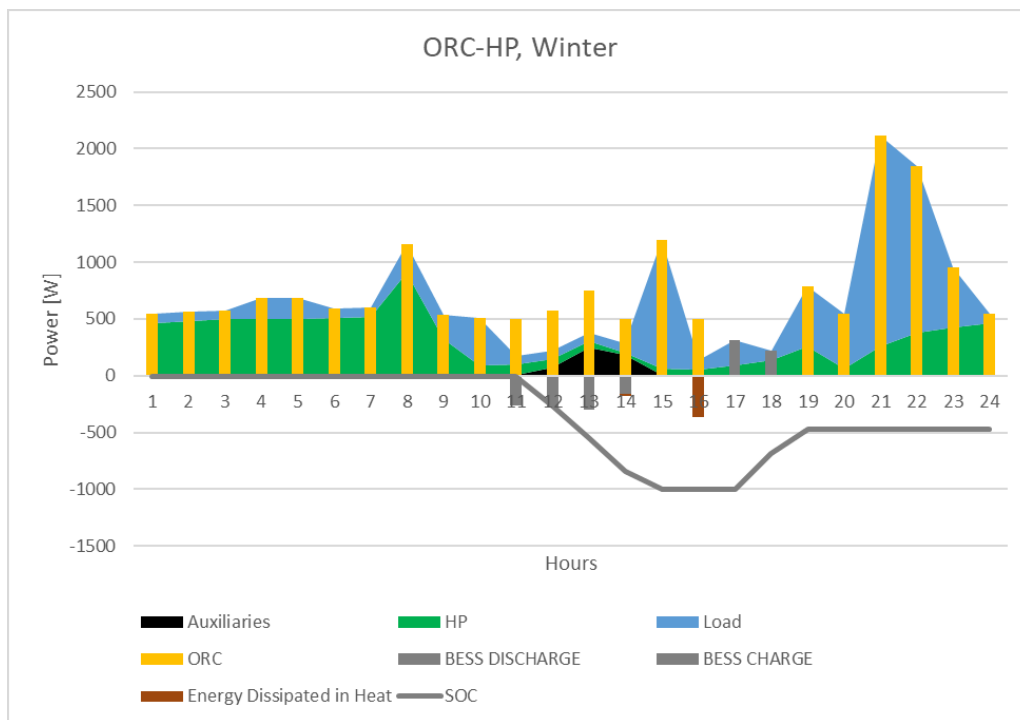
ORC-HP

Figure 64 – Dispatching Graph for the ORC-HP system

- The larger consumption of the auxiliaries is given by the fan devoted to heat rejection, but as previously said this increase does not lead to extreme power consumption.
- Batteries SOC has the same trend of the system without ETCs.
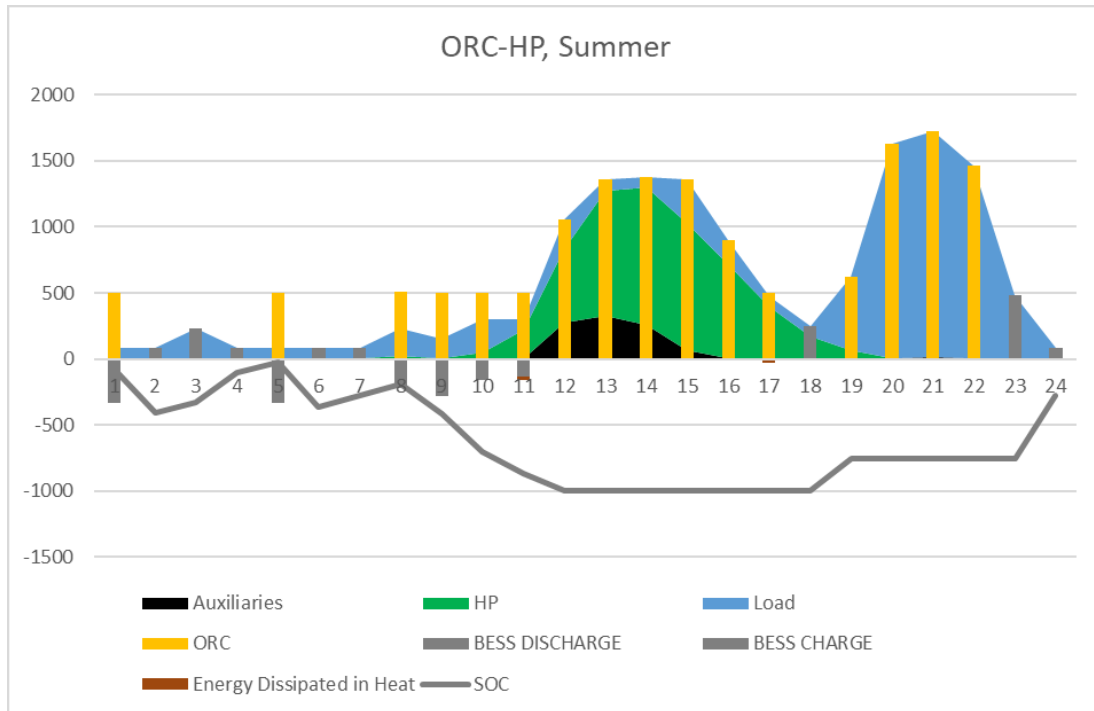
Figure 65 – Dispatching Graph for the ORC-HP system

- An increase of auxiliaries' consumption is present also in summer. The period of heat rejection is the same of operations of ETCs, meaning that they produce more heat that is possible to store, but still economically speaking, it is better to consume some biomass for heat rejection and gather more solar power with a larger collectors' field.

ORC-VCC

Figure 66 – Dispatching Graph of the ORC-VCC system

Figure 67 – Dispatching Graph for the ORC-VCC system

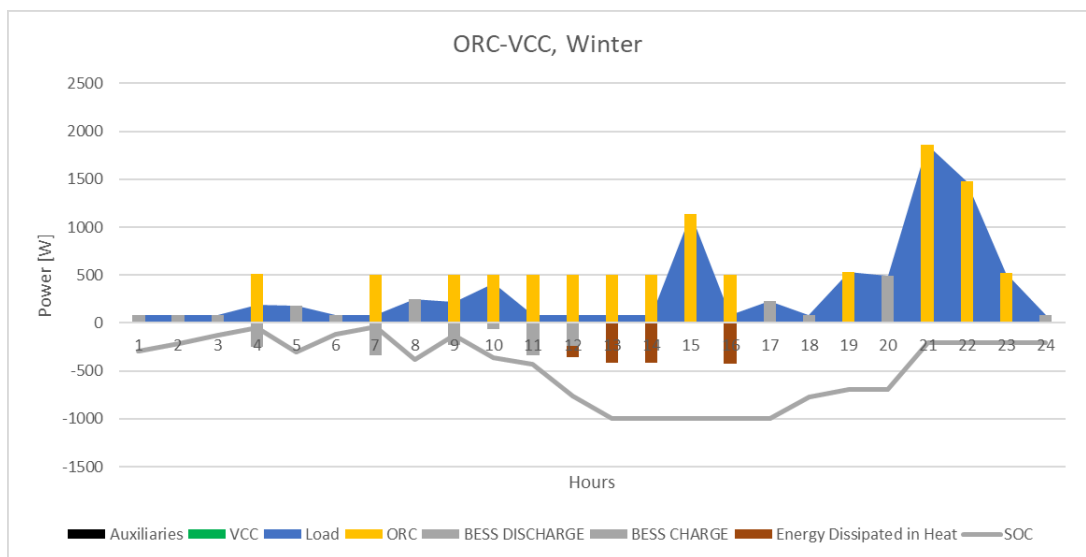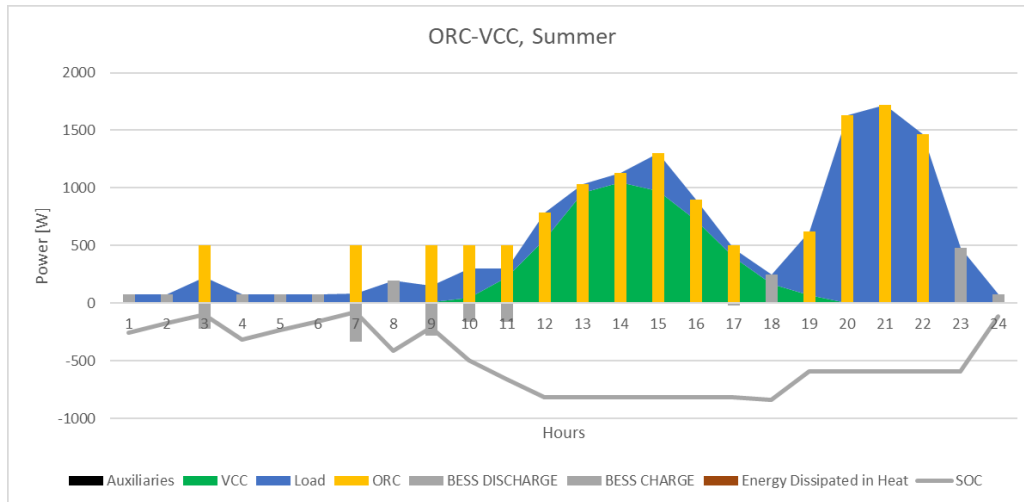- As previously showed, heat rejection is less intense for the ORC-VCC, hence in both the cases the auxiliaries are not switched on.

Thermal

ORC-HP

The Figure 68 shows the three different dispatching graphs for each season.

The most important outcomes are:

- Heat rejection is present both in winter and in summer: the collectors' field seems oversized with respect to the energy demand, but from an economical standpoint it is better to burn some biomass and reject some heat with the fan, but gather as much solar power as possible.
- Boiler operations diminish along with the seasons and with the increase of radiation availability, and thanks to a better exploitation of batteries that reduce significantly the heat demand during night time. Batteries does not seem very effective during winter: in the graph it is possible to notice that they discharge just one hour. This is because the control strategy did not take into account that peak periods for ORC-HP system are during night time in winter.
- With a bigger storage, we would be able to reject less, but at the same time, with the actual specific cost, this increase was not economically justified.
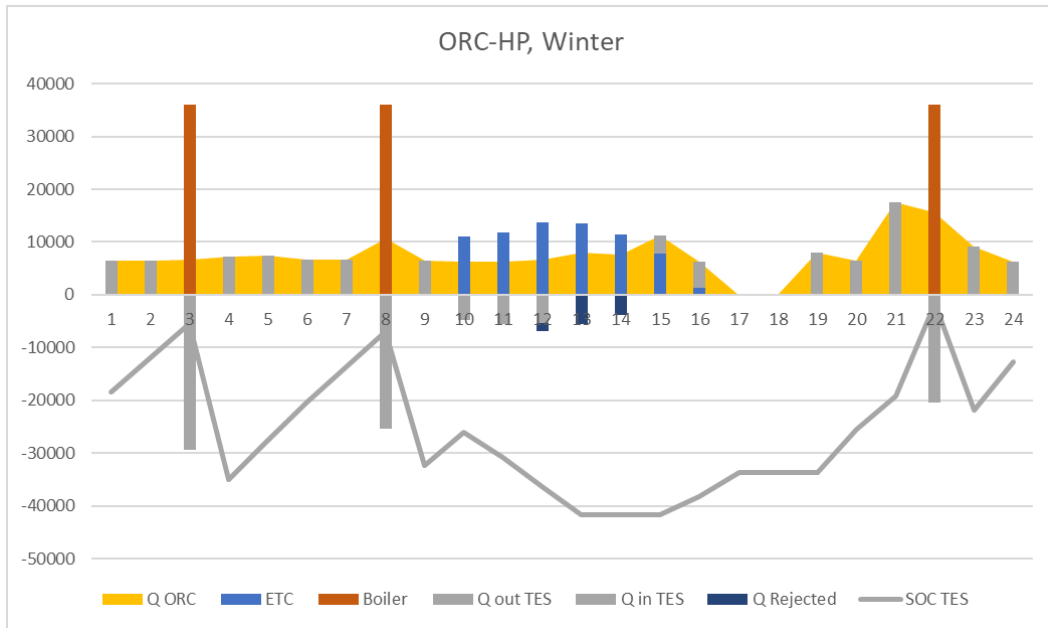
Figure 68 – ORC-HP Dispatching Graph
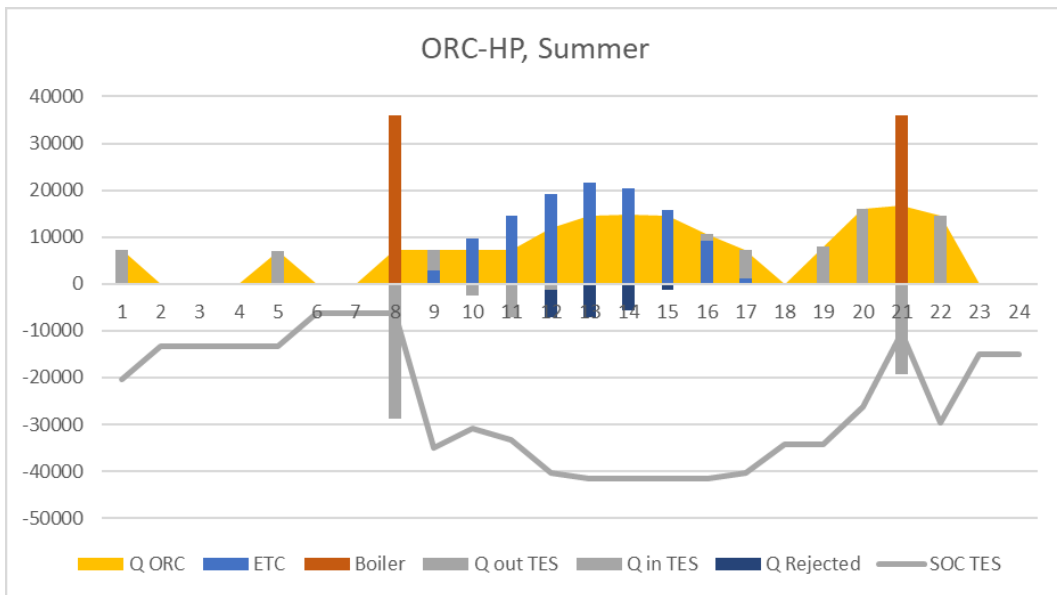
Figure 69 – ORC-HP Dispatching Graph

ORC-VCC

The most important outcomes are:

- It is possible to see the assumption made on the boiler operations when batteries are discharging. In fact, in such periods, the boiler can operate at lower conditions with respect to the minimum: it provides the same amount of energy, but in a smaller interval of time. This assumption is made because otherwise it would

occur that the TES is saturated and fan for heat rejection must be switched on, leading to an overconsumption of BESS or, even worse, to switch on the micro ORC.

- Boiler operations are drastically decreased: it is switched on only one or two times per day, even less tha ORC-HP system, that have to deal with heat rejection.

Figure 70 – ORC-VCC Dispatching Graph

Figure 71 – ORC-VCC Dispatching Graph

5.4   μORC + TES + Boiler + BESS + ETCs + PV

PV panels are integrated only with ORC-HP: this choice is justified by the higher electric consumption of the system compared with ORC-VCC, 4.6 MWh/year and 4.1MWh/year respectively. Moreove, it is more expensive with respect to the ORC-VCC, thus it has been decided to investigate on this last integration.

Pv panels will produce electric energy, and if larger than the demand, they cover it and the surplus is stored, otherwise they just charge the batteries.
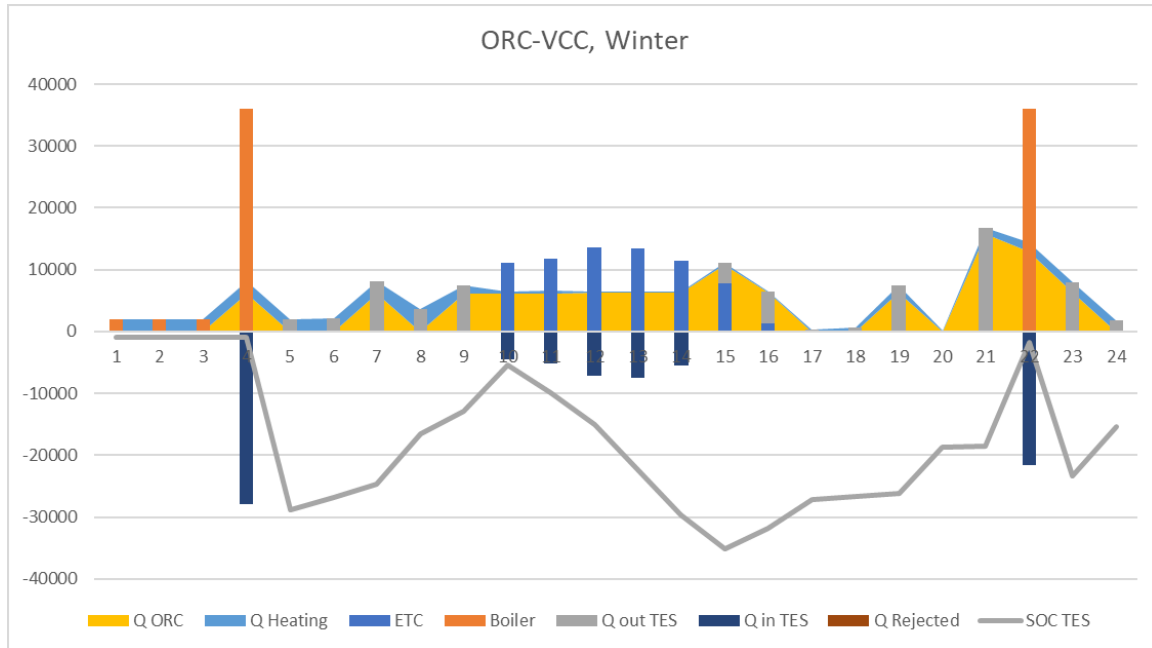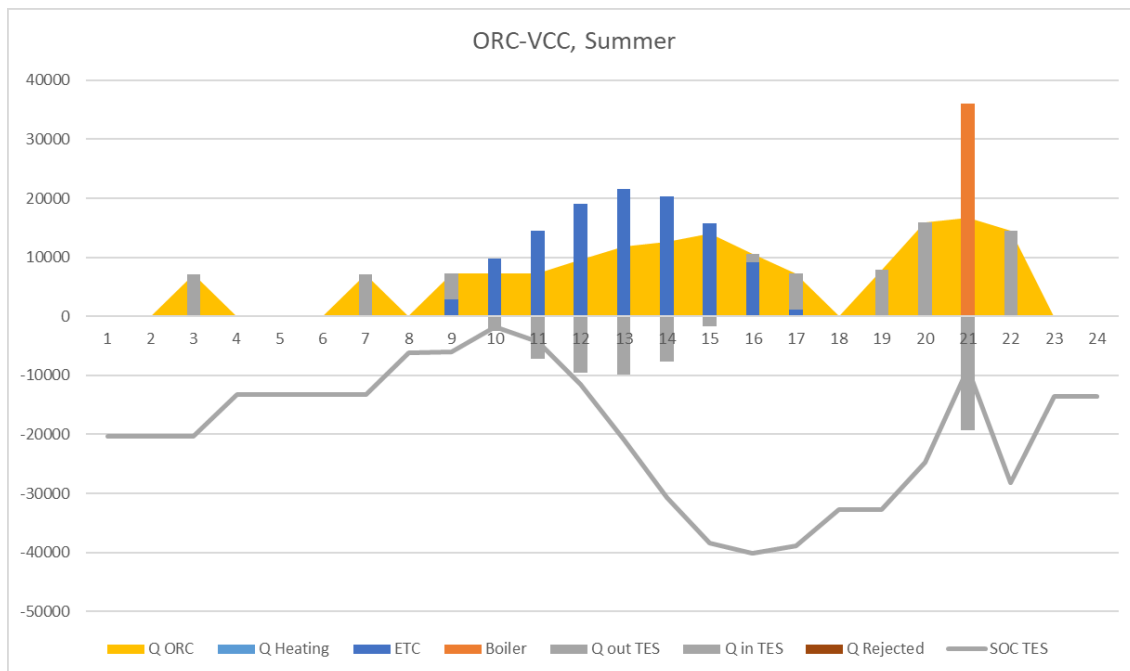
5.4.1   Preliminary design

PV panel will affect the electric dispatching; hence, we want to investigate if there is the chance to lower the ORC nominal power thanks to the introduction of PV panels, keeping the yearly unmet load equal to zero. In this case, it seems reasonable to lower down the ORC nominal power with respect to the previous case, for two main reasons:

- There is another device devoted to electric energy production
- Batteries can be charged also by the PVs, and discharge whenever the ORC can cover just part of the demand.
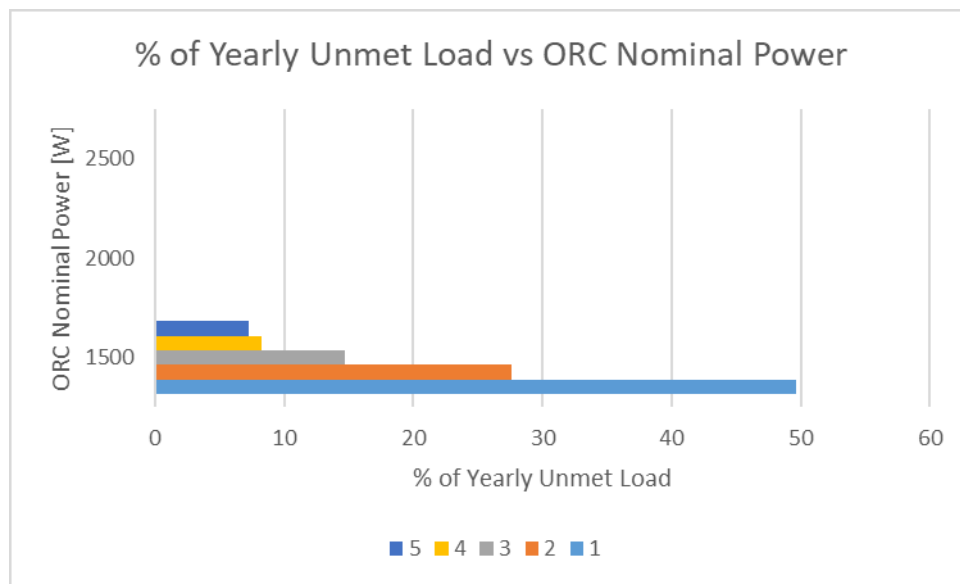
Figure 72 – Percentage of Yearly Unmet Load for different ORC nominal Powers and different number of PV panels.

This chart has been made for 1 kWh of BESS capacity: BESS system lowers the percentage of unmet load, but not as deeply as the PV panel. From the figure it is possible to notice that the introduction of 1 photovoltaic panel allows to reduce the nominal power of the micro ORC by 500 W, in fact, the unmet load is still equal to zero with 2 kW of

micro ORC nominal power. On the other hand, still with 5 panels the unmet load is 7% if the nominal power of the ORC is lowered by 1 kW.

Table 17 – Annuity and Percentage of Unmet Load for the 1.5 kW micro ORC as a function of BESS capacity and Number of Panels

Annuity [€] / Unmet Load [%]		Number of Panels				
		1	2	3	4	5
BESS Capacity [Wh]	1000	6163 / 49%	6192 / 27%	6257 / 14%	6338 / 8%	6407 / 7%
	1500	6215 / 45%	6238 / 20%	6310 / 4%	6390 / 1%	6458 / 0%
	2000	6281 / 43%	6300 / 15%	6371 / 3%	6450 / 1%	6519 / 0%
	2500	6349 / 43%	6365 / 14%	6435 / 2%	6517 / 1%	6584 / 0%

From Table 17 it is possible to notice that there is the chance to have an unmet load equal to zero with at least five panels and 1.5 kWh BESS capacity for a micro ORC with 1.5 kW of nominal power. The equivalent annuity is 6458€, which is slightly decreased with respect to the system without PV (6595€), while for bigger size of BESS it overlaps with the case without PV. Furthermore, the annuity for larger size of micro ORC is equivalent to the case without PV.

Since the maximum power of the ORC would be 1500 W, the maximum heat input given by the boiler, i.e. the size of the boiler, can be lowered. According to the results of the simulation, the maximum heat input required by the ORC is 20 kW, that is half of the estimated capacity at the beginning of the simulation. According to this new value, ETCs field area, TES capacity and finally the minimum of the boiler set, should be designed.

With a simple calculation it is possible to estimate the maximum amount of surplus hot stream given by the boiler working at its minimum, which is given for the highest minimum boiler set, i.e. 0.9:

$$M_{boiler} = \frac{\dot{Q}_{boiler}}{c_p \Delta T_{storage}} \cdot 3600 \cdot 0.9 = 648 \, kg$$

Thus, it is meaningless to analyse scenarios with TES capacity larger than 1000, because they lead to higher costs without introducing significant benefit. Here are presented two different charts, as a function of the minimum set and collectors'area: the first refers to a TES capacity equal to 500 kg and the second one to a TES capacity equal to 1000 kg.

Figure 73 shows that is not wothy to operate with a high minimum boiler set because it would exceed the TES capacity, leading to a waste of fuel. In fact it is the most expensive scenario.
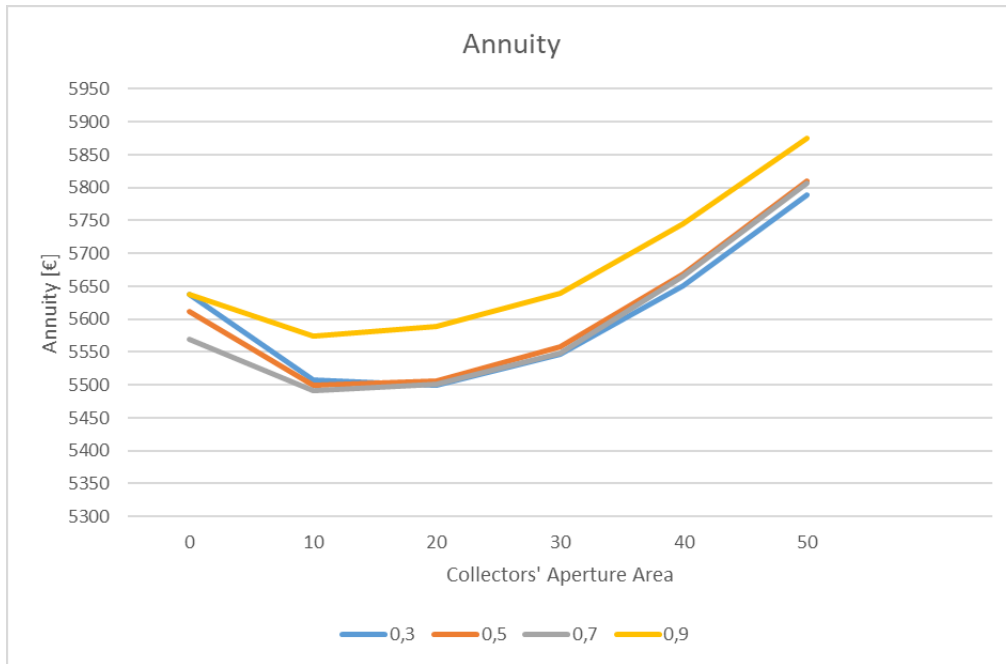
Figure 73 – Annuity for a TES capacity equal to 500 kg. The minimum is for 10 m^2 of collectors'area. Moreover, it is noteworthy that with such capacity it is meaningless to run the boiler at high minimum set, because a significant amount of the heat is rejected by the fan.

Since the maximum amount of hot stream produced by the boiler at the highest minimum set is lower than the TES capacity, Figure 74 shows that it is worthy to operate it at 0.9.
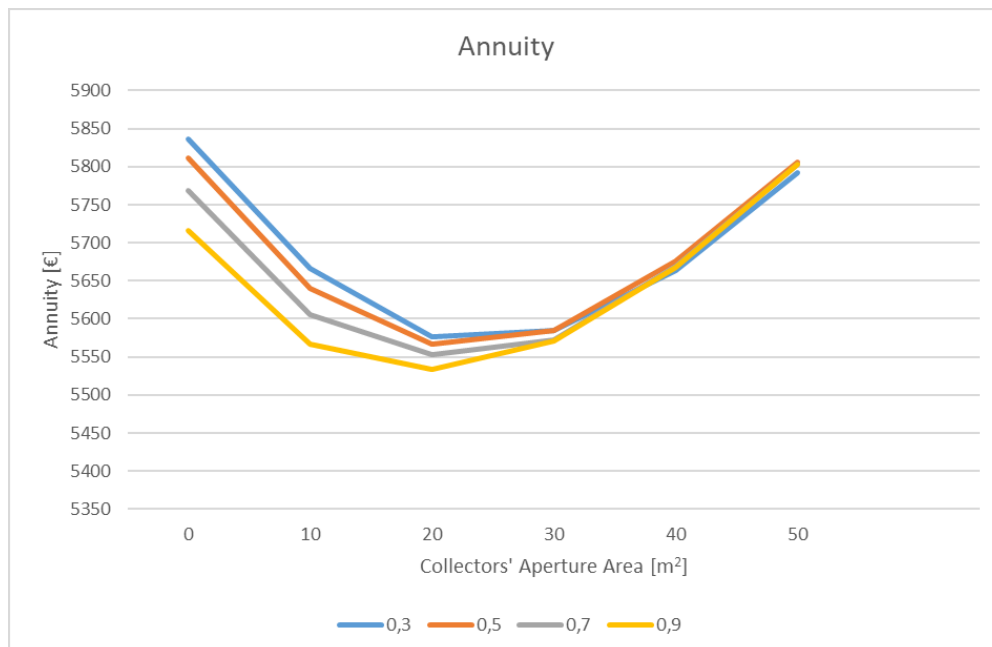
Figure 74 – Annuity for a TES capacity equal to 1000 kg. For a bigger TES capacity, the minimum obviously shifts towards higher values of collectors' area.

The increase of TES capacity does not lead to economic benefits: in fact, it is possible to notice that the cheapest scenario is for 500 kg of TES capacity and 10 m^2 of collectors' aperture area.

With respect to the case without PV panels we can state that the system is lighter and more compact: a smaller engine, a smaller hot storage, and a smaller collectors' field. Moreover, thanks to the reduction of the μORC nominal power, the engine operates closer to its nominal condition, leading to higher LF and higher efficiency. For such system the efficiency raises up to 0.1025, the new LF is equal to 56%, while biomass consumption has incresed due to the reduction of collectors' area that leads to lower solar fraction (16%).

Table 18 – Results of the Preliminary Sizing

	Size Storage [kg]	Minimum of Boiler [%]	ORC Nominal Power [W]	η_I	Annuity [€/y]	Biomass Consuption [kg]	BESS Capacity [kWh]	ETCs Gross Area [m^2]	PVs Gross Area [m^2]
ORC -HP	500	0.7	1500	0.1025	5,499	$8.1036\cdot10^3$	1.5	16.60	8.125

5.4.2 Check of the Results

Table 19 - Tollerances on Energy Balances and Check on the Maximum of the Boiler

Check	1st Principle Energy Balance	Electric Balance	Q boiler max
Value	$<10^{-7}$	$<10^{-13}$	< 20 kW

5.4.3 Dispatching Graph

Electricity

The most important advantage introduced by the PV is the chance to switch off the μORC and having always fully charged batteries that are able to support the engine while it is running at its maximum and to cover an eventual missed load, as its is possible to notice in the peak of the dinner, Figure 75.
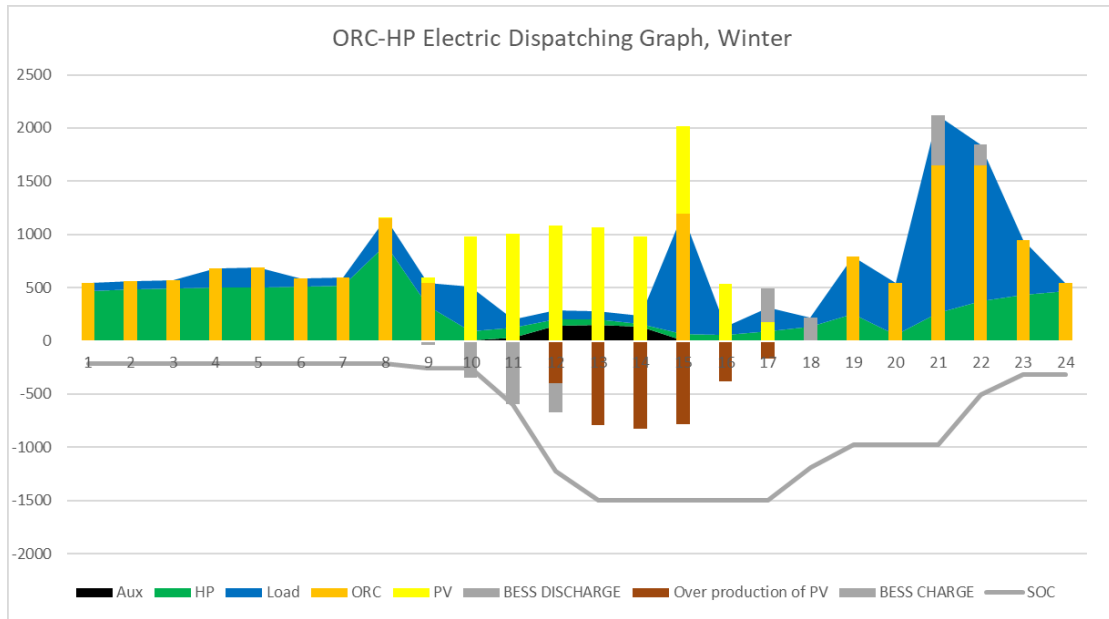
Figure 75 – Dispatching Graph of the ORC-HP, Winter

On the other hand, 5 panels seem to be too much, the over production of PV panels is approximately half of the power produced (54%), or alternatively it should be developed a better control strategy that integrate better BESS with PV. Moreover, heat rejection, although it is present, is powered by the PV panels without consuming biomass.
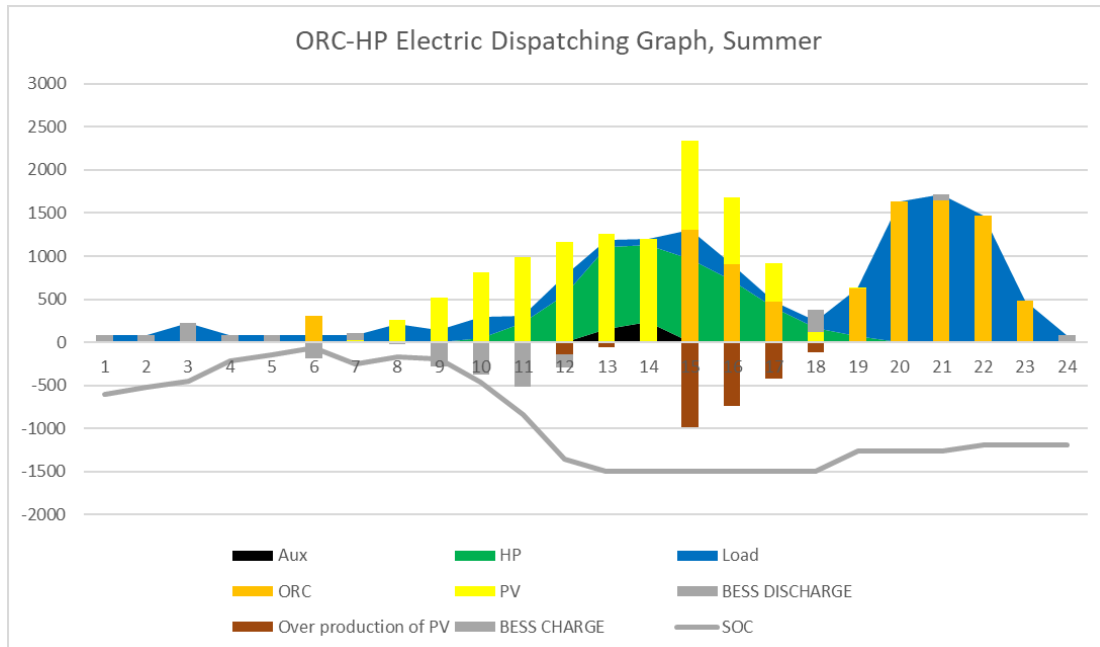
Figure 76 – Dispatching Graph of the ORC-HP, Summer

During summer, PV panels meet the energy demand of the peak of mid-day. Morevoer, they are able to fully charge the batteries that discharge during base load of night time, avoiding costly operations at part load of the micro ORC.

Thermal

The heat rejected by the system is concentrated in winter, because demand and production are shifted and a small TES has been selected to minimize the annuity, i.e. it is not possible to store thermal power and keep it for the dinner peak. There is also a smaller fraction in summer, but in both cases, are powered by the PV.

The boiler is switched on more often on winter mainly because the base load during night time is higher, and renewable sources are not operating in such period, and the storages, both thermal and electric are almost empty, or not sufficiently charged. Moreover, according to the new TES capacity, boiler operates more often because the TES can not store energy for many hours due to its smaller dimension.

Figure 77 - Dispatching Graph of the ORC-HP, Winter

Figure 78 – Dispatching Graph of the ORC-HP, Summer

5.5 PV+BESS

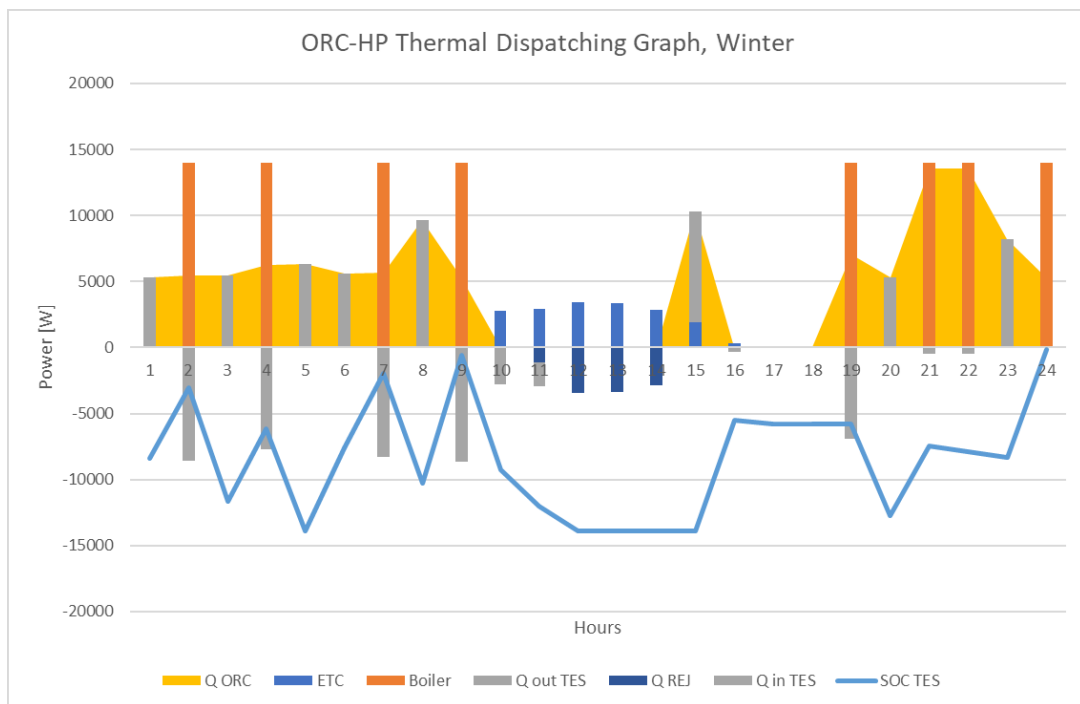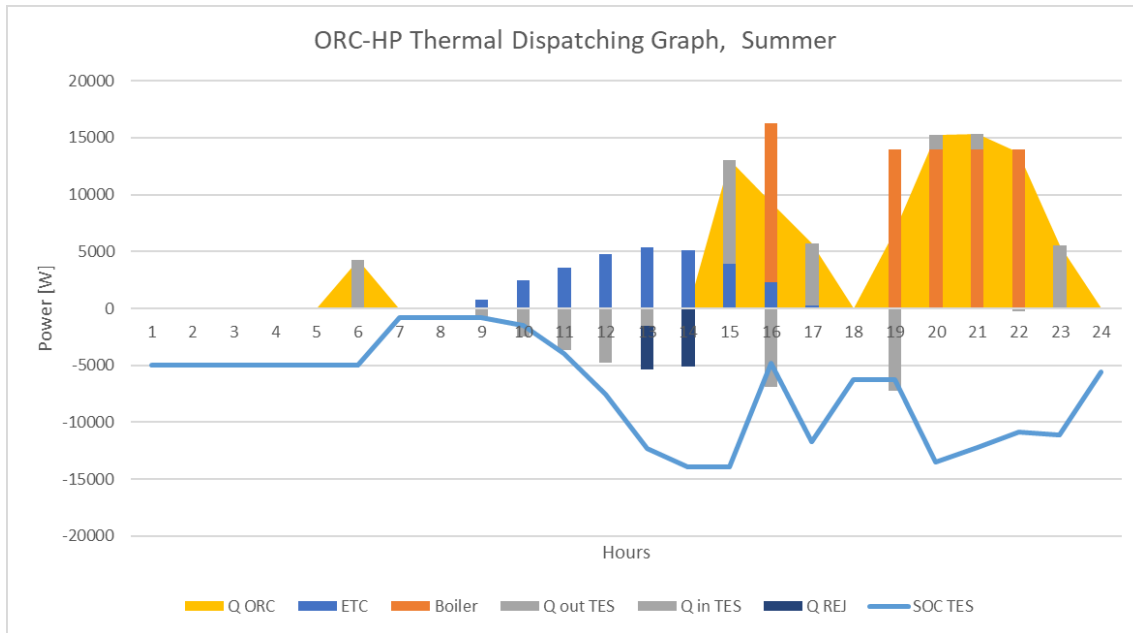The results of the Photovoltaic field coupled with batteries can be easily summarised in one chart, Figure 79.

The figure shows dot-dashed iso-percentage of unmet load compared with the annuity of the system.

In the range of annuity of the micro ORC plant, the system shows a a reliability in the range of 90-95%. The number of panel required to obtain such reliabilities ranges between 25-30, which is quite high and, most important, extremely bulky: it means a gross area approximately equal to 50 m^2. Moreover, the energy produced throughout the whole year is three times the energy demand. This is a consequence of the shift between the production and the consumption, which is not coupled, leading the system to a high production during mid-day to cover the dinner peak and nigh-time base load. Moreover, the data of the radiation includes also cloudy day, or zero-irradiation day, meaning that according to the input, the panels should provide maybe more than a single day energy demand: in fact, the most important drawback of such technology is the non-dispatchability.

Batteries' dimension is still reasonable, because it is approximately 20 kWh, i.e. two Tesla PowerWall 2 for instance.

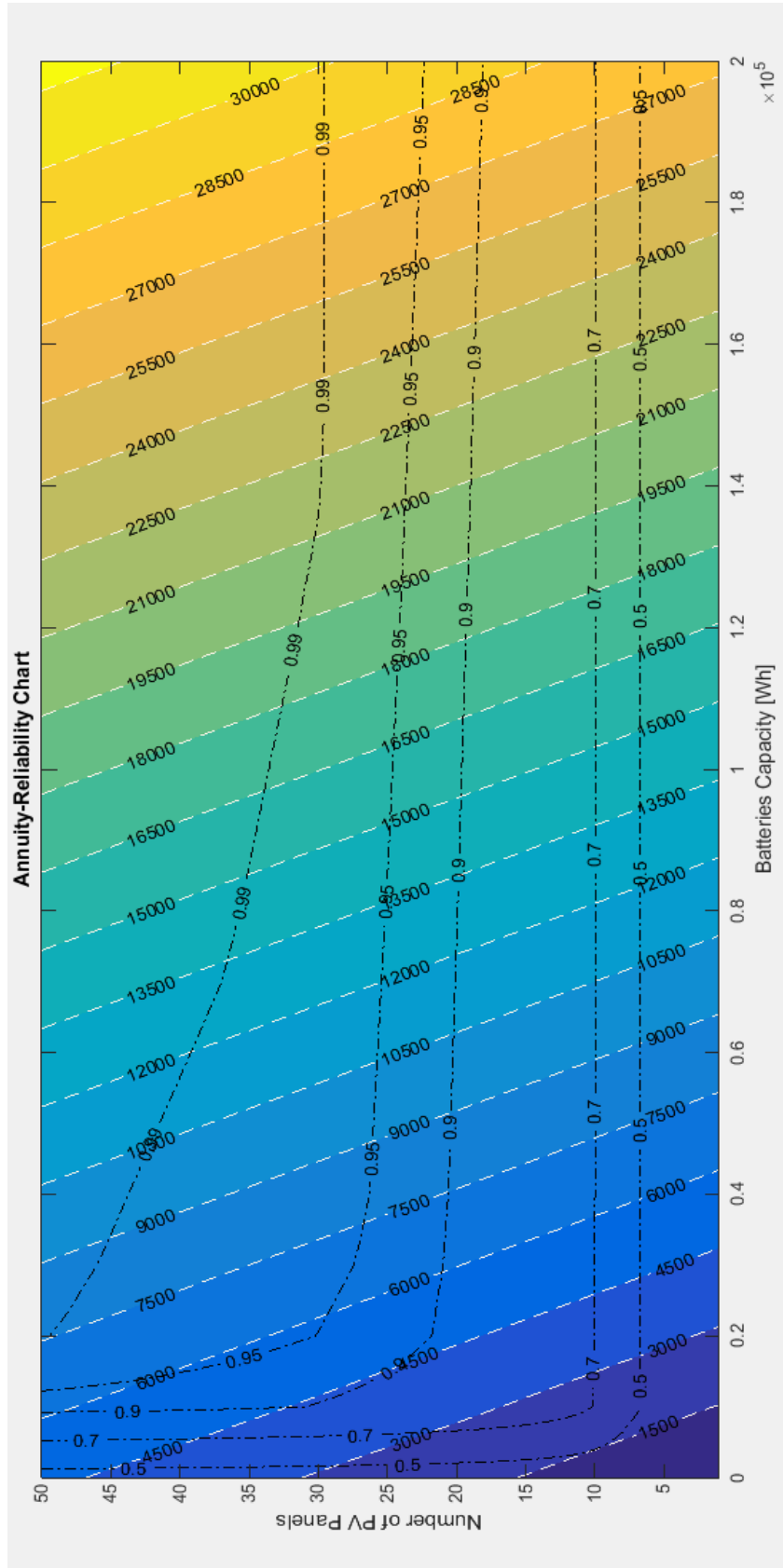Dispatching graphs are not presented because they are trivial.

Figure 79 – Annuity-Unmet Load Chart.

6 Results Discussion and Conclusions

The result of the preliminary design confirms that fully renewable plants are not economically sustainable without subsidies. This is even more evident looking at the annuity of the different plant layouts presented, which are quite high, despite the benefits introduced by a trigeneration system, able to provide all the needs of the utility. This is even more true in the economic scenario of Greece: an economy which is slightly recovering from the financial crisis, that in the past had a system of feed-in tariffs and incentives for such plants, but nowadays is burdened by the public debt and austerity measures. Looking at the annuity of the systems it is possible to notice how different are the weights of variable and equipment costs according to the degree of renewable introduced. The equipment cost is a portion that can cover the 50% of the annuity, and if not subsidised it is not affordable: it is reflected also on the LCOE of the best system which is still five times the actual cost of electricity in the NIIs provided by the diesel generators.

As first it has been analysed a simple layout, considering only the ORC, the TES and the biomass boiler, that should be able to provide a reliability of 100%. The system is a 2500 W of nominal power of the micro ORC, a TES capacity of 1500 kg and a biomass boiler as back-up with a a nominal thermal power output equal to 40 kW; the annuity is 8064 €/y for ORC-VCC and 7995 €/y for ORC-HP. The main drawback was the electric energy surplus dissipated in heat given by the limitations of the engine. It has been tried to include BESS, which introduces benefits to the system, maily expressed by the biomass consumption, which decreases. The capacity of battery installed is 1 kWh for each system, which leads also to a smaller TES (1000 kg). They experience a decrease in the annuity equal to 7073 €/y for the ORC-VCC and 7301 €/y for the ORC-HP respectively. To obtain a further reduction of biomass consumption, ETCs have been investigated and 40 m^2 is the aperture area which minimise the annuity (if coupled with a bigger TES, i.e. 1500 kg), which are 6595 €/y for the ORC-VCC and 6863 €/y for the ORC-HP respectively. ORC-HP shows higher annuity, also because the electric energy required is higher due to yearly HP operations, thus leading to the integration of PV panels, which are able to provide electric energy without fuel consumption. The employment of PV panels involves a reduction of the nominal power of the micro ORC (1500 W), hence a reduction of the biomass boiler (20 kW) and of aperture area of the ETCs (10 m^2), thus a reduction of TES capacity (500 kg). On the other hand, batteries capacity is increased to better exploit the energy gain introduced by PVs (1.5 kWh). The annuity of the system is 5499 €/y.

The best system, economically speaking, is the micro ORC with the highest integration of renewable, but it is true also in terms of dimensions, because it must be kept in mind that the solutions investigated are targeted to a single-family utility. The PV panels plus the ETCs gross area is approximately 23 m^2 which is perfectly compatible with the roof of the house, as well as the TES capacity, which is 500 kg.
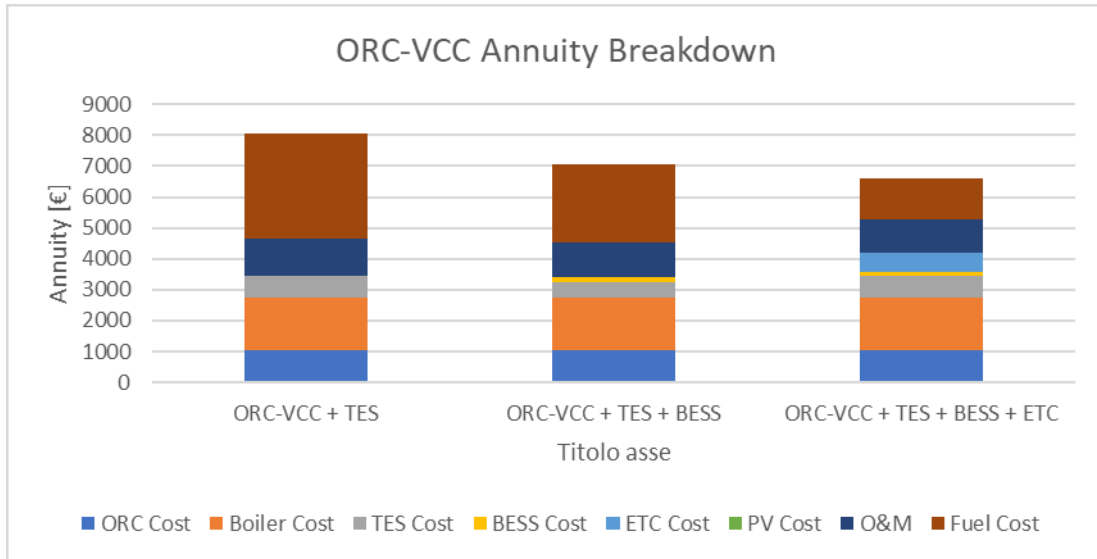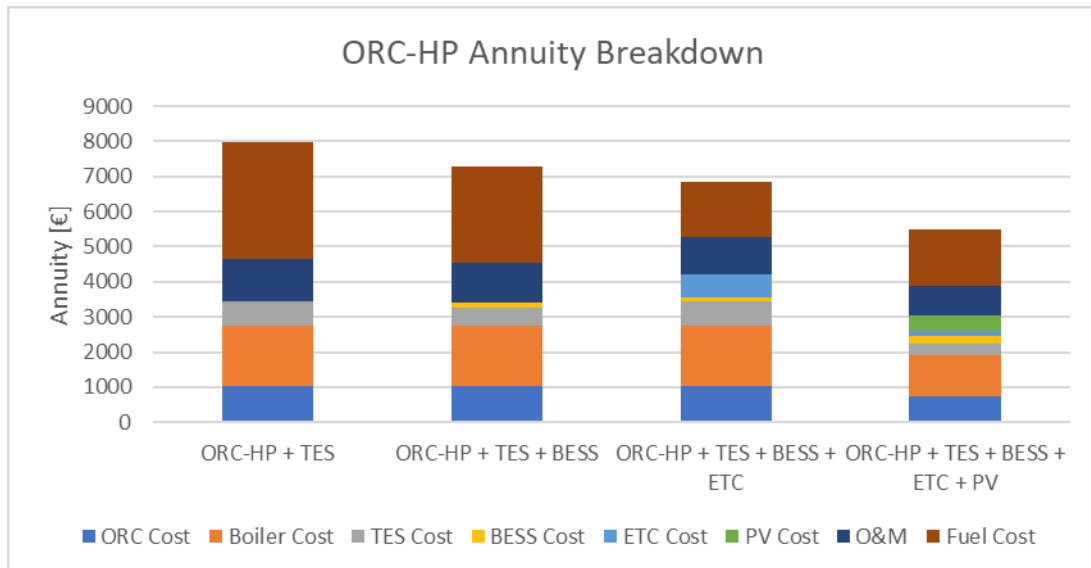

Figure 80 – Annuity Breakdown of the ORC-VCC system.

Figure 81 - Annuity Breakdown of the ORC-HP system.

Figure 80 shows the annuities, which decrease increasing the degree of integration of renewables: this is mainly due to the trade-off between the biomass consumption and the cost of the new item, since fixed cost like ORC and biomass boiler keep constant.

In Figure 81 it is possible to notice the same trend, but a consistent reduction of the annuity is given by the reduction of the size of the micro ORC and boiler.

The annuities analised for the PV-BESS plants refer to a 20,25,30 panel, with fixed 20 kWh BESS capacity, as showed in Figure 82.
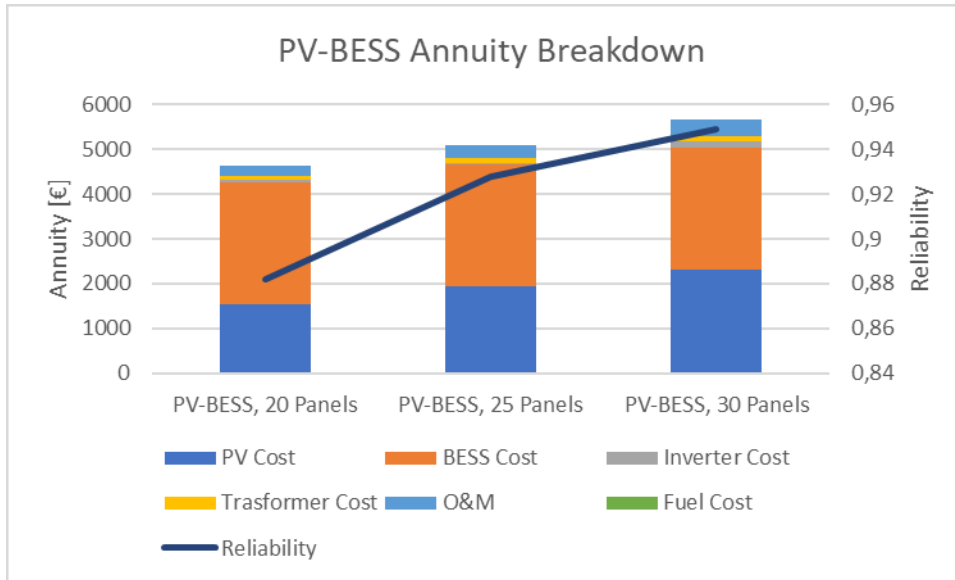
Figure 82 – Annuity Breakdown of the PV-BESS systems and their reliability.

From Figure 79 it is possible to notice that after a certain threshold the BESS capacity is affecting the reliability no more, and in the range of annuity considered the threshold was approximately 20 kWh.

A final remark should be done regarding the control strategies of the components. The control strategies and heurisitcs were not optimal for the system considered, many improvements should be done, which could lead to even higher lowering of the annuities. BESS control strategy should be made seasonal for the ORC-HP system, while it is fitting for the ORC-VCC system. Also, PVs control strategy can be improved: for instance, it could be interesting to evaluate the benefits of PVs if instead of charging the batteries when they are not able to cover the electric load, they lower the load for the micro ORC. Control strategies deeply affects the biomass consumption and the operations of each component.

7 Nomenclature

Acronymis

BESS	Battery Energy Storage System
BOP	Balance Of Plant
CCHP	Combined Cooling Heating and Power
CHP	Combined Heat and Power
COP	Coefficient of Performance
CRF	Capital Recovery Factor
DoF	Degree of Freedom
ETC	Evacuated Tube Collector
HP	Heat Pump
HTF	Heat Transfert Fluid
LCOE	Levelized Cost of Electricity, USD/MWh or USD/kWh
LF	Load Factor
MF	Mass Fuel
ORC	Organic Rankine Cycles
OTEC	Ocean Thermal Energy Conversion
PB	Power Block
PV	PhotoVoltaic panel
R&D	Research and Development
SF	Solar Fraction
TES	Thermal Energy Storage
USD	United States Dollar
VCC	Vapour Compression Cycle
WHR	Waste Heat Recovery

Nomenclature
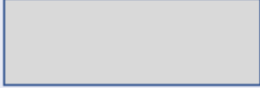
A	Surface, m^2
Cost	cost, €
Cp	constant pressure heat capacity, kJ/kgK
E	energy of the batteries
G	Radiation
M	Mass of fluid in the storage, [kg]
p	pressure, bar
Pel	Electric Power
Q	Thermal Power, kW or MW
T	temperature, °C
U	global heat transfer coefficient, kW/(m2K)
V	volume flow rate, m^3/s

W	power, kW or W
β	tilt angle
η	efficiency
ϑ	Zenith angle, or incidence angle
ρ	Density, kg/m^3

Subscripts

0	optical efficiency, referred to the ETCs efficiency
amb	ambient conditions
aux	auxiliaries
ava	available
batt	batteries
boiler	boiler
coll	collector
cond	condensation (condition) or condenser (plant component)
d	diffure
diss	dissipated
eva	evaporator
gen	generator
htf	heat transfer fluid
i	incident, referred to Radiation, otherwise hour "i"
I	first law
II	second law
inv	inverter
Lorentz	Lorentz efficiency
loss	dispersion to the environment
max	maximum
mec	mecanical
min	minimum
ml	mean logaritmic
nom	nominal
pp	pinch point
rej	rejected
req	required
spec	specific
sto	storage
th	thermal
tot	total
trasf	trasformer
wf	working fluid
z	zenith

Flow Chart Legend	
	Input Data
	Function or Equation
	Choice
	Output

8 References

[1]   IEA, "International Energy Outlook 2017," 2017.

[2]   "Bruntland Report."

[3]   "KYOTO PROTOCOL TO THE UNITED NATIONS FRAMEWORK CONVENTION ON CLIMATE CHANGE," 1998.

[4]   European, "What is Horizon 2020? - European Commission." [Online]. Available: http://ec.europa.eu/programmes/horizon2020/en/what-horizon-2020. [Accessed: 12-May-2018].

[5]   "HORIZON 2020 -Work Programme 2016 -2017 'Secure, Clean and Efficient Energy.'"

[6]   EPA, "Global Greenhouse Gas Emissions Data | Greenhouse Gas (GHG) Emissions | US EPA." [Online]. Available: https://www.epa.gov/ghgemissions/global-greenhouse-gas-emissions-data. [Accessed: 12-May-2018].

[7]   "Energy Efficiency Training Week."

[8]   D. Bhatia, "Review on Combined Cooling , Heating and Power (CCHP) Systems coupled with Fossil Fuels with Energy , Economic and Environmental Considerations Review on Combined Cooling , Heating and Power (CCHP) Systems coupled with Fossil Fuels with Energy , Econo," no. January, 2016.

[9]   A. S. Daniel Maraver, Fernando Sebastián, and Javier Royo, "Environmental assessment of CCHP (combined cooling heating and power) systems based on biomass combustion in comparison to conventional generation."

[10]   F. R. Tsakiris, "Energy Development in the Non-Connected Islands of the Aegean Sea Internship report," 2010.

[11]   "Hellenic Statistical Authority - ELSTAT." [Online]. Available: http://www.statistics.gr/en/home/. [Accessed: 15-May-2018].

[12]   I. - International Energy Agency, "Energy Policies of IEA Countries - Greece Review 2017."

[13]   M. Šúri, T. A. Huld, E. D. Dunlop, and H. A. Ossenbrink, "Potential of solar electricity generation in the European Union member states and candidate countries," *Sol. Energy*, vol. 81, no. 10, pp. 1295–1305, Oct. 2007.

[14]   J. K. Kaldellis, "Social attitude towards wind energy applications in Greece," *Energy Policy*, vol. 33, pp. 595–602, 2005.

[15]   Ministry of Development, "ENERGY OUTLOOK OF GREECE."

[16]   "21 more islands in the list of electric connections | EnergyWorld Magazine." [Online]. Available: https://www.energyworldmag.com/21-islands-list-electric-connections/. [Accessed: 15-May-2018].

[17] S. Quoilin and M. Orosz, "Rural Electrification through Decentralized Concentrating Solar Power: Technological and Socio-Economic Aspects," *J. Sustain. Dev. Energy J. Sustain. dev. energy water environ. syst*, vol. 1, no. 13, pp. 199–212, 2013.

[18] A. L. S. Diaf, M. Belhamel, M. Haddadi, "Technical and economic assessment of hybrid photovoltaic/wind system with battery storage in Corsica island." .

[19] IEA, "Renewables 2017 IEA publication." [Online]. Available: https://www.iea.org/publications/renewables2017/. [Accessed: 04-Jun-2018].

[20] R. Fu, D. Feldman, R. Margolis, M. Woodhouse, and K. Ardani, "U.S. Solar Photovoltaic System Cost Benchmark: Q1 2017," 2009.

[21] S. Tselepis, "ELECTRIFICATION WITH SOLAR POWERED MINI-GRIDS, A CASE STUDY FOR THE ISLAND OF KYTHNOS," pp. 7–3, 2003.

[22] W. K. G-Cramer, M. Ibrahim, "PV SYSTEM TECHNOLOGIES, State-of-art and Trends in Decentralised Electrification."

[23] L. L. K. * Ali Al-Karaghouli, "Optimization and life-cycle cost of health clinic PV system for a rural area in southern Iraq using HOMER software."

[24] J. G. Fantidis, D. V. Bandekas, C. Potolias, and N. Vordos, "The effect of the financial crisis on electricity cost for remote consumers: Case study samothrace (Greece)," *Int. J. Renew. Energy Res.*, vol. 1, no. 4, pp. 281–289, 2011.

[25] R.K. Akikur, R. Saidur, H.W. Ping, and K.R. Ullah, "Comparative study of stand-alone and hybrid solar energy systems suitable for off-grid rural electrification: A review."

[26] J. Freeman, I. Guarracino, S. A. Kalogirou, and C. N. Markides, "A small-scale solar organic Rankine cycle combined heat and power system with integrated thermal energy storage," *Appl. Therm. Eng.*, vol. 127, pp. 1543–1554, Dec. 2017.

[27] B. F. Tchanche, G. Lambrinos, A. Frangoudakis, and G. Papadakis, "2011 - Tchanche - Low-grade heat conversion into power using organic Rankine cycles A review of various applications," *Renew. Sustain. Energy Rev.*, vol. 15, pp. 3963–3979, 2011.

[28] G. Qiu, Y. Shao, J. Li, H. Liu, and S. B. Riffat, "Experimental investigation of a biomass-fired ORC-based micro-CHP for domestic applications," *Fuel*, vol. 96, pp. 374–382, 2012.

[29] J. Freeman, I. Guarracino, S. A. Kalogirou, and C. N. Markides, "A small-scale solar organic Rankine cycle combined heat and power system with integrated thermal energy storage," *Appl. Therm. Eng.*, vol. 127, pp. 1543–1554, Dec. 2017.

[30] J. Freeman, K. Hellgardt, and C. N. Markides, "An assessment of solar-powered organic Rankine cycle systems for combined heating and power in UK domestic applications," 2015.

[31] "LoadProGen Repository." [Online]. Available: https://www.dropbox.com/sh/auahaeuhmiqlgkp/AACXfH1M83huQYOuR2NW6e xoa?dl=0. [Accessed: 10-Jun-2018].

[32] ASHRAE, "ASHRAE STANDARD." .

[33]   "Weather Data | EnergyPlus." [Online]. Available: https://energyplus.net/weather. [Accessed: 10-Jun-2018].

[34]   "MITSUBISH FH SERIES HEAT PUMPS."

[35]   K. H. N. Min Soo Kim,Hansaem Park, "Performance investigation of heat pump–gas fired water heater hybrid system and its economic feasibility study."

[36]   Y. Zhang, E. Long, Y. Li, and P. Li, "Solar radiation reflective coating material on building envelopes: Heat transfer analysis and cooling energy saving," *Energy Explor. Exploit.*, vol. 35, no. 6, pp. 748–766, 2017.

[37]   E. Macchi and M. Astolfi, *Organic Rankine Cycles (ORC) Power Systems.* .

[38]   "Turboden ORC technology for the wood industry."

[39]   B. F. Tchanche, S. Quoilin, S. Declaye, G. Papadakis, and V. Lemort, "Economic feasibility study of a small scale organic rankine cycle system in waste heat recovery application," *ASME 2010 10th Bienn. Conf. Eng. Syst. Des. Anal. ESDA2010*, vol. 1, no. September 2015, pp. 249–256, 2010.

[40]   F.-P. Langue, "Biomass market trends and bioenergy sector views on EU policy," 2015.

[41]   E. Carlon *et al.*, "Efficiency and operational behaviour of small-scale pellet boilers installed in residential buildings," 2015.

[42]   "SMART 350 kW - Smart Heating Technology." [Online]. Available: http://www.smartheating.cz/en/smart-350-kw/. [Accessed: 13-Jun-2018].

[43]   B. D. Neyer *et al.*, "Collection of criteria to quantify the quality and cost IEA Solar Heating and Cooling Program," vol. 61, no. 0, pp. 1–56, 2015.

[44]   I. Renewable Energy Agency, "Renewable Energy Cost Analysis: Biomass for Power Generation," vol. 1, no. 5, 2012.

[45]   K. B. Sotirios Karellas, "Energy–exergy analysis and economic investigation of a cogeneration and trigeneration ORC–VCC hybrid system utilizing biomass fuel and solar power."

[46]   "Thermomax DF100." [Online]. Available: http://www.powernaturally.co.uk/working/content/uploads/2015/07/Kingspan-DF100-data-sheet.pdf. [Accessed: 11-Jun-2018].

[47]   A. Samer Yasin, N. Y. Fathi, and A. K. Ali, "General Polynomial for Optimizing the Tilt Angle of Flat Solar Energy Harvesters Based on ASHRAE Clear Sky Model in Mid and High Latitudes," vol. 6, no. 2, pp. 29–38, 2016.

[48]   "MIDC: Solar Position and Intensity (SOLPOS) Calculator." [Online]. Available: https://midcdmz.nrel.gov/solpos/solpos.html. [Accessed: 11-Jun-2018].

[49]   Apricus, "Apricus Ap pressure Drop curve." .

[50]   J. Freeman, I. Guarracino, S. A. Kalogirou, and C. N. Markides, "A small-scale solar organic Rankine cycle combined heat and power system with integrated thermal energy storage," *Appl. Therm. Eng.*, vol. 127, pp. 1543–1554, Dec. 2017.

[51]   H. Fugmann, B. Nienborg, G. Trommler, A. Dalibard, and L. Schnabel,

"Performance evaluation of air-based heat rejection systems," *Energies*, vol. 8, no. 2, pp. 714–741, 2015.

[52] M. Schimpe *et al.*, "Energy efficiency evaluation of a stationary lithium-ion battery container storage system via electro-thermal modeling and detailed component analysis," *Appl. Energy*, vol. 210, no. November 2017, pp. 211–229, 2018.

[53] I. Renewable Energy Agency, "Electricity storage and renewables: Costs and markets to 2030," 2017.

[54] H. Darhmaoui and D. Lahjouji, "ScienceDirect Latitude Based Model for Tilt Angle Optimization for Solar Collectors in the Mediterranean Region," *Energy Procedia*, vol. 42, no. 42, pp. 426–435, 2013.

[55] "PEIMAR SG300M."

[56] R. Fu, D. Feldman, R. Margolis, M. Woodhouse, and K. Ardani, "U.S. Solar Photovoltaic System Cost Benchmark: Q1 2017," 2009.

[57] T. Khatib, "Optimization of a grid-connected renewable energy system for a case study in Nablus, Palestine," *Int. J. Low-Carbon Technol.*, vol. 9, no. 4, pp. 311–318, 2014.